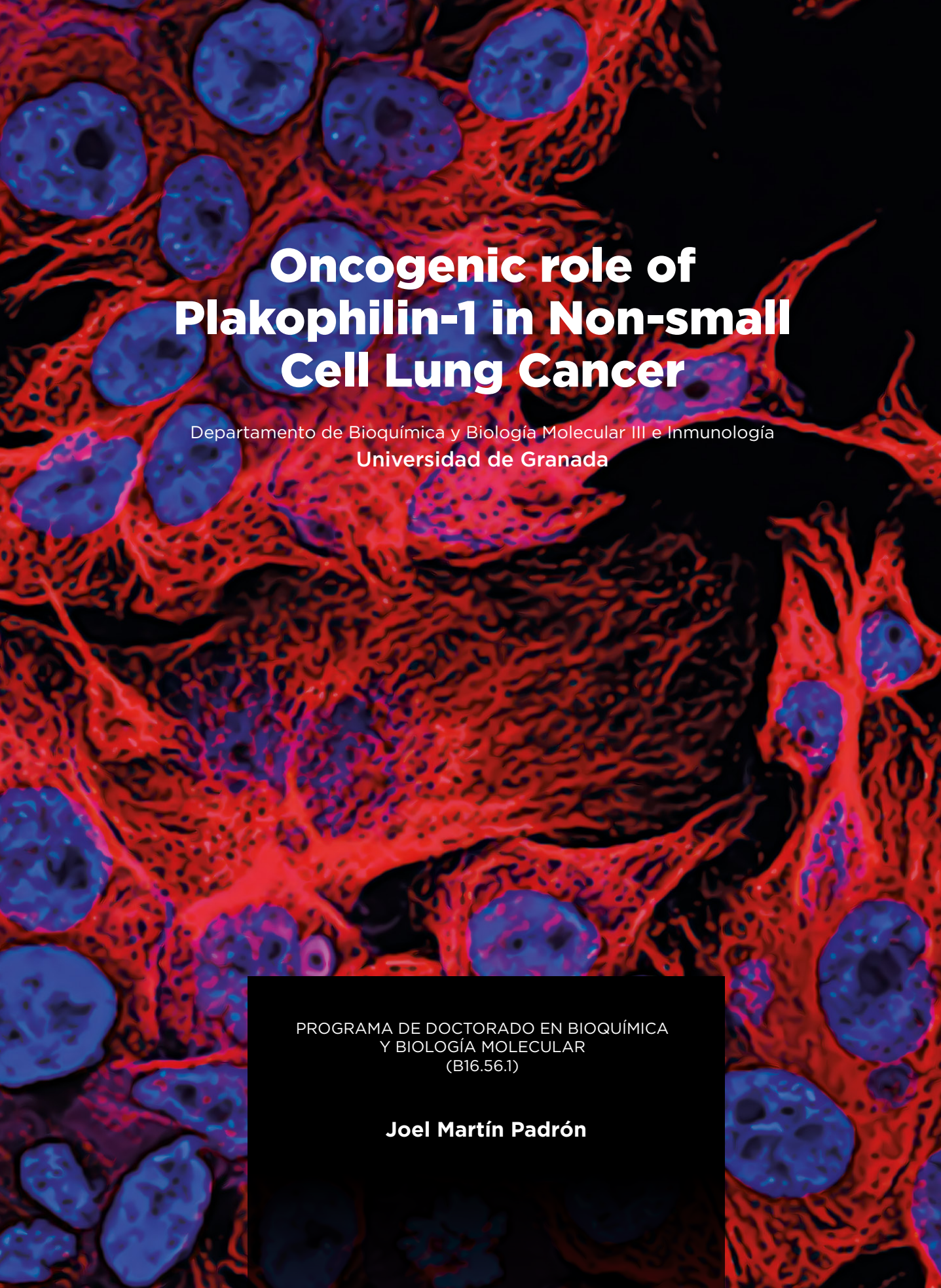

Oncogenic role of Plakophilin-1 in Non-small Cell Lung Cancer

Departamento de Bioquímica y Biología Molecular III e Inmunología
Universidad de Granada

PROGRAMA DE DOCTORADO EN BIOQUÍMICA
Y BIOLOGÍA MOLECULAR
(B16.56.1)

Joel Martín Padrón

Editor: Universidad de Granada. Tesis Doctorales
Autor: Joel Martín Padrón
ISBN: 978-84-1306-464-2
URI: http://hdl.handle.net/10481/60167

Oncogenic role of Plakophilin-1 in Non-small Cell Lung Cancer

Departamento de Bioquímica y
Biología Molecular III e Inmunología.
Universidad de Granada

UNIVERSIDAD DE GRANADA

Centro Pfizer - Universidad de Granada - Junta de Andalucía
de Genómica e Investigación Oncológica (GENyO)

PROGRAMA DE DOCTORADO EN BIOQUÍMICA Y
BIOLOGÍA MOLECULAR
(B16.56.1)

GENYO
PFIZER-UNIVERSIDAD DE GRANADA-JUNTA DE ANDALUCIA
CENTRE FOR GENOMICS AND ONCOLOGICAL RESEARCH

Joel Martín Padrón

Tesis Doctoral
Granada, 2020

Porque ya no están todos los que son, pero sí son todos los que están.

Para la vieja y la nueva guardia (ellos/as saben quiénes son): "GRACIAS" nunca tuvo tanto significado para mí como hoy.

INDEX

ABSTRACT

Plakophilin 1 (PKP1) is a member of the arm-repeat (armadillo) and the plakophilin gene families. PKP1 is best known for being an essential component of the desmosome. While the loss of desmosome function has been related to increased cell migration and pro-oncogenic activity, intriguingly, our group has robustly observed that PKP1 is among the top overexpressed proteins in Squamous Cell Lung Cancer (SqCLC). To shed light on these contradictory observations, we have developed some different *in vitro* and *in vivo* functional models of PKP1 gain/loss in Squamous Cell Lung Cancer.

Interestingly, on the one hand, the CRISPR-Cas9 *PKP1* knock-out clones displayed more cell dissemination, but their cell proliferation was severely damaged *in vitro*. On the other hand, ectopic PKP1 expression in the NCI-H2170 cell line clearly showed the promotion of cell proliferation and cell survival. Furthermore, xenograft engraftment caused by PKP1 expression was concluded from *in vivo* experiments. These phenotypical results may place PKP1 as a new oncogene in Squamous Cell Lung Cancer.

Importantly, a functional relationship between PKP1 and the oncogene C-MYC was identified as the cause of these pro-oncogenic activities. Several functional experiments were performed, and results showed that PKP1 can bind the 5'UTR of C-MYC mRNA to enhance its translation, and C-MYC directly interacts with the PKP1 promoter, enhancing its transcription. These new observations have revealed a mechanistic feedforward loop, unveiling C-MYC as an important transcriptional regulator of PKP1, and PKP1 as a novel post-transcriptional regulator of C-MYC.

In summary, these results support PKP1 as a valuable diagnosis biomarker for squamous cell carcinoma and confirm it as a new promising target for the development of therapeutic opportunities in this tumor subtype (and potentially others), especially taking into account that PKP1 inhibition can affect C-MYC expression, which is recognized as a "most wanted" target for cancer therapy.

INTRODUCTION

CANCER

DEFINITION AND BIOLOGY

Cancer can be defined as a set of genetic diseases characterized by the presence of abnormal cells with uncontrolled grow in the body. It is a complex and multistage process in which genetic changes progressively accumulate and transform healthy cells into malignant tumors (Hanahan & Weinberg, 2011). These changes are the result of the interaction between genetic factors and environmental agents as chemical, physical, and external biological carcinogens.

Aging is considered a global risk, and chronic infections is also an important factor for low- and middle-income countries. Furthermore, some life habits as alcohol consumption, tobacco use, physical inactivity, and unhealthy diet are worldwide proved risk factors to suffer cancer (STEWART & WILD, 2014).

Regarding cancer biology, whereas healthy cells mature to specific cell type, cancer cells have a lower degree of specialization and remain in an immature stage. They mainly do it through avoiding anti-growth signals, replicating in an uncontrolled way without grow factor signals, and getting the ability to invade the same or adjoining tissues (which is known as metastasis and represents a significant cause of cancer death worldwide) (Massagué & Obenauf, 2016).

Cancer cells can also influence the surrounded microenvironment, evading and taking advantage of the immune system, avoiding programmed cell death and apoptosis signals, and improving tumor irrigation through promoting angiogenesis (Hanahan & Weinberg, 2011).

Furthermore, it is well known that tumors are composed of several different cell types and act as complex tissues in which every cell type interacts with each other. It should be underlined the role of the tumor-associated stroma, which is formed by healthy cells and contributes to the tumor microenvironment development and the expression of some cancer hallmarks(Tlsty & Coussens, 2006).

THE DOGMA OF CANCER DEVELOPMENT

The current dogma of cancer states that every single tumor cell has a monoclonal origin, although they are not genetically identical. It is because tumor cells suffer what is called a "microevolution" process during the tumor development, which is composed by mutations (genetic alterations), competition, and cell selection (Greaves & Maley, 2012)(Image 1).

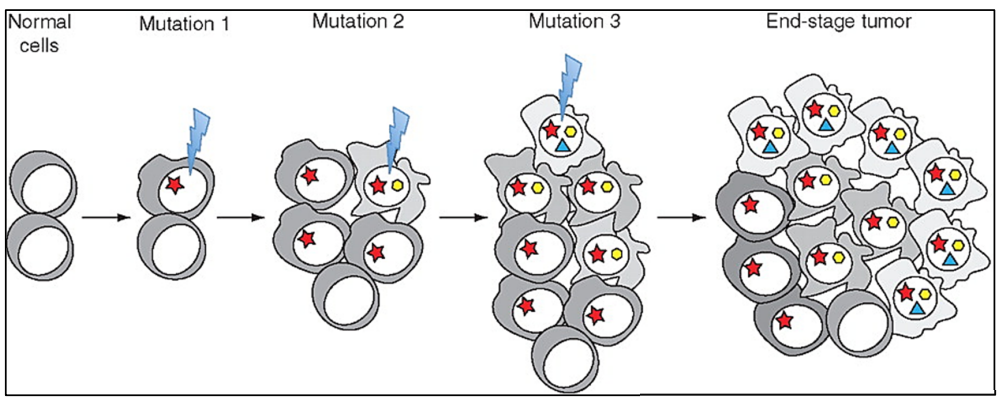

Modified from (Jonkers, 2012).

Image 1. Cancer development through the "microevolution" process in which repeated cycles of genetic mutations in driver genes and clonal expansion generate the end-stage tumor.

Carcinogenesis implies progressive accumulation of gene alterations during tissue growth over the years until it becomes evident. During this dynamic process, those cells that are acquiring genetic alterations, which give them growth advantages, are being selected and will be the majority in the developed tumor. That is why cancer is triggered by mutations in those genes that control cell proliferation (Lodish, Berk, & Zipursky, 2000). Finally, mortality caused by cancer is the result of invading and spread cancer cells into normal tissues due to this uncontrolled clonal expansion.

CANCER-TRIGGERING MUTATIONS

Mutations that trigger the processes leading cancer take place in three types of genes: proto-oncogenes, tumor-suppressor genes, and DNA-repair genes.

- Proto-oncogenes(Lee & Muller, 2010): the mutation of these normal genes creates oncogenes, and the altered proteins resulted from the expression of these oncogenes can stimulate cell growth and/or invasiveness. Sometimes, increased expression of the normal protein can induce the changes which are necessary to trigger cell transformation and tumorigenesis.

- Tumor-suppressor genes(L.-H. Wang, Wu, Rajasekaran, & Shin, 2018): their normal function is to regulate the cell cycle, avoid excessive proliferation, and promote specific cell localization. The inactivation of both alleles in these genes can cause aberrant proteins or loss of expression, inducing tumorigenesis. This biallelic inactivation can be caused by mutation, methylation, or loss of heterozygosity (due to loss of chromosomal fragments or homologous recombination).

- DNA-repair genes(Carrassa & Damia, 2017): they work rectifying errors from the wrong incorporation of nucleotides during DNA replication, and repairing alterations induced by radiation and chemicals. Mutations in these genes can induce cancer when they stop being able to repair accumulated errors in proto-oncogenes and tumor-suppressor genes.

THE GLOBAL BURDEN OF CANCER

According to the World Health Organization (WHO) data (STEWART & WILD, 2014), cancer is the second leading cause of death worldwide and a major cause of morbidity. Due to its complexity and difficult treatment, it is responsible for about 1/6 of deaths with an estimation of 9.6 million cancer deaths in 2018, and predictions estimate 20 million new cancer cases annually by 2025.

The highest cancer death rates occur in low- and middle-income countries (approximately 70%), and bad diet and behavioral habits cause around 1/3 of deaths from cancer, meaning between 30% and 50% of cancer deaths could be prevented.

In terms of incidence by gender: in men, from highest to lowest, the most common cancer types are lung, prostate, colorectal, stomach, and liver; whereas in women are breast, colorectal, lung, cervix, and thyroid. These sites also represent the most common causes of cancer death.

Finally, in light of these data, it is clear that the worldwide economic impact of cancer is highly significant and remains increasing. An example is the total annual economic cost of cancer in 2010, calculated at approximately US$ 1.16 trillion (STEWART & WILD, 2014).

CANCER IN SPAIN

According to the Spanish National Institute of Statistics (INE), in 2010, tumors were the second leading cause of death in Spain (28.1 out of every 100 deaths), only behind circulatory system diseases, and with an ascending trend between 2000 and 2010.

Furthermore, tumors were the second cause of death in women and the first in men and the age groups between 5 and 14 years, and between 40 and 79 years (35.7% and 42.7% of the total, respectively) regardless of gender.

Regarding the tumor type, responsible for the highest mortality were: lung, bronchi, and trachea cancers (with 1.6% more deaths in 2010 than in 2009) and colon cancer (3.6% more deaths). By gender, cancers that caused the most deaths in men were lung, bronchi, and trachea cancers; while it was breast cancer in women.

The standardized mortality rate due to tumors in 2010 in Spain was 152.4 per 100,000 inhabitants. Between 2000 and 2010, this rate fell by almost 11%, but the weight of deaths due to tumors became more critical, representing 26.4% in 2000 and increasing to 28.1% in 2010.

Finally, despite those above, the cancer mortality rate in 2010 in Spain was one of the lowest in the European Union, with 153 deaths per 100,000 inhabitants, behind Cyprus, Finland, and Sweden. This fact contrasts with the values of Hungary, Poland, and the Baltic States, which exceed 190 deaths per 100,000.

LUNG CANCER

LUNG CANCER DEFINITION AND CLASSIFICATION

In lung cancer, tumor cells can be found in the epithelium that lines the entire respiratory tree, from the trachea to the finest terminal bronchiole, and the cells found in the pulmonary alveoli.

All lung cancer tumors have common cellular and molecular origin and derive from pluripotent cells capable of presenting different phenotypes depending on the accumulated mutations and the received stimuli (with the subsequent specific clinical and prognostic implications). All these differences between patients have driven to stablish different lung cancer subgroups.

The World Health Organization (WHO) and the International Association for the Study of Lung Cancer (IASLC) adopted the same histological classification of lung cancer in 2004 (Defranchi et al., 2009), and the WHO published a final revised version in 2015.

According to morphological, immunohistochemical and genetic characteristics, lung cancer is classified in two main groups, each one ranging from I to IV stage depending on tumor progression: Small Cell Lung Cancer (SCLC) (20% of patients), and Non-small Cell Lung Cancer (NSCLC) (80% of patients). This last group is, in turn, subclassified in three subtypes: adenocarcinoma (40% of patients), squamous cell carcinoma (25% of patients), and large cell carcinoma (10% of patients).

On the one hand, Squamous Cell Lung Cancer tumors are frequently located in the lung core and, compared to lung adenocarcinoma, they tend to grow more slowly, and metastasize later.

On the other hand, lung adenocarcinomas, which are more frequently found in the pulmonary periphery, usually present a worse prognosis in all stages.

Accurate histological lung cancer subclassification is crucial since therapeutic approaches depend on their histological type. Nowadays, lung cancers are tending to be classified in the different subtypes attending to particular genetic alterations related to drive and maintain lung cancer development. Interestingly, these new classification parameters open the possibility of developing personalized and specific novel targeted therapies (Travis et al., 2015).

LUNG CANCER EPIDEMIOLOGY AND ETIOLOGY

Lung cancer is the most frequent cancer worldwide, representing 11,6% of all cancers and 18,4% of all cancer deaths in the estimations provided by the GLOBOCAN database for 2018(Image 2). In terms of gender prevalence, it has the first position in men and the third in women.

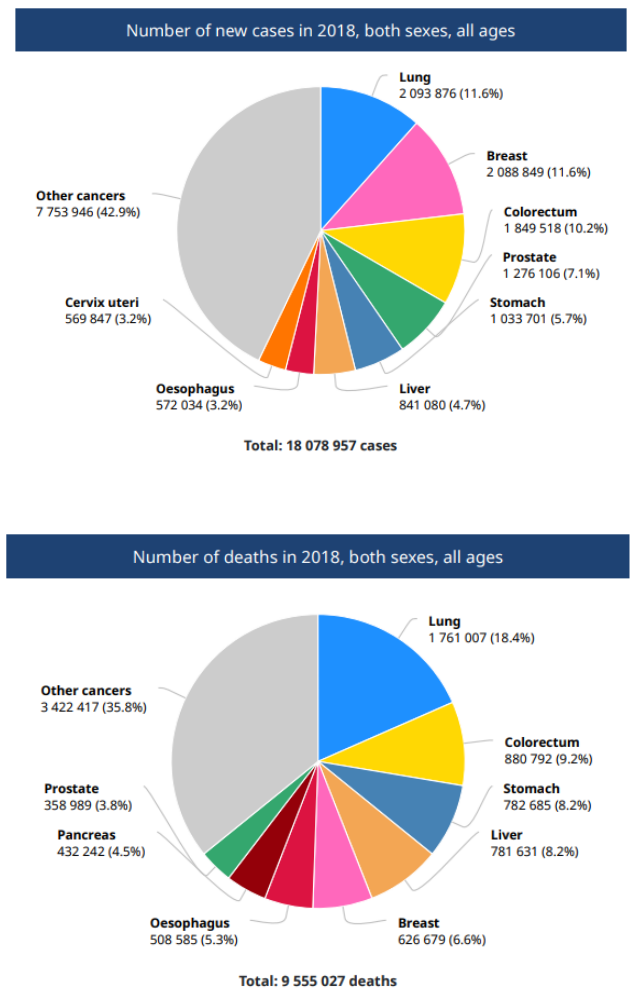

Image 2. Lung cancer statistics for 2018 provided by the GLOBOCAN database.

The highest age-standardized lung cancer rates are in North America, East Asia, and Europe; whereas the lowest are in many African and some Asian countries, although China includes more than 1/3 of all newly diagnosed cases (Bray et al., 2018).

The predominant cause of lung cancer worldwide is tobacco smoking, including second-hand smoke. Smoker-derived tumors present ten times more mutations than those derived from never-smokers. Other causes of lung cancer include exposure to different breathable toxic compounds like those contained in air pollution.

In terms of prevalence, adenocarcinoma predominates in women never-smokers; while male smokers usually develop squamous cell carcinoma. Finally, Small Cell Lung Cancer typically occurs in heavy smokers, presenting the most aggressive phenotype (Pesch et al., 2012).

LUNG CANCER PROGNOSIS AND DIAGNOSIS

Lung cancer patients have a 5-years overall survival of around 10–15%, being one of the most aggressive malignant neoplasms. Poor survival of lung cancer patients is mainly due to close to 80% of patients are diagnosed with metastasis and/ or in advanced stages, which are more resistant to traditional chemotherapy. Furthermore, around 30-70% of patients at initial stages develop recurrence after treatment(Lacasse, Wong, Guyatt, & Cook, 1999)(Loubeyre, Copercini, & Dietrich, 2005)(Rivera & Mehta, 2007). However, specific therapies based on histology and genetic classifications start to be successful.

The diagnosis of lung cancer is based on the recommendations of the International Association for the Study of Lung Cancer (IASLC), published in its 7th edition (Mirsadraee, Oswal, Alizadeh, Caulo, & van Beek Jr, 2012) and, most recently, its 8th edition (Goldstraw et al., 2016). The combination of microscopic cell and tissue morphology (to differentiate tumoral cells from healthy cells), and immunohistochemistry (to identify specific cancer cell markers) allow to histologically classify the samples into the different lung cancer subtypes (Vannini, Fanini, & Fabbri, 2013) and facilitate the treatment selection for the patients.

Napsin A and Thyroid transcription factor 1 (TTF-1), as well as the Surfactant apoprotein A (SP-A) (which is expressed in around 50% of adenocarcinomas), are the recommended markers for the diagnosis of lung adenocarcinoma; while the most useful markers for the diagnosis of Squamous Cell Lung Cancer are p63, p40 and Cytokeratin 5/6 (CK 5/6).

Furthermore, cytokeratin 7 (CK7) for lung adenocarcinoma, and desmocollin 3 (DSC3) and Desmoglein 3 (DSG3) for Squamous Cell Lung Cancer are also considered potential good markers. (González Baron, 2006).

It is important to remark the need of further research regarding lung cancer diagnosis since approximately 16% of diagnosticated lung carcinoma are negatives for some of the subtype-specific markers or positives for both, adenocarcinoma and squamous carcinoma markers.

LUNG CANCER GENETICS

Although much about genetic risk has to be learned, there is an extensive collection of studies that show the importance of genetics in the development of cancer and its value in diagnosis (biomarkers) and correct treatment selection.

In regards to lung cancer, genes included in regulating telomerase production and nicotinic acetylcholine receptors have been identified in three separate loci associated with lung cancer (5p15, 6p21, and 15q25) in several large collaborative genome-wide studies. Furthermore, many studies to determine susceptibility to particular lung tumor subtypes have been extensively achieved:

On the one hand, EGFR, ALK, BRAF, PIK3CA, ROS1, HER2 (ERBB2) and KRAS driver mutations and ALK or ROS1 fusions(Pao & Hutchinson, 2012) have been frequently found in adenocarcinoma tumors. Furthermore, other remarkable adenocarcinoma tumours mutations and/or alterations have been found in such important genes as: RBM10, ARID1A, U2AF1 (Imielinski et al., 2012), RELN, CFTR, DACH1, ABCB5, and HGF (Govindan et al., 2012).Finally, currently approved drugs as crizotinib (for ROS1 and ALK fusion)(J. J. Lin & Shaw, 2017), and erlotinib or gefitinib (for EGFR mutation)(J. J. Yang et al., 2017), are being used as target therapy of adenocarcinoma, and there are several drugs in phase 2 or 3 which target some of the other described mutations (Hirsh, 2015)(Cousin et al., 2018).

On the other hand, the squamous differentiation pathway (in 44% of cases) and the oxidative stress response pathway (in 30% of the cases) are recurrently affected in Squamous Cell Lung Cancer. Furthermore, the most frequent mutations or somatic alterations in copy number, which are recognized as drivers of tumor initiation and progression from patients with Squamous Cell Lung Cancer, have been detected in TP53, PTEN, CDKN2A (P16), PIK3CA, KEAP1, and MLL2 (Network, 2012)(Drilon, Rekhtman, Ladanyi, & Paik, 2012), FGFR1, SOX2(Weiss et al., 2010), C-MYC, NFE2L2, CDK6, MDM2, NF1, DDR2, and FOXP1 (Network, 2012). Finally, although 50% of squamous lung carcinomas have mutations or other genetic alterations which are susceptible to be molecular targets, just some drugs as Dasatinib (for DDR2 mutation) and FGFR1 tyrosine kinase inhibitor (for FGFR1 amplification) are presently in the market, and a drug targeting PIK3CA is currently under approval consideration in the United States Food and Drug Administration (FDA).

Regarding small cell carcinomas, more research effort is necessary in order to shed light on the molecular origins of this tumor subtype. Although it is known that most of these lung tumors present RB1 and TP53 mutations and express neuroendocrine markers(Zheng, Liu, Fallon, & Zhong, 2015), none single molecularly targeted drug has been successfully developed.

Non-small and small cell lung carcinomas usually also contain several numerical and structural chromosome alterations and epigenetic changes that result in aberrant expression of oncogenes and silencing of tumor-suppressor genes. Due to these aberrations in combination with the previously described alterations, lung cancer treatment continues to be a challenge, and it is crucial to know the tumor histological type, the tumor extension, and its genetic characteristics to select a correct personalized treatment which may be more likely to work and reduce side effects.

LUNG CANCER TREATMENT

There are many types of lung cancer treatment, each one with different side effects, which can be used alone or in combination depending on the general health of the patient, lung cancer type, location, size, stage, and whether it has spread. It is important to mention that patients can also take part in research studies, called clinical trials, in order to get access to developing treatments.

NON-SMALL CELL LUNG CANCER TREATMENT

Regarding Non-small Cell Lung Cancer (NSCLC), surgery is the preferent treatment to remove stage I and II NSCLC tumors. Depending on how advanced it is, surgery can be used to remove the entire tumor, or to eliminate part of it. Furthermore, surgery can also be used to excise tumors which are causing pain or pressure, and even to help other treatments to work better(Howington, Blum, Chang, Balekian, & Murthy, 2013). It has been demonstrated that adjuvant chemotherapy after tumor extirpation may prevent cancer from returning, mainly for patients in stage II and IIIA(collaborative group, 1995).

A combination of chemotherapy and radiotherapy treatments is recommended to those patients with lung tumors in stage III that cannot be removed by surgery. Finally, lung tumors in

stage IV are typically treated with chemotherapy, whereas radiotherapy is used only for symptoms palliation(Ramalingam & Belani, 2008)(Amini, Yeh, Gaspar, Kavanagh, & Karam, 2014).

It is important to remark that chemotherapy treatment is used in many occasions in lung cancer patients before radiotherapy or surgery to facilitate subsequent tumor extirpation or to increase the effectiveness of radiation.

Among the most commonly used chemotherapy drugs are cisplatin, carboplatin, gemcitabine, docetaxel, pemetrexed, paclitaxel, and vinorelbine. These drugs can be used alone or in combination, and patients are frequently submitted to a second round of chemotherapy(Masters et al., 2015).

Although chemotherapy and radiotherapy have demonstrated their efficacy in the fight against lung cancer, some improvements in mortality and morbidity of the patients must be achieved. Furthermore, these treatments cannot discriminate between normal cells and cancer cells, frequently causing high number of side effects.

The introduction of targeted therapies, specifically designed to attack cancer cells through mainly targeting genomic mutations (that help tumors to grow, divide, and/or spread in each particular patient), has been one of the most important developments in lung cancer medicine. In this sense, people who have lung tumors containing certain molecular biomarkers can be treated with a targeted drug alone or in combination with chemotherapy, even in advanced stages(Tsimberidou, 2015).

Most targeted therapies are either small-molecule drugs (used for targets which are inside cells) or monoclonal antibodies (to specific targets on the outer surface of cancer cells). Regarding Non-small Cell Lung Cancer, these treatments include: Erlotinib, Afatinib and Gefitinib for mutations in the epidermal growth factor receptor (EGFR) gene(Yamaoka, Ohba, & Ohmori, 2017); Bevacizumab, which targets the vascular endothelial growth factor (VEGF)(Russo et al., 2017); and Crizotinib and Ceritinib, which block the ALK receptor tyrosine kinase(Gainor et al., 2015).

However, more research is crucial in this new field since many times lung cancer patients may develop tumor resistant to targeted treatment due to the continuous mutational changes suffered by cancer cells(Pakkala & Ramalingam, 2018).

Interestingly, immunotherapy has recently emerged as a promising treatment against lung cancers. This biological therapy helps the immune system of the patient to fight cancer through different strategies and with shallow side effects. Although immunotherapy treatments for NSCLC have evolved the most and have demonstrated successful results, there are also some of these drugs in clinical trials for SCLC(Freeman-Keller, Goldman, & Gray, 2015). Due to this smart treatment approach is revolutionizing present cancer therapy, it will be explained more in detail later in the text.

SMALL CELL LUNG CANCER TREATMENT

Regarding Small Cell Lung Cancer, a minimal percentage of patients in the early-stage of tumor development may benefit from surgery, and chemotherapy is the recommended treatment regardless of the SCLC stage. Furthermore, radiotherapy may be used in combination with chemotherapy in the early stages, and radiotherapy of the brain is used in patients whose cancer has spread to this organ or as a prophylactic procedure in those patients who are responding to the treatment(Byers & Rudin, 2015).

IMMUNO-ONCOLOGY

The immune system consists of several cell types, molecules, and organs that have the mission to protect the body from infections and diseases. The immune system is classically classified in two categories: the innate immune system, which provides first defense barrier, and the adaptative immune system, including those immune system members which can remember most invading organism or antigens, allowing a more rapidly reaction in a subsequent interaction.

Immuno-oncology is an emerging and promising cancer research field which is focused on finding ways to empower the human body in order to better fight tumoral cells through either stimulating the components of the immune system itself or to enhance the immunological response through the addition of external components(Finn, 2012). Then, Immunotherapy targets the immune system, not the tumor itself, displaying a different side effect profile that may be advantageous from conventional therapies.

IMMUNOTHERAPY IN CANCER

It is known that the immune system can suppress and/or promote cancer growth (Schreiber, Old, & Smyth, 2011), for example, chronic inflammation can lead local immunosuppression in a tumoral context, favoring cancer development. On the contrary, acute inflammation can enhance T cells function and dendritic cells maturation, promoting antitumor effects (Shalapour & Karin, 2015).

Tumoral cells can often avoid recognition and elimination by the immune system(Drake, Jaffee, & Pardoll, 2006) through any of the following mechanisms: producing ligands for co-inhibitory receptors, avoiding antigen presentation, recruiting immune suppressor cells, and/or secreting immune response inhibition factors.

According to the American Cancer Society (ACS), over 900 clinical trials are currently evaluating the effects of immunotherapy in cancer through different therapeutic approaches as cancer vaccines, monoclonal antibodies, and non-specific immunotherapies. Furthermore, combined

CRISPR-Cas9 and immune-based therapies, as well as neoantigen therapies approaches and Janus Kinase (JAK) family of proteins inhibitors (Pesu et al., 2008), are demonstrating a promising future and, likely, they will soon impact clinical practice (Xia et al., 2019) (Schumacher & Schreiber, 2015).

The most important achievements which have contributed significantly to the development of Immunotherapy in cancer are those related to monoclonal antibodies used as blockers against CTLA-4 receptor and PD-1/PD-L1 interaction, and the chimeric antigen receptor T-cell therapy (CAR T cell therapies) (Buchbinder & Hodi, 2015) (L. Chen & Han, 2015) (Kalos et al., 2011) (Grupp et al., 2013)(Brentjens et al., 2013).

Immunotherapy is postulated as a promising treatment not only to cancer but also to several diseases such as autoimmune pathologies, in which the immune system plays a central role. Furthermore, Immunotherapy is currently positively impacting the global socioeconomic scenario thanks to its promising results regarding cancer treatment in terms of patient survival and life quality(Emens et al., 2017).

IMMUNOTHERAPY IN LUNG CANCER

A significant effort is being made in the development of new immune-based lung cancer treatments since lung cancer is frequently diagnosed in late stages, when surgery, chemotherapy, and radiation are minimally effective. In fact, there are many immuno-based lung cancer treatments currently approved, mainly for subsets of patients with advanced NSCLC. It should be noted some monoclonal antibodies as Bevacizumab (targeting the VEGF/VEGFR pathway)(Russo et al., 2017), and Necitumumab (targeting the EGFR pathway)(Brinkmeyer & Moore, 2016); and many Immunomodulators as Atezolizumab, Durvalumab, and Pembrolizumab (Targeting the PD-1/PD-L1 pathway),or Nivolumab (also targeting the PD-1/PD-L1 pathway and approved not only for subsets of patients with advanced NSCLC but also for those with metastatic SCLC previously treated with conventional treatments)(Kumar et al., 2017)(Ready et al., 2019).

An impressive improvement in lung cancer patient outcomes is being observed when they are treated with immunotherapy, alone or in combination with standard treatments(Visconti, Morra, Guggino, & Celetti, 2017). Even so, several immune-based drugs are currently in clinical trials for lung cancer treatment and many other diseases, and more basic research is needed to completely understand the immune landscape and its implications in the development and treatment of diseases.

PLAKOPHILIN-1(PKP1)

PKP1 FAMILY AND STRUCTURE

The human gene encoding the PKP1 protein, which was crystallized in 2005(Choi & Weis, 2005), covers 50 kb of genomic DNA, is located on chromosome 1q32, and contains 15 exons. PKP1 belongs to the plakophilin (PKP) proteins, which are members of the p120-catenin subfamily of armadillo-related proteins and are composed of four main members:

On the one hand, Plakophilins 1,2 (and their isoforms PKP1b, and PKP2b), and Plakophilin 3 (PKP3), are mainly characterized as desmosomal proteins, and they share 55% similarity in the sequence of the armadillo repeats and 50% with the armadillo domain of p120-catenin (Image 3).

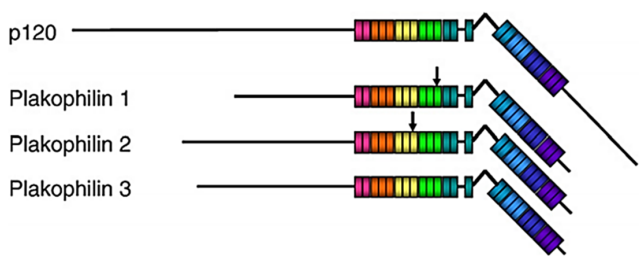

Adapted from (Mechthild Hatzfeld, 2007)

Image 3. Armadillo domain structure of PKP1, 2, and 3 compared to p120catenin. Black arrows point PKP1b and PKP2b isoforms obtained by alternative splicing.

On the other hand, Plakophilin 4 (PKP4) shares between 65 and 81.5% similarity in the armadillo repeat sequences with p120 catenin, δ-catenin, and ARVCF, and all of them crucially participate in stabilizing cadherin-mediated adhesion in adherens junctions(P Z Anastasiadis & Reynolds, 2000) (Mechthild Hatzfeld, 2005) (Mechthild Hatzfeld, 2007).

The plakophilins have a long amino-terminal domain, a central domain of nine arm repeats, and a short carboxyl-terminal domain (Bass-Zubek, Godsel, Delmar, & Green, 2009). Although the armadillo domain has structural and protein interaction functions in other p120-catenin family members, all protein interactions which have been observed in plakophilins, PKP1 included, take

place in the N-terminal domain, and the role of the central armadillo domain remains unknown. Furthermore, all plakophilins are basic proteins (Hofmann et al., 2006), and this could have effects in their interactions with other proteins.

The PKP1 protein contains nine armadillo repeats, and it is the smallest of the plakophilins (with a molecular weight of 82 KDa), it is practically insoluble (Wolf et al., 2010), and the only positively charged desmosome protein (Schmidt et al., 1997). It is believed that this positive surface on the armadillo domain has the function of binding to ligands not yet identified (Mechthild Hatzfeld, 2007).

Furthermore, the arm repeat structure of PKP1 contains a long and flexible insert between the fifth and sixth arm repeats, which produces a significant fold in the arm domain without affecting its packing (Choi & Weis, 2005) (Image 4).

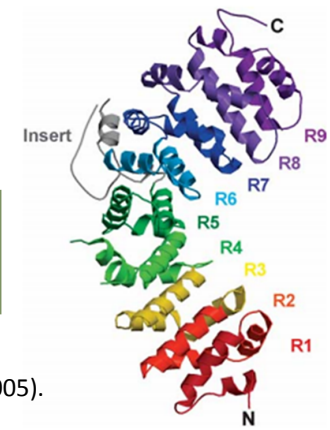

Image 4. Ribbon diagram of the PKP1 arm repeat domain. It illustrates the significant fold in the PKP1 arm domain without affecting its packing (Choi and Weis, 2005).

Adapted from (Choi & Weis, 2005).

The amino-terminal domain of PKP1 robustly interacts with DSP (Desmoplakin), recruiting it to the intercellular binding zone(Kowalczyk et al., 1999). PKP1 also interacts with DSG1 (Desmoglobin-1) and keratins, and some studies also relate it to PG (plakoglobin) and DSC1a(Desmocollin-1a)(South, 2004). Besides, plakophilins may associate with actin, actin regulating proteins, and microtubules (M Hatzfeld, Haffner, Schulze, & Vinzens, 2000).

Finally, as it was previously mentioned, PKP1 presents two isoforms ("a" and "b"), resulting from alternative splicing, and the mRNA of each isoform can also be presented in two alternatives 3´UTR polyadenylated forms (Schmidt et al., 1997). PKP1a is smaller (with 726 amino acids), and PKP1b contains a sequence of 21 additional amino acids encoded by exon 7 and located in the

third armadillo repeat. Both isoforms differ in abundance and behavior, although more research is necessary to bring light to its biological significance.

PKP1 BIOLOGICAL FUNCTIONS

Plakophilins 1, 2, and 3 reveal distinct expression patterns and, although they have partially redundant functions, mainly mediate distinct effects on desmosomal adhesion (Mechthild Hatzfeld, 2007). For example, it has been demonstrated that PKP1 overexpression increased desmosome size and number in tissue cells in culture (Kowalczyk et al., 1999) (M Hatzfeld et al., 2000), indicating that PKP1 significantly imparts intercellular cohesion and protects the epidermis from mechanical stress.

All three plakophilins have been observed in the nucleus (Bonne, van Hengel, Nollet, Kools, & van Roy, 1999) (Heid et al., 1995) (Mertens, Kuhn, & Franke, 1996)(Schmidt & Jäger, 2005) (Schmidt et al., 1997) but the nuclear localization of PKP1 is the most abundant.

PKP1 isoform "a" is more abundant than "b" and, while PKP1a is located in desmosomes, cytoplasm and, nucleus, PKP1b is only located in the nucleus (but none in the nucleolus)(Schmidt & Jäger, 2005). It is believed that the insertion of 21 amino acids present in the isoform "b" may be responsible for the abundance of PKP1b in the nucleus (Schmidt et al., 1997).

NLS (nuclear localization signals) motifs have not been found yet in the PKP1 sequence (Mechthild Hatzfeld, 2010). What is known is that the carboxyl-terminal of PKP1 (especially the last 40 amino acids) (Neuber et al., 2010) is required for its location in the plasmatic membrane while the amino-terminal end is involved in its nucleus location (Mechthild Hatzfeld, 2010) (M Hatzfeld et al., 2000)(Kowalczyk et al., 1999). However, it is not discarded that PKP1 could be associated with other proteins that contain NLS to be able to migrate to the nucleus.

Chromatin DNase I digestion revealed a decreased pool of nuclear PKP1, suggesting that PKP1 specifically associates with nuclear components. Furthermore, DNA damage resulted in the partial displacement of PKP1 from the nucleoplasm to the nucleolus, inducing increased cell survival and linking PKP1 to DNA damage response. In agreement, the association of PKP1 to single-stranded DNA (ssDNA), but not double-stranded DNA (dsDNA) have been demonstrated *in vitro*(Sobolik-Delmaire, Reddy, Pashaj, Roberts, & Wahl III., 2010), although it is postulated

that *in vivo* PKP1 may have greater affinity for binding RNA instead of ssDNA (Mechthild Hatzfeld, 2010).

Interestingly, although PKP1 nuclear functions are still unknown, data suggest that its nuclear location correlates with cell growth, and it may even promote it (Mechthild Hatzfeld, 2010).

PKP1 plays a vital role in cell migration and calcium-dependent stability of desmosomes. In normal tissues, desmosomes adopt a calcium-independent state (also called "hyper-adhesion")(Garrod, Berika, Bardsley, Holmes, & Tabernero, 2005) (Kimura, Merritt, & Garrod, 2007) (Wallis et al., 2000). In contrast, during wound healing and tissue regeneration, desmosomes lead to weaker intercellular adhesion through becoming calcium-dependent and allowing tissue remodeling (Kimura et al., 2012) (Wallis et al., 2000).

Nevertheless, the cytoplasmic localization of PKP1, and also PKP3, suggests an additional role of these proteins beside their involvement in cell-cell junction. Thus, PKP1 and PKP3 have been identified in stress granules, which are cytoplasmic aggregates of latent translation initiation complexes, and RNA binding proteins (RBPs). During cellular stress, mRNA is stably accumulated in them but without being translated.

RBPs direct several mRNAs processes such as translation, stability, transport, processing, and localization (Collins, Kurland, Biggs, & Penny, 2009) (Glisovic, Bachorik, Yong, & Dreyfuss, 2008), and it has recently been revealed that PKP1 and PKP3 containing messenger ribonucleoproteins (mRNPs) include PKP2 and DSP mRNAs, and affect their availability to be translated(Fischer-Kešo et al., 2014).

In agreement, FXR1, G3B, and PABPC1 have been found together with PKP1 or PKP3 in stress granules (SGs) when cells were exposed to environmental stress (i.e., heat shock or oxidative stress) (Hofmann et al., 2006). These three RBPs affect the turnover and translation of mRNAs in the cytoplasm, suggesting a possible role of PKP1 as well as PKP3 in post-transcriptional gene regulation (Wolf et al., 2010)(Wolf & Hatzfeld, 2010).

Furthermore, plakophilins have recently been associated with cell translation machinery, suggesting that they can play a role in post-transcriptional regulation and cell growth. PKP1 has been shown to stimulate translation *in vitro* and in cell lines(Wolf et al., 2010)(Wolf & Hatzfeld, 2010), and it has been demonstrated a direct association of PKP1 with the translation initiation factor eIF4A1 through its N-terminal head domain. PKP1 can recruit eIF4A1 to the initiation

complex and stimulates its helicase activity in a concentration-dependent manner, leading an increase in translation to the point of almost doubling it (Wolf et al., 2010) (Wolf & Hatzfeld, 2010), and correlating with a cell size and proliferation increment (Dusek & Attardi, 2011). Interestingly, eIF4A1 has also been found in stress granules together with PKP1.

In summary, these data suggest that PKP1, and also PKP3, exerts some functions in RNA translation, and RNA metabolism, and, although no RNA binding motifs have been discovered, this association could occur through direct electrostatic interactions due to the high alkalinity of these PKPs (Hofmann et al., 2006).

PKP1 EXPRESSION AND REGULATION

EXPRESSION

Although the sequences of all p120-catenin family proteins are highly related, the corresponding genes are scattered throughout the human genome, leading to the conclusion that the expression of these genes does not seem to be coordinately regulated. Furthermore, it is essential to mention that the organization of exons is highly conserved among genes related to p120-catenin, including plakophilins, suggesting that they have mainly followed the same evolutionary path (Mechthild Hatzfeld, 2007).

Plakophilins reveal overlapping but distinct expression patterns in the epidermis. Plakophilins 1, 2, and 3 show tissue-specific expression patterns similar to cadherins. Specifically, PKP1 presents a higher expression in the suprabasal layers of stratified epithelia (where desmosomes are larger and numerous). It is also present in the basal and granular layers and absent in the stratum corneum of complex epithelia (South, 2004) (Mechthild Hatzfeld, 2007)(Bass-Zubek et al., 2009) (Neuber et al., 2010).

REGULATION

There are several armadillo proteins which have been related to signaling functions as transcriptional regulation (β-catenin and p120), or specific signaling cascades as the Rho pathway (p 120 and PKP4).

PI3K / AKT pathway regulates PKP1 but not the rest of plakophilins. This pathway is triggered by several receptors, such as insulin or insulin-like growth factors, and phosphatidylinositol-3 kinase (PI3K) plays a key role in the cascade. PI3K / AKT pathway induces a cascade of kinases that ends in the phosphorylation of PKP1 through AKT2 in four motifs within the amino-terminal domain. These phosphorylations produce a lower affinity of PKP1 to DSG1, and as a consequence, it results in lower cell adhesion. PKP1-phosphorylated protein pool accumulates in the cytoplasm due to greater stability and a longer half-life of this PKP1 form, leading to higher proliferation rates through PKP1 cytoplasmic interaction with eIF4A1 (Wolf et al., 2013)(Wolf et al., 2010)(Wolf & Hatzfeld, 2010).

On the contrary, PKP1 non-phosphorylated pool interacts with DSP in desmosomes and promotes adhesion in the absence of growth factors, playing a tumor suppressor role. It is important to note that the PKP1 phosphorylated form, which will be located in the cytoplasm as a result of growth factors stimulation, will play an oncogenic role through inducing protein synthesis and cell proliferation (although it can still bind to desmosomes, but with less stability).

Furthermore, a loss of PKP1 expression can also contribute to decrease cell adhesion and to induce metastatic phenotypes in contexts in which the PI3K / AKT pathway is not activated. This scenario is very similar to the one found in β-catenin regulation (Wolf et al., 2013).

PKP1 could also be able to exert a remodeling function modulating the actin organization presumably through the Rho signaling pathway (Neuber et al., 2010) (Wolf et al., 2013). However, although the function of p120 protein and its direct homologs in regulating the actin cytoskeleton via small Rho-GTPases is well established (Panos Z Anastasiadis, 2007) (Dohn, Brown, & Reynolds, 2009)(Ghose, Min, & Lin, 2015) (Keil, Wolf, Huettelmaier, & Hatzfeld, 2007)(Schackmann, Tenhagen, van de Ven, & Derksen, 2013), the PKP1 role remains unknown.

PKP1 AND DISEASES

SKIN HEREDITARY DISEASES

GENETIC ORIGINS

In 1997, the first hereditary disorder of desmosomes was described(McGrath & Mellerio, 2010) and called Ectodermal Dysplasia or Skin Fragility Syndrome (EDSFS) (Orpha Number: 158668; OMIM 604536). This rare autosomal recessive disease, in which patients carry a complete ablation of the PKP1 gene, is classified as a suprabasal form of Epidermolysis Bullosa Simplex.

Pathogenic mutations have been described not only in PKP1 but also in many other desmosomal genes as DSG1, DSG2, DSG4, PG, PKP2, DSP, DSG1, etc. (McGrath & Mellerio, 2010).

The prevalence of the Ectodermal Dysplasia or Skin Fragility Syndrome (EDSFS) is unknown, due to the few existing patients, 13 cases have been described to date (Kashyap, Shanker, & Sharma, 2015), and the variety of mutations they present, mainly in splicing sites (Abdalla & Has, 2014) (McGrath & Mellerio, 2010) (Rietscher et al., 2016)(Sprecher et al., 2004). Furthermore, the disease is frequently associated with significant morbidity, although it does not seem to affect life expectancy.

Finally, those subjects with haploinsufficiency do not seem to show any clinical disorder, evidencing a recessive origin of the disease. Furthermore, milder phenotypes have been found in patients with mutations near to the carboxyl-terminal domain, indicating that PKP1 protein remains at least partially functional (at least partially(Neuber et al., 2010).

SYMPTOMS

Although it is impossible to establish a genotype-phenotype correlation in EDSFS patients because of its very low prevalence, Ectodermal Dysplasia or Skin Fragility Syndrome (EDSFS) symptoms can be classified into three groups:

1. Frequent symptoms: skin fragility, palmoplantar hyperkeratosis with painful cracking of the skin, and chronic cheilitis(McGrath & Mellerio, 2010)(McGrath et al., 1997)

2. Additional manifestations: growth retardation, ectodermal development abnormalities, hypohidrosis, and nail dystrophy and hypotrichosis or alopecia (McGRATH et al., 1999)(McGrath et al., 1997)(Vázquez-Osorio et al., 2017)(Ersoy-Evans et al., 2006).

3. Uncommon symptoms: pruritus, dental caries, recurrent systemic infections, follicular hyperkeratosis, and perianal erythema (Whittock et al., 2000)(Boyce et al., 2012)(Hamada et al., 2002)(Steijlen et al., 2004)(Boyce et al., 2012).

Furthermore, skin biopsies show acanthosis, acantholysis, and a reduced number of compromised desmosomes, underlying the essential role of PKP1 in desmosomal formation and function, mainly in the spinous layer of the epidermis (McGrath & Mellerio, 2010)(Image 5).

Adapted from (McGrath & Mellerio, 2010)

Image 5. Clinical features of EDSFS. The main manifestations include perioral cracking, alopecia or hypotrichosis, and palmoplantar keratoderma, frequently with fissuring.

TREATMENT

Treatment is based on healing and prevention of symptoms, such as blisters formation and infections, since this disease (EDSFS) has no cure. For example, palmoplantar hyperkeratosis treatment includes keratolytics, topical vitamin D lotions, topical or systemic retinoids, etc.

PLAKOPHILINS AND CANCER

Overexpression of Plakophilins 1, 2, and 3 is not consistently observed in different tumor types, although it is a quite common event in cancer(Wolf et al., 2010)(Wolf & Hatzfeld, 2010).
Plakophilins 1, 2, and 3 have a context-dependent role that could depend on the protein phosphorylation status. They play a structural and protective role against cancer in desmosomes but stimulate proliferation in the cytoplasm (and possibly in the nucleus) through releasing or translating components with oncogenic potential, and/or activating signaling pathways involved in tumor development (Dusek & Attardi, 2011)(Wolf et al., 2010) (Wolf & Hatzfeld, 2010).Then, the regulatory mechanisms that control the balanced distribution of Plakophilins 1, 2, and 3 in different cellular compartments may contribute to carcinogenesis (Mechthild Hatzfeld, 2007).

This context-dependent localization suggests that all plakophilins could modulate gene expression in the nucleus, as it has already been demonstrated to PKP2, which can interact with β-catenin and potentiates the endogenous transcriptional activity of β-catenin-LEF / TCF (Dusek & Attardi, 2011).

Furthermore, high levels of PKP3 have been found in several lung adenocarcinoma samples, and it correlated with the stage of the disease, worse prognosis, and poor survival. It suggests that PKP3 may act as an oncogene, and it could be useful in lung cancer as both: prognostic marker and therapeutic target (Furukawa et al., 2005).

Interestingly, recent observations suggest that PKP2 and PKP3 may be involved in epithelial-mesenchymal transition (EMT), which has particular relevance in tumor cells metastasis (Neuber et al., 2010)(Takahashi et al., 2012).

As for the rest of plakophilins, the contribution of PKP1 in cancer may be context-dependent and determined by the status of distinct signaling pathways: while an increment in PKP1 could contribute to cancer progression by increasing the translation and proliferation, the loss of PKP1 would also lead to carcinogenesis and / or metastasis, causing loss-of-contact inhibition and an increase in motility(Wolf et al., 2010) (Wolf et al., 2013) (Wolf & Hatzfeld, 2010) (Image 6).

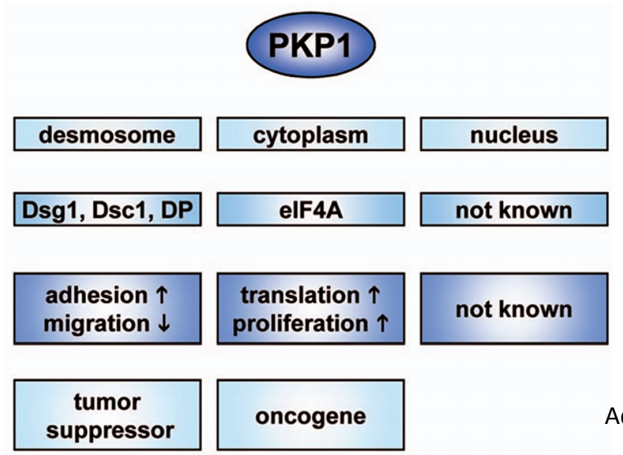

Image 6. Summary of localizations, interaction partners, and functions of Plakophilin 1.

Adapted from (Wolf & Hatzfeld, 2010).

Thus, although PKP1 has been found deregulated in several cancer types, its role in carcinogenesis remains unclear due to contradictory results reported between different studies: upregulation, downregulation, or maintenance levels (Mechthild Hatzfeld, Wolf, & Keil, 2014).

A decrease in PKP1, and also PKP3, gene expression has been correlated with desmosome instability, lower cell adhesion, increase in migration, and worse prognosis in several cancer types. However, overexpression of PKP1 and PKP3 has been detected in different tumors such as head and neck, lung and prostate carcinoma, and Ewing's sarcoma (Wolf & Hatzfeld, 2010).

It is well known that an increase in protein synthesis is essential for cell growth and proliferation, and alterations in this process, which usually occur by mutational activation of key signaling pathways, are also a frequent event in cancer.

Interestingly, the activation of cap-dependent translation is enough to transform fibroblasts into tumor cells in cell culture, and the ectopic expression of eIF4E in transgenic mice increases the incidence of several cancer types as hepatomas, angiosarcomas, lung adenocarcinoma, and

lymphomas. Furthermore, eIF4E has been found highly expressed in head and neck, and breast tumors, correlating with worse patient prognosis (Siddiqui & Sonenberg, 2015).

Whereas most mRNAs have short and poorly structured 5'UTR regions, those proteins which are important for cell growth, cell survival, and cell cycle (or are involved in malignancy), usually show an mRNA with highly structured 5'UTRs (for example, C-MYC, VEGF, survivin, etc.), these mRNAs are poorly translated under normal conditions, and their translation is increased in the presence of high levels of eIF4E. In those tumors in which PKP1 is overexpressed, complex mRNA translation could be enhanced by the role of PKP1 in recruiting eIF4A1 to the translation initiation complex, and in stimulating its helicase activity. Besides, an increase in eIF4E also promotes the nucleus-cytoplasmic transport of mRNAs encoding vital growth-regulating proteins, such as cyclin D1 (Wolf & Hatzfeld, 2010) (Wolf et al., 2010).

C-MYC

THE MYC GENE FAMILY

The MYC gene family is one of the most extensively studied in biology, and it is composed of the protooncogenes C-MYC, N-MYC, and L-MYC.

The C-MYC gene (also called MYC) was firstly identified in the early eighties in the translocated region t (8; 14) (q24; q32) of the Burkitt lymphoma/leukemia (Dalla-Favera et al., 1982). Subsequently, amplified sequences of N-MYC in Neuroblastoma cells, and L-MYC in small cell lung tumors, were discovered due to their homology to V-MYC (viral homolog of C-MYC)(Henriksson & Lüscher, 1996).

The C-MYC gene is located in the chromosomal band 8q24, consists of three exons, and its transcription usually begins in exon II, at an AUG codon, generating a protein of 439 amino acids (64 KDa). Furthermore, there are two alternative start codons which produce two minority protein isoforms: a second AUG codon in exon II, which originates a 339-amino-acids isoform (MYCS), and a CUG codon in exon I, which produces a 454-amino-acids isoform (p67MYC)(Hann, King, Bentley, Anderson, & Eisenman, 1988)(Spotts, Patel, Xiao, & Hann, 1997).

The most abundant isoform of C-MYC (64 KDa) is a transcription factor, which is part of the basic-proteins family with helix-loop-helix motifs and leucine zippers (bHLH-LZ). Moreover, its amino acid sequence presents highly conserved motifs called MYC boxes, and four MYC boxes have been identified so far: MBI, MBII, MBIII, and MBIV, being all of them essential for C-MYC protein activity(Meyer & Penn, 2008).

MBI and II are found at the N-terminus of the protein, and they serve as transactivation domain (TAD) by performing multiple interactions with several interacting partners. In contrast, MBIII and IV are located next to the nuclear localization signal (NLS), which indicates the subcellular localization of the protein. Finally, the C-terminal end contains what is called the basic region (BR), and the bHLH-LZ domains. The latter is the C-MYC binding site with the small bHLHZip protein MAX. This protein-protein interaction generates functional heterodimers with DNA-binding ability at specific DNA sequences in the genome, which are known as E-boxes(Meyer & Penn, 2008) (Image 7).

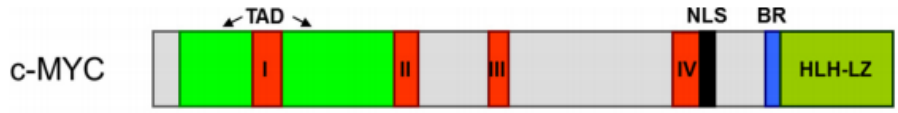

Adapted from (Bachmann & Geerts, 2018)

Image 7. Representation of a mammalian C-MYC protein, indicating the transcriptional activation domain (TAD), the central portion, the canonical nuclear localization sequence (NLS), the basic region (BR), and the region involved in DNA binding via interaction with MAX(HLH-LZ).

BIOLOGICAL FUNCTIONS OF C-MYC

C-MYC protein is considered a member of the protein group so-called "super-transcription factors" since it can regulate the transcription of a large number of protein-coding or non-coding genes (approximately 10-15% of the entire genome).

C-MYC mainly acts as an activator of transcription and cellular processes through the stimulation of the RNA polymerase I, II, and III, but it also can act as a repressor in specific contexts. Although it is well known that some proteins, as histone acetyltransferases (HATs) and transformation/transcription domain-associated protein (TRRAP), are important partners for C-MYC transcriptional function, how C-MYC can regulate transcription remains under discussion. On the one hand*, Lin, C. Y. et al*. suggested that the C-MYC gene can act stimulating only the transcription of active genes without acting on silenced genes (C. Y. Lin et al., 2012). On the other hand, *Sabò et al*. questioned this model and postulated that C-MYC, with the help of other transcription factors, can activate specific genetic signatures(Sabò et al., 2014).

What is entirely sure is that C-MYC acts regulating several cellular processes (cell cycle, metabolism, protein biogenesis, signal transduction, cell adhesion, translation, transcription, among others), which are involved in many biological functions, such as cell growth, proliferation, survival, apoptosis, and differentiation. For example, C-MYC induces the transcription activation of some cell cycle regulatory factors such as Cyclin D1, CDK4 or E2F1, and the inhibition of cyclin-dependent kinase inhibitors (CDKs) as p21, promoting cell cycle progression from the G0 / G1 to the S phase. It can also act stabilizing the proapoptotic p53 protein or indirectly inhibiting antiapoptotic proteins such as BCL2 (Meyer & Penn, 2008). Negative regulation of C-MYC is necessary for cell cycle exit and subsequent differentiation.

Furthermore, C-MYC can influence the regulation of other biological processes such as genomic instability, immune surveillance, and angiogenesis.

In general, C-MYC affects cell cycle regulation, apoptosis, and metabolism positively, whereas it affects cellular differentiation and cell adhesion negatively. Lack of coordination and deregulation of these C-MYC activities presumably contribute to neoplastic phenotypes, which are mainly characterized by deregulated growth, and glycolytic metabolism. For example, an increased apoptotic rate caused by C-MYC may be abrogated by mechanisms acquired in tumor to inhibit apoptosis, such as loss of p53 and p19-Arf or activation of the Bcl-2 family of proteins(Cory & Adams, 2002).

EXPRESSION AND REGULATION OF C-MYC

During embryogenesis, the N-MYC, L-MYC, and C-MYC genes are expressed in several tissues: N-MYC is expressed at low levels in the kidney, intestine, brain, pre-B cells, and other newborn tissues(Zimmerman, Legouy, Stewart, Depinho, & Alt, 1990); L-MYC is expressed in developing lung and Kidney tissues, and in specific compartments of the brain and the neural tube related to differentiation and proliferation processes(Hatton et al., 1996); and the C-MYC gene is expressed mainly in undifferentiated cells with a higher rate of proliferation, while their expression is undetectable in differentiated cells(Hurlin, 2013).

Regarding C-MYC regulation, the formation of C-MYC / MAX heterodimers induces the functional activation of C-MYC (Image 8), triggering the transcriptional regulation of its target genes through interaction with their promoter regions. Interestingly, MAX protein is constitutively expressed, and their C-MYC affinity is greater than by itself, but, in the absence of C-MYC, it forms MAX / MAX homodimers with no transcriptional activity.

The MXD protein family (of which MAD is the main representative) has opposite functions to C-MYC. On the one hand, MAD competes with C-MYC to join MAX, preventing the C-MYC / MAX heterodimers formation. On the other hand, MAX / MAD heterodimers bind specifically to the E-boxes sequences, repressing transcription of the same target genes which are activated by C-MYC / MAX heterodimers(Meyer & Penn, 2008)(Dang, 2012)(Lüscher & Vervoorts, 2012)(Conacci-Sorrell, McFerrin, & Eisenman, 2014).

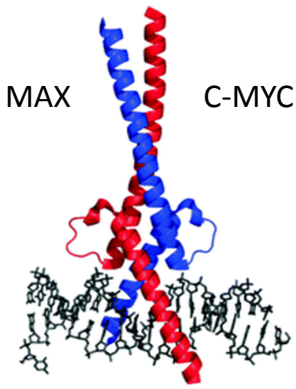

Image 8. Crystal structure of the C-MYC (red) / MAX (blue) heterodimer formation and its interaction with DNA.

Adapted from (Nair & Burley, 2003)

Although there are multiple signaling transduction pathways which lead to rigorously regulate C-MYC transcription (as the repression of C-MYC transcription induced by the interaction of growth factors with specific C-MYC promoter regions), C-MYC expression is also regulated at translational, mRNA stability, protein activation, and degradation levels. Besides, C-MYC has been related to miRNA expression, mitochondrial biogenesis, translation progression, and DNA replication (through non-transcriptional mechanisms). (Meyer & Penn, 2008)(Dang, 2012)(Lüscher & Vervoorts, 2012)(Conacci-Sorrell et al., 2014).

The C-MYC protein contains two crucial amino acids in the MBI, which have an essential role in its stability and activity: a Serine in position 62 (Ser62) and a Threonine in position 58 (Thr58). The phosphorylation of the Ser62 stabilizes and activates C-MYC, whereas the subsequent phosphorylation of the Thr58 induces its ubiquitination and degradation (Hann, 2006) (Conacci-Sorrell et al., 2014). It must also be reminded that the formation of the C-MYC / MAX heterodimers is an essential requirement to activate C-MYC functions, constituting another C-MYC regulation point at the protein level. Furthermore, C-MYC mRNA has a very short half-life, and its interaction with some miRNAs could also play a role in its activity(Jackstadt & Hermeking, 2015).

Finally, it has been described that C-MYC and the eukaryotic initiation factor 4F complex are linked through a feedforward loop that affects the regulation of several cellular processes as cell growth, differentiation, proliferation, and oncogenesis(C.-J. Lin, Malina, & Pelletier, 2009).

C-MYC AND TUMORIGENESIS

It is widely demonstrated that deregulation of C-MYC expression leads to tumorigenicity in a huge variety of tumors as cervical carcinoma, lymphoma, breast cancer, colon cancer, lung cancer, etc. (Kalkat et al., 2017).

Loss of regulation in C-MYC expression occurs by different genetic mechanisms that lead to the transformation of several cell types into neoplastic. The most common alterations include amplification, numerical and structural chromosomal alterations (such as translocation), viral insertion at the promoter region, point mutations (for example, those occurring in upstream signaling pathways that enhance C-MYC stability), and activation of super-enhancers within the C-MYC gene.

Regarding lung cancer, gene overexpression or gene amplification of each member of the MYC family has been documented (C-MYC, L-MYC, N-MYC) (Marion M Nau et al., 1985) (Wong et al., 1986):

On the one hand, around 20% of SCLC tumors contain mutually exclusive genomic amplifications in any MYC family genes, including C-MYC, L-MYC and N-MYC (Peifer et al., 2012) (Sos et al., 2012). C-MYC genomic amplifications have been identified in 6–25% of SCLC primary human tumors (Gazzeri et al., 1991)(George et al., 2015) and in 30–50% of SCLC cell lines (Johnson, Brennan, Ihde, & Gazdar, 1992)(Sos et al., 2012), and N-MYC is also frequently amplified and expressed in this lung cancer subtype (M M Nau et al., 1986). These genomic alterations are associated with poor outcome, tumor progression, and treatment resistance, but how the MYC family members impact these processes remains unknown *in vivo* (Brennan et al., 1991)(Johnson et al., 1987)(Sos et al., 2012).

On the other hand, C-MYC genomic amplification has been detected in 8- 20% of NSCLC with poorest prognosis (Iwakawa et al., 2011) (Seo et al., 2014) (Wolfer & Ramaswamy, 2010) and it is overexpressed in around 70% of this lung tumor subtype (Richardson & Johnson, 1993).

The relevance of C-MYC expression in lung cancer development can be illustrated by the experiments achieved by *Ehrhardt et al*., in which the development of multifocal adenocarcinomas from the alveolar epithelium in transgenic mice were observed after the induction of lung-specific murine C-MYC expression (Ehrhardt et al., 2001).

Finally, it is demonstrated that C-MYC cooperates with other oncogenes as C-RAF in NSCLC metastasis (Rapp et al., 2009), and K-RAS in nonmetastatic NSCLC (Soucek et al., 2008) (FUKAZAWA et al., 2010); and C-MYC amplification in combination with loss of the tumor suppressors TP53 and RB1 are prevalent oncogenic events in Small Cell Lung Cancer (SCLC)(Mollaoglu et al., 2017).

C-MYC TARGETING

C-MYC is recognized as a "most wanted" target for cancer therapy. The studies in transgenic mice models have suggested that regulation of oncogenic C-MYC could induce tumor regression (for example through transient C-MYC inactivation) (Morton & Sansom, 2013), but the development of drugs that directly target C-MYC continues to be a big challenge since it is conditioned by different factors: C-MYC is a transcription factor that affects essential physiological functions for the maintenance of normal tissues; it lacks a defined ligand binding site for small molecules (making very difficult the inhibition of C-MYC activities using strategies similar to those used for kinases); and it is predominantly located in the nucleus (targeting nuclear C-MYC protein pool is technically impractical).

Some preliminary experiments in mice pointed out that the size of C-MYC-overexpressing tumors was markedly reduced after generic ganciclovir treatment in SCLC (Nishino et al., 2001), but, over the years, it has become clear the need to design new strategies to overcome the challenge of identifying a clinical-viable pharmacophore capable of directly target C-MYC. These strategies are based on impairing its transcription, interfering with its mRNA, or reducing C-MYC protein stability and function. The current catalog of inhibitors includes direct and indirect targeting through traditional small molecules and natural chemicals, RNA and antisense technology, and peptides or mini proteins such as the "Omomyc" protein (Whitfield, Beaulieu, & Soucek, 2017).

BACKGROUND AND JUSTIFICATION

SqCLC is a major subtype of Non-small Cell Lung Cancer (NSCLC) and represents around 30% of all lung tumors. SqCLC begins to develop in cells lining the inner wall of the airways (usually near the bronchi) and is more closely related to smoking than other subtypes (Bender, 2014).

In two independent studies using different microarray hybridization technologies, our group has found PKP1 as the most overexpressed gene in SqCLC versus normal lung tissue samples (Angulo et al., 2008)(Sanchez-Palencia et al., 2011). Furthermore, these results have been supported by other researchers (Hou et al., 2010)(Bhattacharjee et al., 2001), who also found significant PKP1 overexpression in SqCLC versus normal tissue.

Desmosomes have been reported to mainly possess tumor suppressor properties by promoting cell-to-cell cohesion and restricting cell mobility (Dusek & Attardi, 2011). However, although our observations appear to contradict the current assumptions about the biological function of PKP1 as a desmosome component, overexpression of desmosomes members in tumoral cells have been shown in several publications, supporting our data and providing evidences for their oncogenic function (Furukawa et al., 2005)(Hakimelahi et al., 2000)(Kolligs et al., 2000). This apparent paradox reflects real context-dependent differences in the contribution of desmosomes to cancer.

In order to gain insight into the specific biological role of PKP1 in lung cancer, a PKP1 mRNA -expression screening was conducted in 14 NSCLC cell lines, and three of them were selected. Western blot results confirmed that PKP1 was expressed at higher levels in the EPLC-272H, at mid-levels in the SK-MES-1, and at undetectable levels in the NCI-H2170 cell lines. They were used as cellular models in subsequent functional and phenotypical experiments, and most of them are described in this Ph.D. work.

On the one hand, loss-of-function studies to assess the possible role of PKP1 in lung cancer cell growth and survival were previously performed in our laboratory in the selected PKP1-expressing SqCLC cell line called SK-MES-1. Results demonstrated that PKP1 knock-down significantly reduced cell viability, cell proliferation and cell colony formation, and enhanced apoptosis. Furthermore, the execution phase of apoptosis was triggered by the proteolytic cleavage of procaspase-3, and a cell cycle arrest in the G0/G1 phase and an increase in the p21 protein levels were detected.

On the other hand, gain-of-function studies were also achieved through the ectopic expression of PKP1 in the selected SqCLC cell line with a lack of PKP1 basal expression, called NCI-H2170. In agreement with the knock-down model, results showed that ectopic expression of PKP1 significantly promoted cell proliferation.

At this point of the research (when this Ph.D. thesis begins), more experiments were necessary to completely characterize the proliferative role of PKP1 and its functional effects on lung cancer regulation. Furthermore, a functional hypothesis that could completely explain the role of PKP1 in sqCLC became essential (taking into account the available contradictory data that supported both a tumor-suppressive role and an oncogenic function). In order to achieve these goals, a PKP1 Knock-out cellular model was developed, as well as an *in vivo* experiment that allowed us to mimic, as accurate as possible, the human sqCLC complexity. Moreover, high-throughput transcriptomics and proteomics analysis were performed in our previously described PKP1 loss-of-function cellular model and the EPLC-272H cell line respectively, helping us to unveil most of the relevant pathways and protein networks that may link PKP1 with cancer development. Importantly, these experiments, and some others included in this Ph.D. thesis, have led to a relevant scientific publication that supports the data presented(Martin-Padron et al., 2019).

OBJECTIVES

In order to shed light on the oncogenic role of PKP1 in SqCLC, the following objectives were proposed:

1. **Develop and characterize, *in vitro* and *in vivo,* specific PKP1 gain/loss functional models:**

1.1. PKP1 overexpression model: functionally and phenotypically characterize a previously developed PKP1 overexpression model in the NCI-H2170 cell line.

1.2. PKP1 Knock-out model: develop, through the Crispr-Cas9 technology, and fully characterize a PKP1 Knock-out model in the SK-MES-1 cell line.

1.3. Xenograft mouse model: stablish a xenograft mouse model that allows elucidating the *in vivo* role of PKP1 in tumor development and cancer invasiveness in SqCLC.

2. **Determine the molecular mechanisms responsible for the oncogenic role of PKP1 in SqCLC:**

2.1. Transcriptomic analysis: accomplish an mRNA microarray analysis to compare differences in gene expression between a previously developed PKP1 knock-down model in the SK-MES-1 cell line and its respective scramble control.

2.2. Proteomic analysis: achieve a cytoplasmic immunoprecipitation of the endogenous PKP1 protein in a selected SqCLC cell line model to obtain a complete landscape of the PKP1 protein partners.

2.3. Analyze and compare the altered pathways and protein networks obtained in objectives 2.1 and 2.2, and identify possible matches which may connect PKP1 functions and/ or interactions with SqCLC development.

3. **Propose and experimentally validate a functional hypothesis that may explain the oncogenic role of PKP1 in SqCLC.**

MATERIAL AND METHODS

CELL CULTURE

The SK-MES-1 and NCI-H2170 SqCLC cell lines, as well as the NIHeT3 mouse-fibroblast cell line, were cultured in DMEM medium supplemented with 10% FCS. The EPLC-272H cell line was cultured in RPMI-1640 medium supplemented with 20% FCS. L-glutamine, antibiotics and antimycotic agents were added to prevent contamination. HEK293T packaging cells, used for the production of lentiviral particles, were cultured in DMEM medium supplemented with 10% FCS and L-glutamine. All cells were maintained at 37ºC in a humid atmosphere with 5% CO2.

TRANSFECTION

24 h before transfection, $2{\cdot}10^5$ - $5{\cdot}10^5$ cells/well were seeded in 6-well plates in an appropriate medium. For 96-well plate format, $5{\cdot}10^3$ – $5.5{\cdot}10^3$ cells/well were seeded. After 24 h, SK-MES-1 cells were transfected with 7.5 nM of a combination of two siRNAs to target PKP1 (Ambion) or one siRNA to target C-MYC (Santa Cruz Biotechnology), using Lipofectamine RNAiMAX reagent. After 72 h of incubation, the cells were processed for further analysis. As a control, Scramble siRNA (Ambion) was used for each experiment. Down-regulation of PKP1 or C-MYC protein expression was confirmed by Real Time-PCR and western blot analysis, as described below.

RNA ISOLATION AND REAL TIME-PCR

Total RNA was isolated from cultured cells using Trizol reagent (Gibco) according to the protocol of the manufacturer. The RNA concentration and purity for each sample were measured with a Nanodrop 2000c Spectrophotometer (Thermo Fisher Scientific), and 1 µg of RNA was reversely transcribed using random primers and the iScript transcriptase kit (BioRad). The reverse transcription products were amplified using the iTaq Universal SYBR Green Supermix kit (BioRad), and an ABI 7500 Real-Time PCR Detection System (Applied Biosystems). All PCR

reactions involved initial denaturation at 95ºC for 30 s followed by 40 cycles at 95°C for 15 s and 60°C for 60 s.

The following specific primers (Sigma) were used for PCR:

Gene	Primer name	Sequence
PKP1	PKP1_forward	5'-TCAGCAACAAGAGCGACAAG-3'
	PKP1_reverse	5'-TCAGGTAGGTGCGGATGG-3'
TBP	TBP_forward	5'-CACGCCAGCTTCGGAGAGT-3'
	TBP_reverse	5'-GGCACGAAGTGCAATGGTCC-3'
GAPDH	GAPDH_forward	5'-GAAGGTGAAGGTCGGAGTC-3'
	GAPDH_reverse	5'-GAAGATGGTGATGGGATTTC-3'
C-MYC	C-MYC_forward	5'-CCACCAGCAGCGACTCTGAG-3'
	C-MYC_reverse	5'-CCAGCAGAAGGTGATCCAGAC-3'

Each experiment was performed in triplicate. Gene expression was calculated using the 2-ΔΔCt method, and TBP or GAPDH expression was used as housekeeping.

WESTERN BLOT

Cells lysates were prepared in RIPA buffer (150 mM NaCl, 1% NP-40, 0.5% sodium deoxycholate, 0.1% SDS and 50 mM Tris-HCl pH 7.5) containing protease and phosphatase inhibitors (0.2 mM PMSF, 7 mM OV4 and cOmplete Mini EDTA-free Protease Inhibitor Cocktail Tablets (Roche)). Protein concentration was determined using Bradford reagent (Amresco) with BSA as a standard. 25 µg of total proteins were subjected to 10-12% SDS-PAGE gels. The resolved samples were transferred onto PVDF membranes and blocked for 1 h in PBS containing 3% non-fat dry milk and 0.1% Tween. Then, they were incubated overnight at 4°C with primary antibodies (PKP1, Sigma, 1:250; C-MYC, Cell Signaling, 1:1000; PABP, Thermo, 1:1000; β-Actin, Sigma, 1:5000; GAPDH, Sigma, 1:1000), and then secondary antibodies (anti-rabbit HRP, Dako, 1:2000;

anti-mouse HRP, Dako, 1:1000; anti-goat HRP, Dako, 1:2000) at room temperature for 1 h. The IQ Las 4000 (GE Healthcare) chemiluminescence Western blotting analysis system was used. β-Actin or GAPDH were used as internal controls. Bands quantification was carried out by the Plot Lanes tool of ImageJ v1.49c software.

STRIPPING FOR REPROBING

In order to remove primary and secondary antibodies from the Western blot membranes and investigate more than one protein on the same blot, a harsh stripping protocol was performed. Membranes were incubated at 50°C for up to 45 minutes with agitation in a prewarmed stripping buffer (100 ml stock: 20 ml SDS 10%, 12.5 ml Tris-HCl pH 6.8 0.5M, 67.5 ml ultra-pure water, 0.8 ml β-mercaptoethanol). Then, membranes were washed under running water tap for 1 minute and in TBST for 5 minutes. After that, the membranes were ready for the blocking stage.

CLONOGENIC ASSAY

$5 \cdot 10^2$ cells/well were plated in 6-well plates and maintained in complete culture medium for 21 days at 37 °C in the presence of 5% CO2. Colonies were fixed by covering them with a fixative solution containing 2% formaldehyde and 0.2% glutaraldehyde in PBS for 1 h at room temperature. Then, the cells were washed in water and stained with 0.1% crystal violet for 10 minutes at room temperature. All experiments were performed in triplicate.

Quantitative data of the different samples, conditions, and replicates were automatically acquired through measuring the fluorescence emission of those crystal-violet-positively-stained colonies. The Li-Cor Odyssey 9120 Imaging System on the “700 channel” position (Laser Source: Solid-state diode laser at 685 nm) was used for that purpose. Output data were statistically treated in order to get the corresponding p-values.

NIH 3T3 FOCUS FORMATION

The NIH 3T3 murine cells were transduced with a previously developed version of the pLVX-IRES-ZsGreen1 plasmid (Clontech) containing the open reading frame (ORF) of PKP1a (pLVX-PKP1a-IRES-ZsGreen1), as well as with the empty vector (control plasmid). Then, they were sorted to guarantee around 100% of green cells. Positive cells were seeded in a six-well plate at 80% confluence and allowed to grow for 30 days. After that, crystal violet staining and colony quantification were performed by eye following standard procedures. All experiments were done in triplicate.

CELL PROLIFERATION

Resazurin assays were carried out to evaluate cell proliferation. 20 µL of filtered resazurin solution (0.15 mg/ml) (Sigma) was added to each well in order to treat previously seeded cells (96-well plates in suitable confluence and a final volume of 100 µl/well). Cells were incubated at 37 °C in darkness, and a humid atmosphere with 5% CO2 for 4 h. 30 µL of 3% SDS was added to each well. Then, cells were incubated again in the same conditions for 15 minutes, followed by 5 minutes of shaking. Finally, the fluorescence of each well was recorded using a GloMax microplate reader (Promega) with a 560 nm excitation / 590 nm emission filter set. As controls, blank wells (without cells) were used for each experiment. Assays were performed in triplicate.

ANALYSIS OF APOPTOSIS

Apoptosis was evaluated using the FITC Annexin-V Apoptosis Detection Kit I (BD, 556547). Treated cells in 6-well plates at 60 % confluence were harvested using trypsin and washed with cold PBS. Then, pellets were processed following the procedure provided. Finally, samples were examined by flow cytometry using a BD FACSCanto II (BD Biosciences). Each assay was performed in triplicate, acquiring a minimum of 10,000 events per sample.

ECTOPIC EXPRESSION OF PKP1 IN NCI-H2170 SQUAMOUS CELL LINE

The previously described plasmid pLVX-PKP1a-IRES-ZsGreen1 and a version of the pLVX-AcGFP1-N1 vector (Clontech) in which the AcGFP1 sequence was substituted by a PKP1a-EGFP fusion sequence (pLVX-PKP1a-EGFP-N1), as well as their empty vectors, were used in order to ectopically express PKP1a or PKP1a-EGFP fusion proteins respectively.

PKP1a or PKP1a-EGFP-expressing stable transfectants were established according to standard protocols. Lentiviral particles were obtained by transient cotransfection of HEK293T cells using the LipoD293 (SignaGen) reagent. The following plasmids were used in a 2:1:3 ratio: packaging construct psPAX.2 (Addgene), VSV-G plasmid encoding the envelope (Addgene), and second-generation pLVX-PKP1a-IRES-ZsGreen1 or pLVX-PKP1a-EGFP-N1 (or their empty vectors (Clontech)). Supernatants were harvested 48 and 72 h after transfection, clarified by 0.45-µm filtration, and stored at −80 °C.

NCI-H2170 cells at 80% confluence were infected with three transduction cycles in the presence of polybrene (8 mg/ml) in order to obtain stable transfectants. Then, they were analyzed by flow cytometry using a BD FACSCanto II (BD Biosciences), sorted when appropriate using a BD FACSAria (BD bioscience) and subjected to further experiments.

CRISPR-CAS9 GENOME EDITING

One guide RNA was designed for each first three exons of PKP1 gene using the online tool http://crispr.mit.edu/ and cloned into the plasmid pSpCas9(BB)-2A-Puro (Addgene) following a previously described protocol (Ran et al., 2013).

Correct plasmid constructions were transfected into the HEK293T cell line in a 6-well plate at 80% confluence. Transfected cells were enriched by puromycin treatment. In order to test the cut efficiency of the guide RNAs, cell genomic DNA (DNAzol™, Thermo Fisher Scientific) was extracted, amplicons of around 200 bp (that contained the targeted guide RNA sequence) were obtained by PCR, and a surveyor assay (Surveyor Mutation Detection Kit, IDT) was performed.

Designed Guide RNAs (Sigma):

Gene	Exon	sgRNA name	Sequence
PKP1	1	PKP1_sgRNA-1	5´-ACCCTGAGCCACTCCAATCG-3´
	2	PKP1_sgRNA-2	5´-CCTCTAGGTTCCATGTATGA-3´,
	3	PKP1_sgRNA-3	5´- CGACCTCTACTGTGACCCAC-3´

The following specific primers (Sigma) were used for PCR:

Gene	Exon	Primers name	Sequence
PKP1	1	surveyor_Exon1_FW	5´-GTGCCAGAGAGGGACGAAC-3´
		surveyor_Exon1_RV	5´-TAGGTGCGTAGACCCTGCC-3´;
	2	surveyor_Exon2_FW	5´-TGGGAATGTCGGAATCCTGC-3´
		surveyor_Exon2_RV	5´-GGTGCCGGTTTTCTCCACTA-3´
	3	surveyor_Exon3_FW	5´-ATGGCTCAGGTTCCTTCCAC-3´
		surveyor_Exon3_RV	5´-GCAGTCAGGCTAAGGGTGTG-3´

The selected plasmid was transfected into the SK-MES-1 cell line in a 6-well plate, and transfected cells were enriched by puromycin treatment. Genomic DNA of half of the 6-well plate cells was extracted, and the other half cells were kept growing. Genomic DNA was tested using the surveyor assay in order to ensure the guide RNA efficiency. Finally, puromycin-free clonal expansion was carried out with the cells which were kept in culture in order to isolate individual cells and expand them until obtaining a stable cell culture in a 6-well plate. Correct PKP1 knock-out at the genome level was checked by Sanger sequencing for each clone, and the positive-edited ones were analyzed by western blot to confirm PKP1 absence at the protein level.

SCRATCH ASSAY

Cells were cultured on a 6-well plate until 90% confluence, in monolayers, and in the appropriate medium. They were maintained at 37ºC in a humid atmosphere with 5% CO2 for 24 h. After that, cells were refreshed with a restricted medium containing 1% FCS, and wounds were created using a yellow pipette tip. Three wounds were made for each well, and cells were maintained 24 h under described incubation conditions. Each assay was performed in triplicate. Wound healing area was photographed in a phase-contrast inverted microscope (5X objective) with high-quality image capture system, Axiovert 40CFL (Zeiss) model and AxioVision software (Zeiss), and measured by the ImageJ v1.49c software applying the plugin 'MRI Wound Healing Tool' at zero time and after 24 h post wound generation.

MONITORING OF MICE TUMOUR DEVELOPMENT BY IVIS

Mouse models were generated and housed in the animal facility provided by the University of Granada. Animal work was covered under protocol 17/07/2017/095, which was approved by the Institutional Animal Care and Use Committee of the University of Granada.

Twenty 8-week-old NSG immunodeficient male mice were separated into two groups (Treatment and Control) and injected through the tail vein with SK-MES-1 PKP1 knock-out clone 1 cells (Cas9 knock-out 1) or SK-MES-1 clonal cells with an empty cassette for the sgRNA (Cas9 Control) respectively.

Experimental and control cells were previously transduced with luciferase (pUltra-chili-luc, Addgene). Equivalent transfection efficiency was determined by flow cytometry using the dTomato reporter, and *in vivo* tumor evolution was tracked thanks to firefly luciferase expression.

In order to determine the optimal number of cells to be injected in mice, a decreasing number of cells ranging from 10^6 to 10^3 were seeded in a 96-well plate in 200 µL of PBS per well, and 100 µL of a 300 µg/ml dilution of luciferin in PBS was added. The image was taken in the imaging *in vivo* IVIS SPECTRUM system (Caliper Life Sciences, 68 Elm Street Hopkinton, MA 01748, USA) in the "automatic" position.

Experimental and control groups (ten mice each) were tail-vein injected with 0.2 million cells per 100 µL resuspended in PBS. Previously, mice were sedated with isoflurane, and the tail was warmed.

Tumor cell distribution and tumor evolution were followed by *in vivo* luminescence using the previous described "IVIS SPECTRUM system" at days: 0, 1, 4, 9, 15, and 24. For that purpose, each group was injected intraperitoneally with luciferin (3 mg / 100 µL for mice weighing 20 grams), and images were taken 3 minutes later.

On day 24, the two mice groups were sacrificed, their organs were extracted, and their luminescence was measured ex vivo. Finally, all organs were macroscopically analyzed under a magnifying glass and preserved in 4% formaldehyde for further experiments.

HEMATOXYLIN-EOSIN STAINING AND DETECTION OF SPECIFIC HUMAN CELLS MARKERS

In order to detect human-derived tumor masses under the optical microscope, lungs extracted from mice injected with PKP1 knock-out clone 1 or with control cells were fixed in 4% formaldehyde and histologically processed for hematoxylin-eosin staining and inmunocytochemistry analyses against human cytokeratin (DAKO) and human Ki67 antibodies (DAKO). All these procedures were performed using standard protocols from Atrys Health S.A.

TRANSCRIPTOME PROFILING

Three SK-MES-1 siPKP1 biological replicates and three siSC were prepared for transcriptome profiling. Total RNA was extracted using the mirVana commercial kit (Thermo Fisher Scientific). The biotinylated cRNA was hybridized against the HumanHT-12 v4 Expression BeadChip array (Illumina) following the standard Illumina protocols. Finally, samples were randomized before hybridization.

STATISTICAL ANALYSES OF MICROARRAY DATA

Raw data from gene expression microarray were exported from the Illumina GenomeStudio software and analyzed using R (version 3.2.3) with the 'limma' and 'RankProd' packages from Bioconductor (https://www.bioconductor.org). Firstly, we performed quality control on raw data, which included checking internal microarray controls, signal/noise ratio, and proportion of expressed probes according to *Shi et al., 2010*(Shi, de Graaf, et al., 2010). After corroborating that raw data from all samples passed first quality control, background correction was performed using a normal-exponential convolution model (Shi, Oshlack, & Smyth, 2010). Data were then quantile normalized (including controls), and log2-transformed. Finally, internal microarray controls were removed.

Probes that did not have a detection p-value < 0.05 in at least one sample were discarded. The median log2-transformed intensity was calculated for each gene within each sample. At this stage, a clustering analysis (using the Ward method), pairwise correlation plots, and a principal component analysis were performed. This second quality check led to the identification of two aberrant samples (one siPKP1 and one siSC), which were excluded from further analyses. Finally, the differential expression of each gene was assessed using the RankProducts method (Breitling, Armengaud, Amtmann, & Herzyk, 2004). The differential expression was considered statistically and biologically significant if FDR < 0.05 and fold change > 1.5 (up or down).

FUNCTIONAL ANALYSES OF THE MICROARRAY DATA

Gene Set Enrichment Analysis (GSEA; http://software.broadinstitute.org/gsea) was used to analyze enriched pathways and biological functions among the differentially expressed genes. The full set of genes with their log2-transformed relative expression was included for each comparison. All gene set databases but C7 (immunological signatures) were checked. Gene sets with fewer than 3 or more than 500 members were excluded. One thousand permutations were performed. Gene sets with FDR < 0.25 and p < 0.05 were considered significant.

LUCIFERASE ASSAY

C-MYC 5'UTR was cloned between the promoter and Renilla luciferase open reading frame in the psiCHECK™-2 vector (Promega). Conventional enzymatic-restriction cloning strategy with NheI enzyme was followed. C-MYC 5'UTR was amplified from genomic DNA, and NheI restriction sites were included in the sequence of the primers. FireFly luciferase expression in the same bicistronic plasmid was used to normalize transfection. All experiments were performed in triplicate (Representation 1).

Gene	Primer name	Sequence
C-MYC	FW_C-MYC_5UTR_NHEI	5'-ATATATGCTAGCGACCCCCGAGCTGTGCTG-3'
	RV_C-MYC_5UTR_NHEI	5'-ATATATGCTAGCCGTCTAAGCAGCTGCAAGGAG-3'

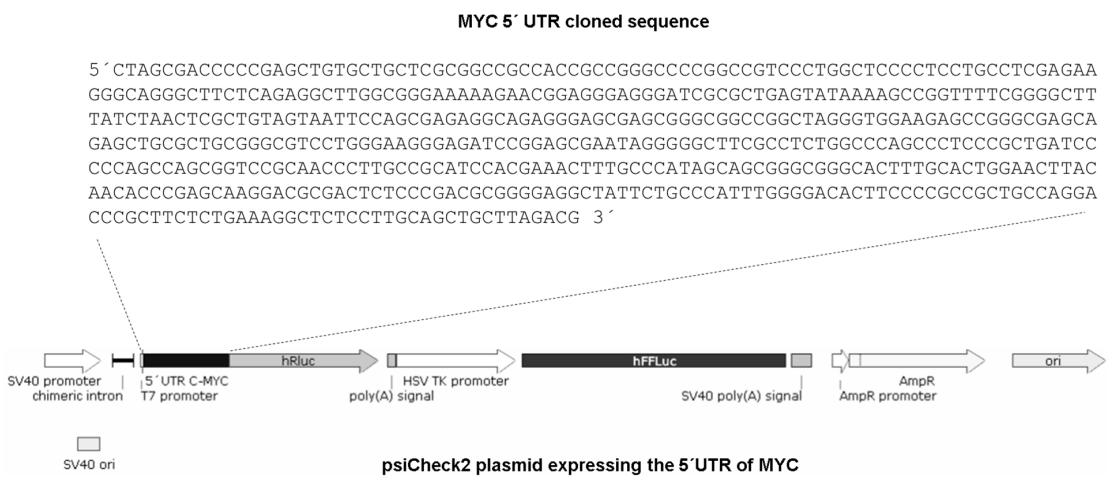

Representation 1. C-MYC 5´UTR cloned sequence in the psiCheck2 plasmid. The 5´UTR of C-MYC is just cloned upstream of the Renilla luciferase gene, conditioning Renilla expression. FireFly luciferase expression is controlled by HSV TK promoter, and FireFly luciferase luminescence is used as normalizer. Legend: SV40 promoter, simian vacuolating virus 40 promoter; SV40 ori, simian vacuolating virus 40 replicational origin; T7 promoter, T7 bacteriophage promoter; 5´UTR C-MYC, 5´UTR sequence of the C-MYC gene ; hRluc, Renilla luciferase gene ; poly(A) signal, polyadenylation signal ; HSV TK promoter, Herpes Simplex Virus (HSV) thymidine kinase promoter.; hFFLuc, FireFly luciferase gene; SV40 poly(A) signal, simian vacuolating virus 40 late polyadenylation signal; AmpR promoter, Ampicillin resistance promoter ; AmpR, Ampicillin resistance gene ; Ori, bacterial replication origin.

PKP1 promoter was cloned upstream the Renilla luciferase gene in the psiCHECK™-2 vector (Promega). Conventional enzymatic-restriction cloning strategy with BglII and NheI enzymes was followed. PKP1 promoter was amplified from genomic DNA through primers including BglII and NheI restriction sites. Firefly luciferase expression in the same bicistronic plasmid was used to normalize the transfection. All experiments were performed in triplicate (Representation 2).

Gene	Primer name	Sequence
PKP1	BglII_FW_PKP1_PROM	5'-ATATATAGATCTTGAGAAACCCAGGGCATCAAG-3'
	RV_PKP1_PROM_NHEI	5'-ATATATGCTAGCGGTGGCGGGAGGCGGGTG-3'

Wildtype PKP1 promoter sequence

5´TGAGAAACCCAGGGCATCAAGAAGTACAGCAAATATGTTCAGTGTTGTTTGCTTTAGGAGGCAAACAGAATGCGATACCTTTTAGAAAGATTTCCATCAAA
GTAAATACTTAAAAAAAAAAAAAAAACACTCAGCTCCTGTTACACACCAAATTCACTGATGTGGGCTCCCTCCACGCCTGGAGAGGATGCTACATGAATAAAGC
TTCACTGCACATGTGTCCCCAGGGGTGAGTGTATATAGGGGAATGCACACAGTGGTCCCAGAATAATAAGTCCAGAGTGAAATTTCAGGGTAAAGCAGCTTTT
CAATTTTTCAGTGAGGATCTGGTTAGGATCCGAGTTAGATTTAATTTACCTTAAATTAACTAGCATTCACGTATTCACCTATTTAAAATATTTTTTATTAAGC
GCCTAATATTATGTGTGCCAGGCATTGTTTTAGAGGTTATAGTGGAGTTTCAGAGAGGATCCGCTGTTCACGTGGTGTTTTACCGGGGTATACTCATGAACAA
CAAATAACCACCGGTTTTACCAAGGCATACCCACTGTGTGGTCTGATATCCCAAGTCTGCTCCTTGATGTGGCCTTACTGCCCCTACCCCACTTTCTTCAGAG
GAAGCTCCTTTAGAGTAGACTGGGTTACCCCCATAAGATGGAGCACTCCTTTGGAGCAAGAGCTATGGTTCTGCCATCAGCCCGGGAGCCTCCACCGCCGGGG
TTGGTCTCTGCTATGACCTCAGTACAGAGGGAGATGGACGCCTGGCTCTCCTGGGCAGCCTGGTCAAGAAAGACTCCTTTCTTTCCTAGAGAGAGGTCTCCCT
CGGTTCCTGAGCTGAGCACATGCTTTCTCAGTGAGCCGGCAGAACAGGACAGAGGGGCGTCTCCCTGGGGCCTCAAGGCTTGCGACGTTTCTTGCTCATGGGG
AGAGGGAAGGGAGAGAAAAAAAAAGAGCGAGCAGGAAGGCGCCCAGCGTCCCACACAGGGGACTCGCAGCCCTGCCCCCAAGAGCGCTGGCTCCGCAGCAGCAG
TGCCCTGCAGCTCCGCGTCTGAGCAGCAGCAGCGCGCGGCCCGGTGGAGTGGGTGGTGCAGGGCAGGGGTGGTATATCCTGTCTGACGGAGGGCGGGCCTCGC
CAGTGCCAGAGAGGGACGAACCAGGGTGGAAGCGCCAGGAGCAGCTGCAGGGAGCCCTCACGCGGACCACGCACTCTATGGCCGTAGGGAGCCGCTGAGAGCG
AGAAGAGCACGCTCCTGCCCGCCCGCTGCACCGCACCTCGCCTCGCCTCTCTGCTCTCCTAGGCCCCGGCCGCGCGCCACCCGCCTCCCGCCACC-3´

psiCheck2 plasmid with wildtype PKP1 promoter sequence

Representation 2. Wild-type PKP1 promoter cloned sequence in the psiCheck2 plasmid. PKP1 promoter was just cloned upstream of the Renilla luciferase gene, conditioning Renilla expression. FireFly luciferase expression is controlled by HSV TK promoter, and FireFly luciferase luminescence is used as normalizer. Legend: PKP1 promoter, wild-type Plakophilin 1 promoter; hRluc, Renilla luciferase gene; poly(A) signal, polyadenylation signal; HSV TK promoter, Herpes Simplex Virus (HSV) thymidine kinase promoter.; hFFLuc, FireFly luciferase gene; SV40 poly(A) signal, simian vacuolating virus 40 late polyadenylation signal; AmpR promoter, Ampicillin resistance promoter; AmpR, Ampicillin resistance gene; Ori, bacterial replication origin.

In both experiments, luciferase luminescence was determined using the Dual-Glo Luciferase Assay System (Promega) and following the provided protocol.

SITE-DIRECTED MUTAGENESIS OF THE PKP1 PROMOTER

PKP1 promoter sequence was cloned upstream of the Renilla luciferase gene in the psiCHECK™-2 vector through conventional enzymatic-restriction cloning strategy with BglII and NheI enzymes, and it was used as PCR template for mutagenesis proposes in the PKP1 promoter.

C-MYC-MAX interacting sites present in the sequence of the PKP1 promoter were predicted by the "MATinspertor" online tool as "MYC-MAX binding sites" and "MYC/MAX heterodimers."

Site-directed mutagenesis was performed by PCR concatenation and using primers with mutations in the C-MYC-MAX interacting site sequences previously detected. Resulting PKP1 mutated promoter was also cloned upstream of the Renilla luciferase gene in the psiCHECK™-2 vector (Promega) through the same strategy used for the previously described PKP1 promoter cloning.

Firefly luciferase expression in the same bicistronic plasmid was used to normalize transfection. Finally, luciferase luminescence was determined using the Dual-Glo Luciferase Assay System (Promega) and following the provided protocol. All experiments were performed in triplicate (Representation 3).

Shared primers used for the PKP1-wild-type and PKP1-mutated promoter cloning in the psiCHECK™-2 vector, and primers with mutations in the C-MYC-MAX interacting site sequences for the generation of the mutated PKP1 promoter are listed below:

Gene	Cloning step	Primer name	Sequence
PKP1	Shared cloning primer	BglII_FW_PKP1_PROM	ATATATAGATCTTGAGAAACCCAGGGCATCAAG
		RV_PKP1_PROM_NHEI	ATATATGCTAGCGGTGGCGGGAGGCGGGTG

Gene	Cloning step	Primer name	Sequence
PKP1	PKP1 promoter Mut 1	Fw-promPKP1-mut-up	5´-GAATAAAGCTTCACTGTCTAGAT GTCCCCAGGGGTG-3´
		Rv-promPKP1-mut1-up	5´-CACCCCTGGGGACATCTAGACAG TGAAGCTTTATTC-3´
		Fw-promPKP1-mut1-Dn	5´-GGTTCCTGAGCTGAGTCTAGACTT TCTCAGTGAGC-3´
		Rv-promPKP1-mut1-Dn	5´-GCTCACTGAGAAAGTCTAGACTCA GCTCAGGAACC-3´
	PKP1 promoter Mut 2	Rv-promPKP1-mut2-Dn	5´-ATATATGCTAGCGGTGGCGGGAG GCGGGTGGTCTAGA GCCGGGGC-3´

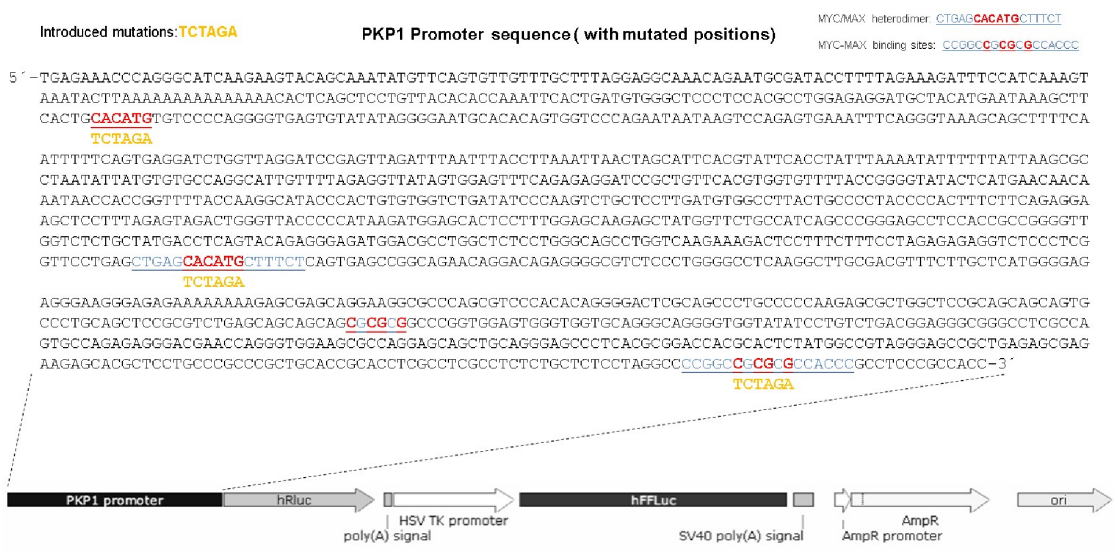

psiCheck2 plasmid with wildtype and mutated PKP1 promoter sequence

Representation 3. Mutated and wild-type PKP1 promoter cloned sequences in the psiCheck2 plasmid. One or another PKP1 promoter variant was just cloned upstream of the Renilla luciferase gene, conditioning Renilla expression. FireFly luciferase expression is controlled by HSV TK promoter, and FireFly luciferase luminescence is used as normalizer. “MYC/MAX heterodimer” recognition sites and “MYC-MAX binding sites” obtained through the "MATinspertor" online tool are provided. In red, the essential recognition sequences. Accessory sequences are in blue. Legend: PKP1 promoter, Plakophilin 1 wild-type or mutated promoter; hRluc, Renilla luciferase gene; poly(A) signal, polyadenylation signal; HSV TK promoter, Herpes Simplex Virus (HSV) thymidine kinase promoter.; hFFLuc, FireFly luciferase gene; SV40 poly(A) signal, simian vacuolating virus 40 late polyadenylation signal; AmpR promoter, Ampicillin resistance promoter; AmpR, Ampicillin resistance gene; Ori, bacterial replication origin.

CO-IMMUNOPRECIPITATION

Immunoprecipitation was performed following a previously described protocol (Munoz et al., 2014) with slight modifications. Nuclear and cytosolic fractions of EPCL-272H cells were collected by scraping, washing with PBS, and pelleting by centrifugation. The pellet was resuspended by gentle pipetting in ice-cold lysis buffer (20 mM HEPES, pH 7.9; 10 mM KCl; 0.2 mM EDTA; protease inhibitors). The cells were allowed to swell for 15 minutes on ice, followed by the addition of NP-40. Nuclei were collected by centrifugation at 200×g for 10 minutes. Nuclei were resuspended in ice-cold buffer (20 mM HEPES pH 7.9; 400 mM NaCl; 10 mM EDTA; 1 mM EGTA; protease inhibitor) and were rocked at 4ºC for 1 hour before centrifugation at 16,100×g (microfuge maximum speed) at 4ºC for 10 minutes.

Cytoplasmic and nuclear extracts were transferred to a new tube and incubated with mouse IgG antibody and Dynabeads Protein G (Novex by Life Technologies) for 1 hour at 4ºC.

The supernatant was incubated with the precipitating anti-PKP1 antibody (Thermo Fisher Scientific) overnight at 4ºC. The next day, the beads were added and incubated during 2 h.

Beads were washed 3X with cold wash buffer (20 mM HEPES pH 7.9; 150-250 mM NaCl; 10 mM EDTA; 1 mM EGTA; 0.5% Triton-X100; 0.1% SDS; protease inhibitor). The final bead pellet was suspended in 25 µL of 3X SDS sample buffer, and the entire sample was loaded. Immunoblotting was carried out following standard protocols.

The Proteomics Facility in the Research Support Central Service at the University of Cordoba (Spain) cleaned-up, digested, separated by UPLC chromatography, and analyzed on a Thermo

Orbitrap Fusion (Q-OT-qIT, Thermo Fisher Scientific) the samples, following standardized protocols.

CO-IMMUNOPRECIPITATION DATA ANALYSIS:

Raw data were processed by the Proteomics Facility in the Research Support Central Service at the University of Cordoba (Spain) using the Proteome Discoverer software (version 2.1.0.81, Thermo Fisher Scientific). MS2 spectra were searched with the SEQUEST engine against different databases (www.uniprot.org). Peptide spectral matches (PSM) were validated using percolator based on q-values at a 1% FDR. With Proteome Discoverer, peptide identifications were grouped into proteins according to the law of parsimony and filtered to 1% FDR.

In our laboratory, the processed lists of immunoprecipitated proteins (PKP1 immunoprecipitation and negative control) were filtered, so only those proteins with at least two unique peptides were retained. Afterward, proteins that were present in the negative control were removed. Finally, proteins which were exclusively nuclear according to GeneOntology (as classified by PANTHER v12.0) but were present in the cytoplasmic list (or vice versa), were excluded. The lists of filtered proteins were analyzed using the functional clustering analysis tool in DAVID 6.8 (https://david.ncifcrf.gov/).

RNA IMMUNOPRECIPITATION (RIP):

RNA immunoprecipitation was performed in the EPLC-272H cell line in duplicate using the Magna RIP Kit (Merk-Millipore) as described in the supplied “Detailed protocol.” Samples were immunoprecipitated using a PKP1 antibody. One RIP reaction (one immunoprecipitation using one antibody) required 100 µL of cell lysate from $2 \cdot 10^7$ cells. Total RNA extraction was performed using TRIzol reagent (Invitrogen). The obtained RNA was converted to cDNA through random primers and used as a template for qPCR. The C-MYC mRNA, cDNA converted, was amplified using the C-MYC primers described below, obtaining a specific amplicon of 115bp:

Gene	Primer name	Sequence
C-MYC	C-MYC_forward	5'-CCACCAGCAGCGACTCTGAG-3'
	C-MYC_reverse	5'-CCAGCAGAAGGTGATCCAGAC-3'

IgG antibody (Life Technologies) was used as a negative control to perform RNA immunoprecipitation. cDNA was also obtained, and C-MYC mRNA, cDNA converted, was amplified by qPCR using the previously indicated C-MYC primers.

Anti-SNRNP70 rabbit polyclonal antibody provided by the Kit was used as a positive control to perform RNA immunoprecipitation. cDNA was obtained and U1 RNA, cDNA converted, was specifically amplified by qPCR using following U1 snRNA primers:

Gene	Primer name	Sequence
SNRNP70	U1_forward	5'-GGGAGATACCATGATCACGAAGGT-3'
	U1_reverse	5'-CCACAAATTATGCAGTCGAGTTTCCC-3'

IMMUNOFLUORESCENCE:

$5*10^4$ cells / well were seeded on 12mm covers and placed in a 24-well plate previously UV sterilized. After 24 hours, cells were fixed with paraformaldehyde (PFA) 4% in 1X PBS for 7 min at room temperature and permeabilized using 0.5% Triton X-100 in 1X PBS for 5 min. The blocking step was performed with 3% BSA in PBS at room temperature for 1 h. The primary antibody was incubated in a humid chamber at 4ºC overnight. The secondary antibody was incubated following the same procedure, and at room temperature for 1 h. The incubation antibody steps were repeated as many times as proteins we wanted to label. Preparations were incubated with a 1:5000 DAPI dilution from a 1ug/ul stock for 5min, placed on microscope slides with mounting medium (Invitrogen ref S36938), and dried at room temperature.

	Name	Dilution	Reference
Primary antibody	PKP1	1:150	Sigma, HPA027221
	Alpha-Tubulin	1:100	Santa Cruz, sc-23948
Secondary antibody	Anti-rabbit ALEXA 488	1:500	Fisher, A-21206
	Anti-mouse ALEXA 555	1:500	Fisher, A-31570
	Anti-rabbit ALEXA 647	1:500	Fisher, A-21244

ANALYSIS OF GLOBAL PROTEIN SYNTHESIS (RIBOPUROMYCYLATION):

De novo-synthesized proteins were quantified by measuring the incorporation of puromycin on native peptide chains. Equal numbers of either treated SK-MES-1 or control cells were incubated with 27 µm/well of puromycin (Sigma-Aldrich, P7255) for 10 minutes in completed DMEM and then 91µM/well of Emetine (Sigma-Aldrich, E2375) was added to the cultures for 5 minutes. Untreated cells incubated without puromycin and just with Emetine were used as negative controls, whereas untreated cells incubated with puromycin and with puromycin and Emetine were used as positives controls. Puromycin incorporation was visualized by western blot, using a specific antibody anti-puromycin (dilution 1:10000) Merck, MABE343) and following standard procedures. Results were quantified by densitometry through the ImageJ software using GAPDH intensity as normalizer (Sigma, Catalog #PLA0302). Three independent experiments were performed.

POLYSOME FRACTIONATION TO ANALYZE RIBOSOMES GLOBAL ACTIVITY:

Ribosomes global activity was quantified by analyzing changes in the polysome profiles. Treated SK-MES-1 and control cells were seeded to reach a maximum of 90% confluence on the day of analysis (1.5 × 106 cells/ treatment). The negative control was treated with Na arsenite (500 µM, 30 minutes) (Sigma, S7400), and untreated cells were included as a positive control. Before lysis, 100 µg/ml cycloheximide (Sigma-Aldrich, C7698) was added to cells for 5 min, and cells were

washed with cold PBS containing 100 µg/ml cycloheximide. Cells were harvested by scraping and lysed in 0.3 ml lysis buffer containing 15 mM Tris, pH 7.4, 15 mM MgCl2, 300 mM NaCl, 1% Triton X-100, 100 µg/ml cycloheximide, 500 µg/ml heparin, 0.2 U/ml RNasin (Promega, N2111), 0.1% 2-mercaptoethanol, and EDTA-free protease inhibitor (Roche, 11873580001). Lysates were cleared by centrifugation at 10,000 rpm for 10 min at 4°C. Supernatants were loaded onto linear gradients of 17.5–50% sucrose in 15 mM Tris, pH 7.4, 15 mM MgCl2, and 300 mM NaCl and centrifuged in a SW60 rotor at 35,000 rpm for 2 h at 4°C. Fractions were eluted from the top of the gradient using a Teledyne Isco (Lincoln, NE) gradient elution system and the polysome profiles were obtained by measuring absorbance at 254 nm. The recorded curves were aligned, and the area under the curve of polysomal ribosomes was calculated and divided by the area of monosomal ribosomes to quantify the rate of active translation. Three independent experiments were performed.

B-GALACTOSIDASE ASSAYS (CHROMOGENIC ASSAY):

Subconfluent PKP1 knock-out and control cells were seeded in p6-well plates and incubated with the fixating solution (2% formaldehyde (vol/vol) and 0.2% glutaraldehyde (vol/vol)) in PBS for 5 min at room temperature. The stained step was performed overnight (12–16 h) at 37 °C (Co2 free) with fresh staining solution (40 mM citric acid/Na phosphate buffer, 5 mM K4 [Fe (CN)6] 3H2 O, 5 mM K3 [Fe (CN)6], 150 mM sodium chloride, 2 mM magnesium chloride and 1 mg ml−1 X-gal in distilled water). The final wash was performed with methanol. Dried dishes were analyzed by bright field or phase-contrast microscopy. All experiments were performed in triplicate.

ABERRANT CELLS COUNTING:

PKP1 knock-out and control immunostaining preparations (labeling DNA with DAPI and alpha-tubulin and PKP1 proteins with specific antibodies) were prepared as previously described. Three slides for each condition were counted (a total of approximately 200 cells for each cell cycle phase). Cells were classified as “normal cell” or “aberrant cell,” according to cell division abnormalities detected by visual criteria, and divided against the total number of cells for each

cell cycle phase in order to obtain a ratio. Finally, the previous calculated aberrant ratios were divided against the normal ratios for each cell cycle phase in order to obtain a ratio fold change.

PROPIDIUM IODIDE (PI) POLYNUCLEATED CELLS ESTIMATION BY FLOW CYTOMETRY:

PKP1 knock-out and control cell cultures were counted in order to obtain 0.5*1 x10^6 cells/ml. Cell preparations were fixed with 70% EtOH (precooled to -20ºC) for 18 hours at -20ºC. Finally, 15µg of propidium iodide (PI) fresh solution (1mg /ml PI (Sigma), and 1mg / ml RNAse A (ThermoFisher) in PBS 1x) was added and incubated in darkness for 30 min at room temperature. Polynucleated cell estimations were calculated by flow cytometry. All experiments were performed in triplicate.

STATISTICAL ANALYSES:

Results are expressed as mean ± S.D. and represent at least two experiments. Statistical differences were analyzed using paired, two-tailed t-tests. Significance was considered when $p < 0.05$.

RESULTS

NCI-H2170 SQCLC CELL LINE ECTOPICALLY EXPRESSING PKP1

CHECKING PKP1 SUBCELLULAR LOCALIZATION:

Ectopic PKP1 levels had been successfully expressed previously in our lab in the NCI-H2170 SqCLC cell line, which was selected for its reported lack of PKP1 expression (Furukawa et al., 2005). As previously described, the PKP1a sequence was cloned into two different lentiviral vectors: pLVX-IRES-ZsGreen1 and pLVX-AcGFP1-N1 (Clontech). Our version of the first plasmid expresses the wild type PKP1a protein, whereas a PKP1a-EGFP fusion protein version was cloned into the second plasmid.

Although PKP1 expression level after transduction had been already tested by qPCR and western blot, subcellular localization of the ectopically expressed PKP1 pool remained unknown. In order to shed light on this question, NCI-H2170 cells were transduced with the plasmids mentioned above and corresponding empty vector. PKP1-EGFP expressing and control cells were subjected to immunofluorescence, labeling tubulin (in red) and nuclei (DAPI in blue). The same labeling was performed for wild-type-expressing and control cells and including PKP1 (in Cyan). (Figure 1 and Figure 2 respectively).

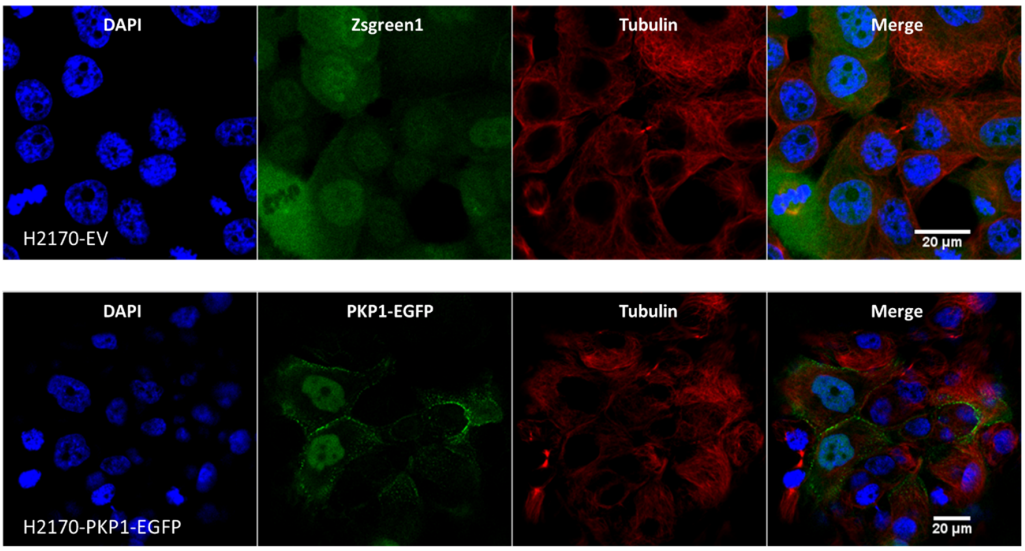

Figure 1. Immunofluorescence of NCI-H2170 control cells (H2170-EV) and NCI-H2170 cells ectopically expressing PKP1 fused to EGFP(H2170-PKP1-EGFP). Scale: 20um; DAPI, 4′,6-Diamidino-2-phenylindole nuclear marker; EGFR, Enhanced Green Fluorescent Protein; Tubulin, anti-tubulin protein antibody; Merge, channels merge. H2170-EV, NCI-H2170 cell line transduced with pLVX-IRES-ZsGreen1 empty vector; H2170-PKP1-EGFP, NCI-H2170 cell line transduced with pLVX-PKP1A isoform fused with EGFR vector.

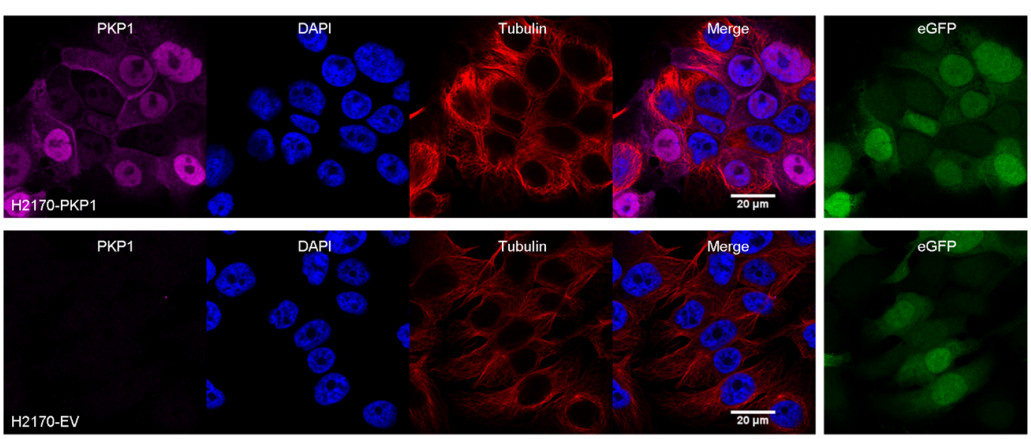

Figure 2. Immunofluorescence of NCI-H2170 control cells and NCI-H2170 cells ectopically expressing PKP1. In both preparations, eGFP signal represents transduction efficiency. In H2170-PKP1cells, PKP1 protein pools go to the cell membrane, nucleus, and cytoplasm. More detailed research is required in order to complete the picture about how these three PKP1 pools contribute, together or by separate, to the phenotype observed. Scale: 20um; PKP1, anti- Plakophilin 1 protein antibody; DAPI, 4′,6-Diamidino-2-phenylindole nuclear marker; Tubulin, anti-tubulin protein antibody; Merge, channels merge; eGFR, Enhanced Green Fluorescent Protein; H2170-EV, NCI-H2170 cell line transduced with pLVX-IRES-ZsGreen1 empty vector; H2170-PKP1, NCI-H2170 cell line transduced with pLVX-PKP1a-IRES-ZsGreen1 vector.

Results demonstrate that PKP1 protein expression in these models follows the expected physiological distribution (protein pools are located in desmosomes, cytoplasm, and nucleus). These findings validated the models and gave credibility and physiological rigor to the subsequent results.

PHENOTYPICAL ASSAYS AND CHARACTERIZATION:

Promotion of cell proliferation induced by ectopic expression of PKP1 in the NCI-H2170 cell line had been previously reported in our group by measuring cell viability through the MTT (3-(4,5-Dimethylthiazol-2-yl)-2,5-Diphenyltetrazolium Bromide) reagent. In this work, we have also confirmed this proliferation promotion (60% increase) using resazurin (p = 0.0005) (Figure 3).

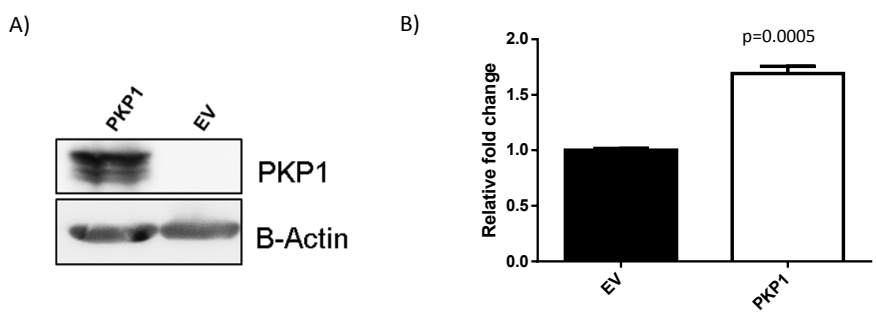

Figure 3. A) Western blot showing ectopic expression of PKP1 in NCI-H2170 SqCLC cell line after pLVX-IRES-ZsGreen1-PKP1A plasmid transduction. B) Relative cell proliferation assay showed a significantly 60% increase in the PKP1 ectopically expressed model (p = 0.0005) at 72h.EV, pLVX-IRES-ZsGreen1 empty vector; PKP1, pLVX-IRES-ZsGreen1-PKP1A isoform; PKP1, Plakophilin 1protein antibody; B-Actin; B-Actin protein antibody.

Furthermore, many other assays were achieved in order to characterize the effects on the phenotype induced by the ectopic expression of PKP1. Enhanced size and number in colony formation was demonstrated (p= 0.0015) (Figure 4A), and, interestingly, Annexin-V assays have revealed a significantly increased percentage of viable cells (97% of total cells) (p = 0.0022) and a significantly reduced percentage of early apoptotic (1% of total cells) (p = 0.0005) and late apoptotic(1.5% of total cells) (p = 0.0144) cells (Figure 4B).

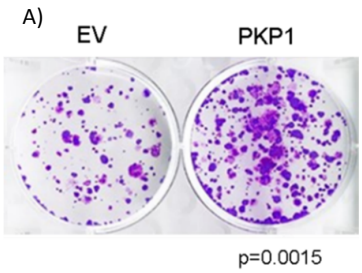

Figure 4. A) Clonogenic assay at 3 weeks revealed an increase in the number and size of colonies after PKP1 ectopic expression; three biological replicates were performed. B) Graphic representation of Annexin-V assay at 72 h after PKP1 ectopic expression, showing a significantly increased percentage of viable cells (p = 0.0022) (Q3) and significantly decreased percentage of early apoptotic (p = 0.0005) (Q4) and late apoptotic (p = 0.0144) (Q2) cells. EV, pLVX-IRES-ZsGreen1 empty vector; PKP1, pLVX-IRES-ZsGreen1-PKP1A isoform; Annexin-V PE-A, Annexin-V linked to R-phycoerythrin;7-AAD-PerCP-Cy 5-5-A, 7-aminoactinomycin D stain; Q1, cell death; Q2, late apoptosis; Q3, living cells; Q4, early apoptosis.

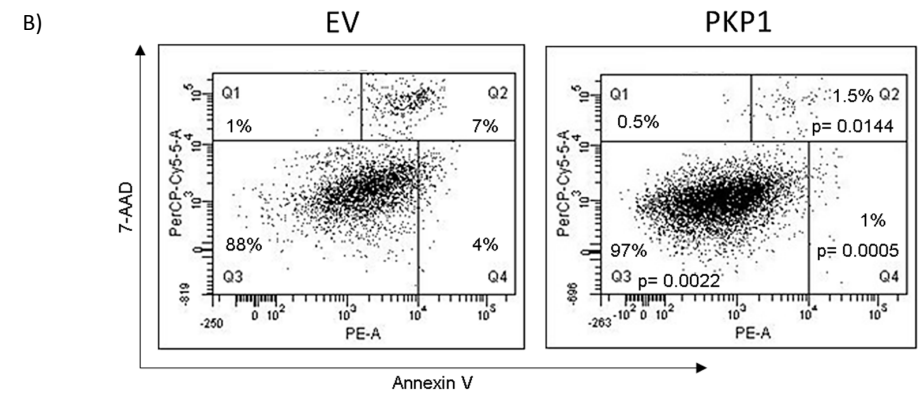

Although more detailed research is required in order to increase our knowledge about the relative importance of each PKP1 pool, our data suggest that PKP1 ectopic expression induce a tumoral phenotype in the NCI-H2170 cell line through enhancing cell proliferation and colony formation and inhibiting apoptosis.

PKP1 ECTOPIC EXPRESSION ON NIH 3T3 MURINE FIBROBLASTS:

In order to confirm the oncogenic effect of PKP1 overexpression, focus formation assays were developed in the NIH 3T3 murine fibroblast cell line. NIH 3T3 cells, which typically grow in monolayer, induce foci formation (that can be stained by crystal violet to be quantified) under an oncogenic signal. These kind of studies have been essential to determine the oncogenicity of important oncogenes like RAS (Clark, Cox, Graham, & Der, 1995). Interestingly, our results show a significant increment in focus formation caused by PKP1 ectopic expression (p = 0.0200) confirming, also in this cellular model, its oncogenic role (Figure 5).

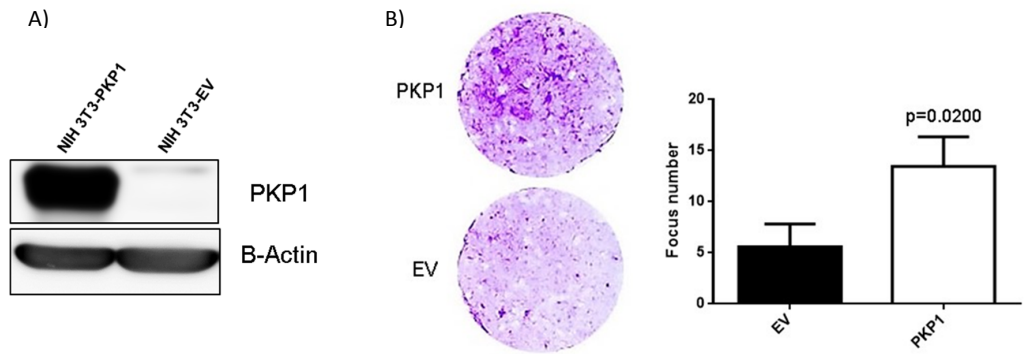

Figure 5. A) Western blot showing PKP1 protein overexpression in the NIH 3T3 cell line. B) Murine fibroblast NIH 3T3 cell line focus assay at 30 days, revealing a significant increase (p = 0.0200) in the number and size of colonies after PKP1ectopic expression; three biological replicates were performed.

IMPROVING PKP1 INHIBITION MODEL

CHARACTERIZATION OF PKP1 CRISPR-CAS9-EDITED CLONES:

Cell proliferation, cell-colony formation, and apoptosis assays in a PKP1 knock-down model had been previously performed in our laboratory. These loss-of-function studies were achieved in the SK-MES-1 cell line (a PKP1-expressing SqCLC cell line whose selection was based on a previous report (Furukawa et al., 2005)). According to that results, PKP1 inhibition significantly affected cell growth and cell proliferation and promoted apoptosis in SK-MES-1.

Nevertheless, we decided to go deeper into the functional role of PKP1 in SqCLC and explore a more extreme phenotype. For this purpose, we achieved the development of a PKP1 knock-out cellular model through the CRISPR-Cas9 technology in the SK-MES-1 cell line.

PKP1 EXPRESSION AND SUBCELLULAR LOCALIZATION

Two positives clones (Cas9 Knock-out 1 and Cas9 Knock-out 2) with no PKP1 expression were detected by western blot (Figure 6A). They were obtained after inducing genetic alterations through a sgRNA designed at exon 3 of the PKP1 gene. Furthermore, a control clone (Cas9 Control), which expresses PKP1, was generated following the same protocol but using an empty vector. PKP1 protein presence/absence and its distribution into cells were also checked by immunofluorescence in both Cas9 Control and Cas9 Knock-out 1 cells (Figure 6B).

A)

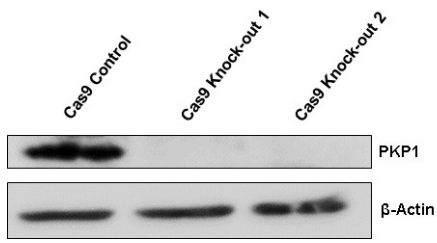

B)

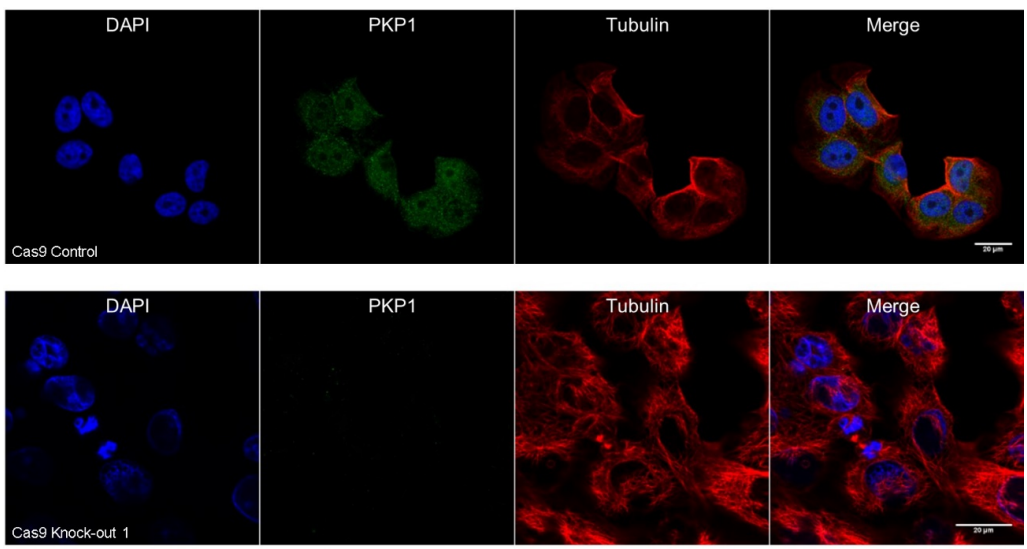

Figure 6. A) Western blot assay showed no PKP1 wild-type expression after targeting with the CRISPR-Cas9 technology. B) Immunofluorescence of Cas9 Control and Cas9 Knock-out 1cells. In Cas9 Control preparation, PKP1 is present in desmosomes, cytoplasm, and nucleus; whereas, in Cas9 Knock-out preparation, the PKP1 signal is removed. Scale: 20um; DAPI, 4′,6-Diamidino-2-phenylindole nuclear marker; PKP1, anti-PKP1 protein antibody; Tubulin, anti-tubulin protein antibody; Merge, channels merge. Cas9 Control, pspcas9(bb)-2a-puro empty vector-treated SK-MES-1 clonal cell line; Cas9 Knock-out 1, pspcas9(bb)-2a-puro sgRNA against PKP1 exon 3 treated SK-MES-1 clonal cell line 1; Cas9 Knock-out 2, pspcas9(bb)-2a-puro sgRNA against PKP1 exon 3 treated SK-MES-1 clonal cell line 2.B-Actin, anti-B-actin protein antibody.

CHARACTERIZATION OF PKP1 CRISPR-CAS9-EDITED AND CONTROL CLONES AT THE GENOMIC AND PROTEIN LEVELS

The control and PKP1 knock-out clones were meticulously analyzed in order to characterize their genomic mutations and the effects in the protein sequence:

Sanger sequencing unveiled two bi-allelic clonal cell lines: PKP1 knock-out clone 1, with homozygous deletions of nucleotide “C”; and PKP1 knock-out clone 2, with deletion of nucleotide “C” in one allele and deletion of ten nucleotides “ACGGGGCACC” in the other (Figure 7A). As mentioned before, these genetic alterations were all located at the nucleotides targeted by the PKP1 sgRNA designed at exon 3. Furthermore, the “ExPASy translate “tool demonstrated that these mutations produced translational frameshift and a premature stop codon (Figure 7B).

A)

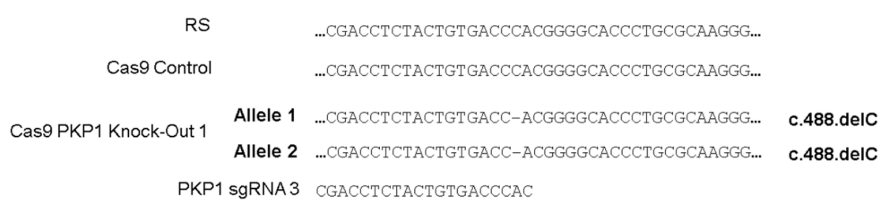

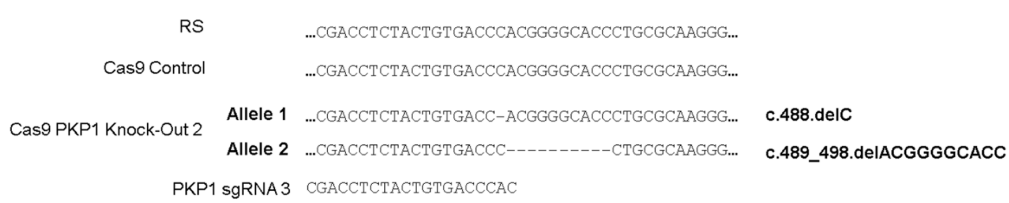

B)

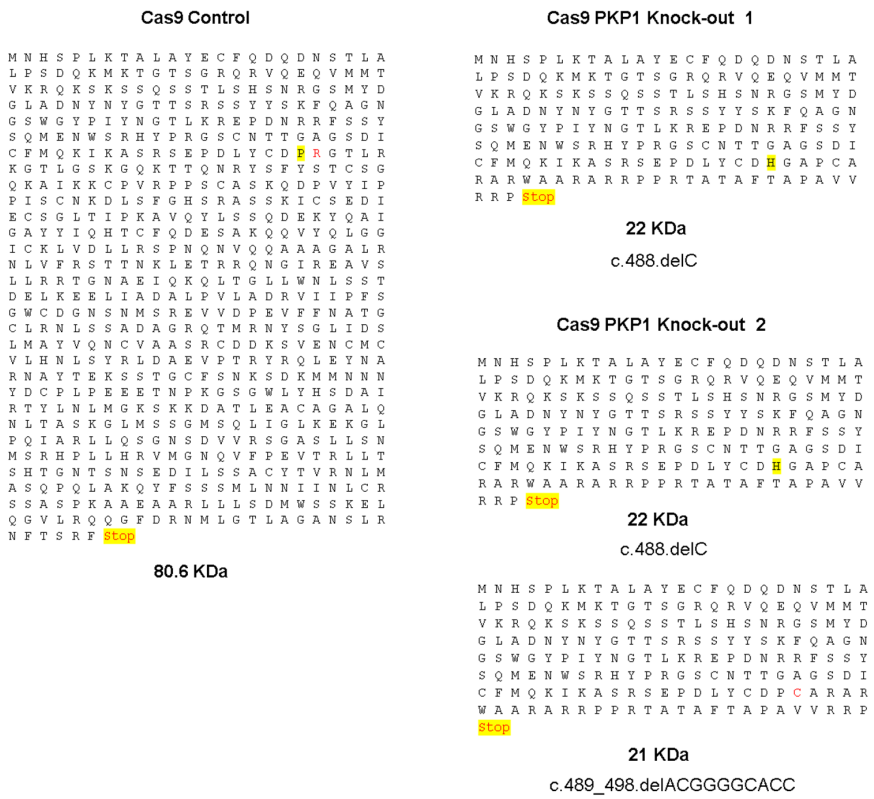

Figure 7. A) Homozygous deletion of the nucleotide "C" in functional knock-out clone 1 and deletion of nucleotide "C" in one allele and deletion of ten nucleotides "ACGGGGCACC" in the other in functional knock-out clone 2 of the SK-MES-1 cell line. B) Control and theoretical PKP1 protein sizes of knock-out and control clones after genetic alterations induced by the PKP1 sgRNA designed at exon 3. RS, genomic referent sequence; Cas9 Knock-out 1, pspcas9(bb)-2a-puro sgRNA against PKP1 exon 3 treated SK-MES-1 clonal cell line 1; Cas9 Control, pspcas9(bb)-2a-puro empty vector-treated SK-MES-1 clonal cell line; PKP1 sgRNA3, guide RNA for Cas9 nuclease against PKP1 exon 3; c.488.delC, "C" nucleotide deletion in 488 coding sequence position. Cas9 Knock-out 2, pspcas9(bb)-2a-puro sgRNA against PKP1 exon 3 treated SK-MES-1 clonal cell line 2; c.489_498.delACGGGGCACC; "ACGGGGCACC" nucleotides deletion between 489 and 498 coding sequence positions; KDa, Kilodaltons.

PKP1 KNOCK-OUT MODELS AND THEIR EFFECTS IN CELL FATE AND BEHAVIOUR

DETECTION OF SENESCENT CELLS

Once the PKP1 Knock-out and control clones were successfully established as cell lines in culture, a high number of senescence-like cells were detected by phase-contrast microscopy at different magnifications in the PKP1 knock-out cultures, compared to control, after several culture rounds. In order to corroborate these observations, B-galactosidase staining experiments were performed, and senescent-like cell quantifications in the resulted phase-contrast images confirmed the significantly increased senescence process in Knock-out 1 ($p= 0.0257$) and Knock-out 2 ($p=0.0111$) clones compare to the control (Figure 8).

A)

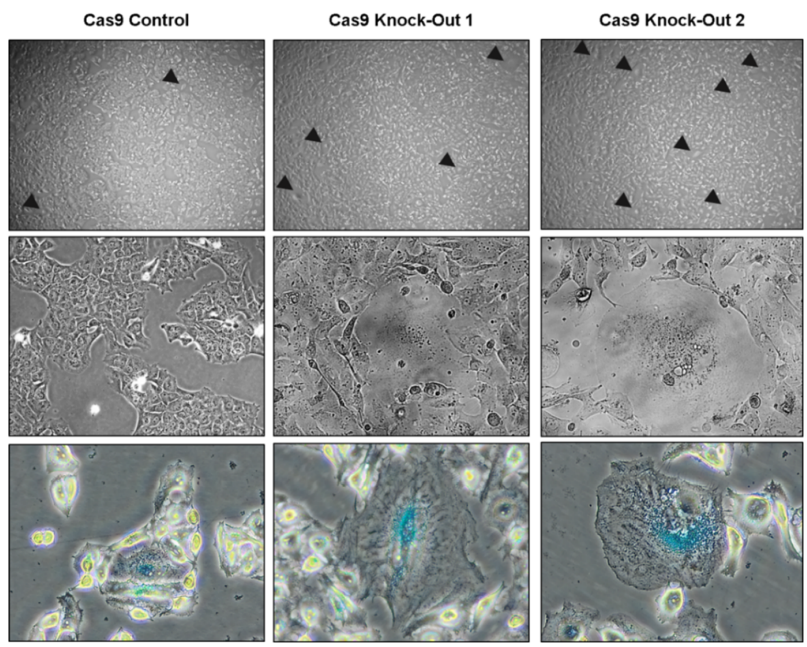

B)

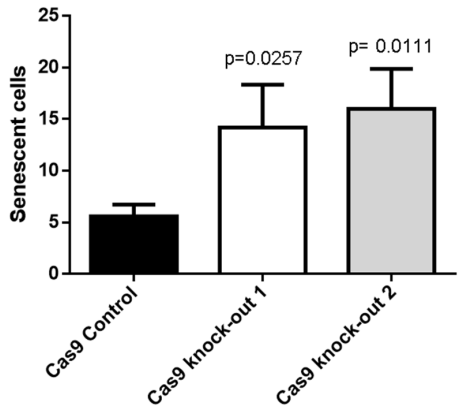

Figure 8. PKP1 depletion increases the number of b-galactosidase-positive senescent-like cells. a) Typical phase-contrast images of senescent-like cells at different magnifications (top and middle pictures) and b-galactosidase phase-contrast images confirming the senescence process (bottom pictures). b) Senescent-like cell quantifications. Cas9 knock-out 1 (p=0.0257) and Cas9 knock-out 2 (p=0.0111) clones significantly presented more senescent-like cells than the Cas9 control clone. Cas9 Control, pspcas9(bb)-2a-puro empty vector-treated SK-MES-1 clonal cell line; Cas9 Knock-out 1, pspcas9(bb)-2a-puro sgRNA against PKP1 exon 3 treated SK-MES-1 clonal cell line 1; Cas9 Knock-out 2, pspcas9(bb)-2a-puro sgRNA against PKP1 exon 3 treated SK-MES-1 clonal cell line 2.

DETECTION OF CELL CYCLE ABERRATIONS:

Another prominent phenotype was detected after several culture rounds of the PKP1 knock-out clones compared to the control: immunostaining revealed cell division aberrations all over the mitosis process. In Cas9 Control cells, tubulin staining, in red, shows proper centrosome maturation and spindle assembly, whereas DAPI staining, in blue, highlights correct chromosome alignment and subsequent segregation. Nevertheless, in Cas9 knock-out 1, tubulin and DAPI staining show defects in all mitotic phases, ranging from abnormal multipolar spindles (prophase and metaphase panels) to chromosome misalignments, segregation errors and lagging chromosomes (anaphase panel), and failed cytokinesis (bottom panel). (Figure 9A) This phenotype was also confirmed by quantifications of aberrant cells in each mitosis phase, suggesting an accumulative process from prophase to cytokinesis (Figure 9B).

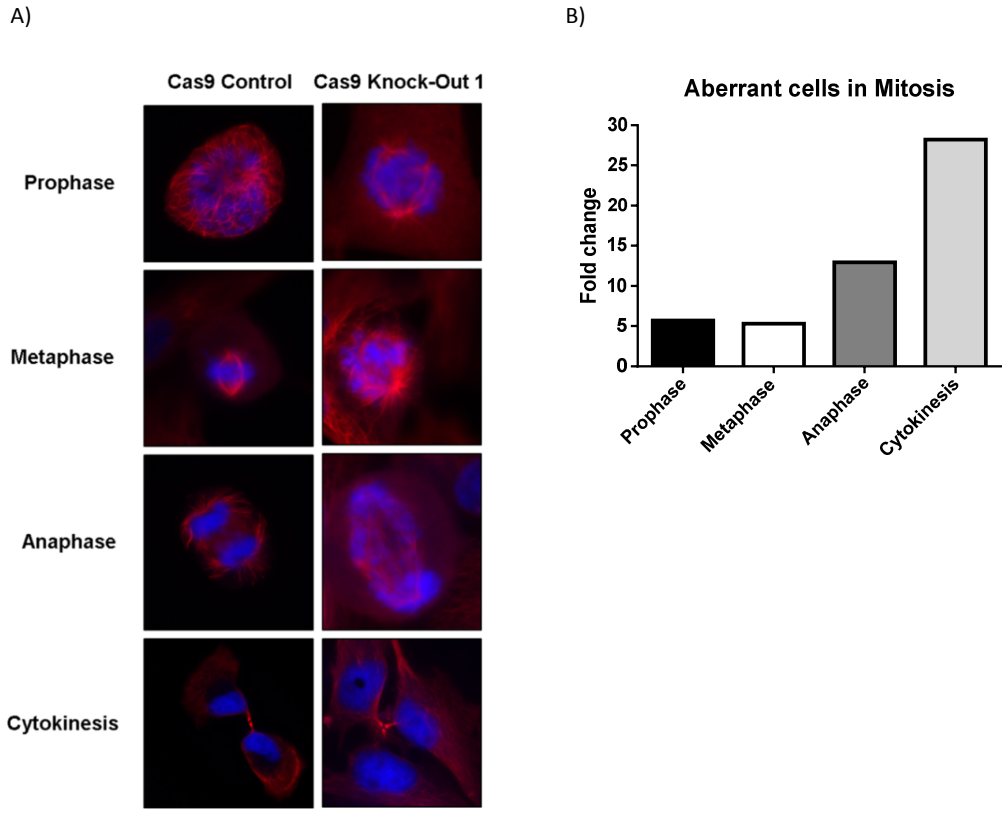

Figure 9. A) Comparison between normal mitosis phases in Cas9 Control cells and aberrant mitosis in Cas9 knock-out cells. In Cas9 Control, tubulin staining, in red, shows proper centrosome maturation and spindle assembly, whereas DAPI staining, in blue, highlights correct chromosome alignment and subsequent segregation. Nevertheless, in Cas9 knock-out, tubulin and DAPI staining show defects in all mitotic phases, ranging from abnormal multipolar spindles (prophase and metaphase panels) to chromosome misalignments, segregation errors and lagging chromosomes (anaphase panels), and finally failed cytokinesis (bottom panel). b) Aberrant cell-counting in the different mitosis phases. Fold change of aberrant cells in the different mitosis phases revealed an increment of aberrant cells in Cas9 Knock-out. It became more evident in the final phases of cell division, suggesting an accumulative process from prophase to cytokinesis. Cas9 Control, pspcas9(bb)-2a-puro empty vector-treated SK-MES-1 clonal cell line; Cas9 Knock-out 1, pspcas9(bb)-2a-puro sgRNA against PKP1 exon 3 treated SK-MES-1 clonal cell line 1.

Furthermore, immunostaining also revealed multinucleated cells in the Cas9 knock-out 1 clone. Propidium iodide (PI) staining and subsequent polynuclear cells counting by cell cytometry after 8 culture rounds showed that Cas9 knock-out 1 cultures significantly exhibited more polynuclear cells than controls (p=0,0142) (Figure 10).

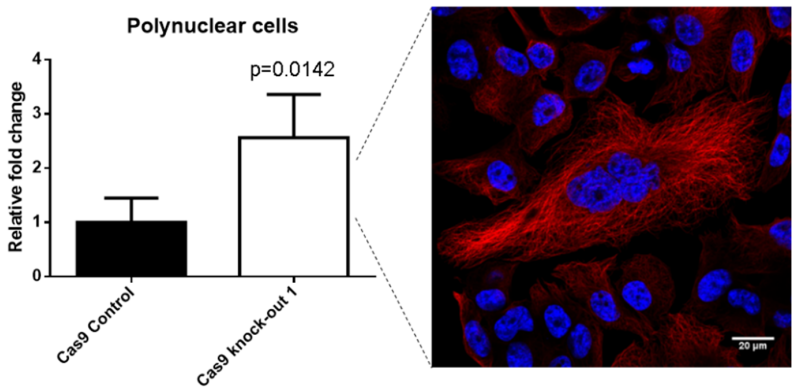

Figure 10. Cas9 knock-out 1 significantly exhibited more polynuclear cells than Cas9 Control cells (p=0,0142) after Propidium iodide (PI) staining and polynuclear cell counting by cell cytometry after 8 culture rounds. A representative image of a multinucleated Cas9 knock-out cell is presented: tubulin staining (in red) shows that all nuclei (DAPI staining in blue) belong to the same cell. Cas9 Control, pspcas9(bb)-2a-puro empty vector-treated SK-MES-1 clonal cell line; Cas9 Knock-out 1, pspcas9(bb)-2a-puro sgRNA against PKP1 exon 3 treated SK-MES-1 clonal cell line 1.

TESTING THE ONCOGENIC PHENOTYPE *IN VITRO*

PROLIFERATION AND COLONY FORMATION

One of the main reasons to develop the PKP1 Knock-out model was trying to improve the depletion in the oncogenic phenotype we had observed previously through siRNA technology in our laboratory (a combination of two siRNAs against PKP1 had been used). Experimental results confirmed the success of this new model: cell proliferation assay showed a 50% relative reduction in cell proliferation in the Cas9 knock-out 1 and 2 cultures ($p = 0.0001$) versus controls at 72 h (Figure 11A). Furthermore, clonogenic assay in the Cas9 knock-out 1($p=0.0096$) and 2 ($p=0.0026$) clones at 3 weeks showed a significant reduction in the number and size of colonies versus controls (Figure 11B).

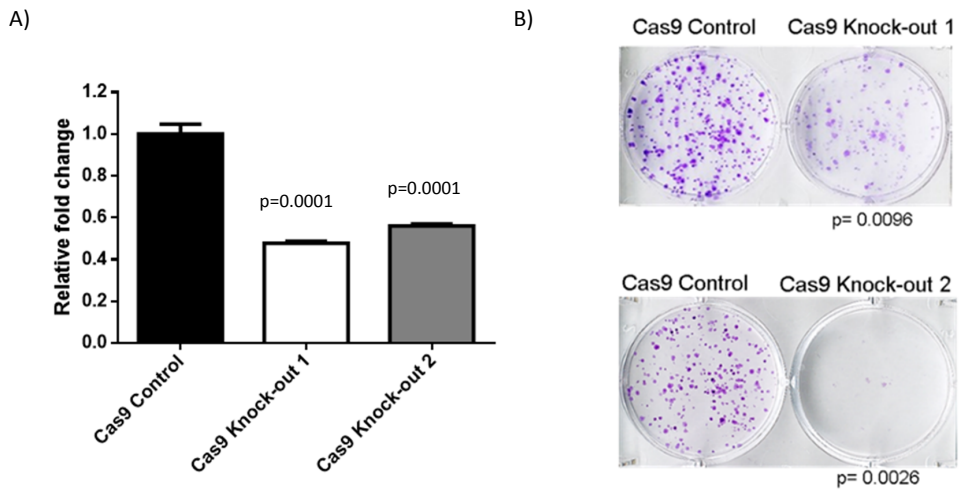

Figure 11. A) Cell proliferation was depleted in PKP1 knock-out 1(p=0.0001) and 2(p=0.0001) in comparison to the control. B) Colony formation showed a reduction in PKP1 knock-out 1(p=0.0096) and 2(p=0.0026) clones in comparison to the control; three biological replicates were performed. Cas9 Control, pspcas9(bb)-2a-puro empty vector-treated SK-MES-1 clonal cell line; Cas9 Knock-out 1, pspcas9(bb)-2a-puro sgRNA against PKP1 exon 3 treated SK-MES-1 clonal cell line 1; Cas9 Knock-out 2, pspcas9(bb)-2a-puro sgRNA against PKP1 exon 3 treated SK-MES-1 clonal cell line 2.

SUCCESSFUL RESCUE OF THE OBSERVED REDUCTION IN THE PROLIFERATION PHENOTYPE

A rescue experiment was achieved in order to discard off-target effects in the phenotype displayed by the PKP1 knock-out clones (Figure 12). PKP1 ectopic expression in the Cas9 Knock-out 1 clone significantly increases the proliferation when it is compared to the Cas9 knock-out 1 clone transduced with the empty vector (p=0.0303). However, no significant differences are observed between neither the Cas9 Knock-out 1 clone ectopically expressing PKP1 and the Cas9 Control clone transduced with the empty vector (p= 0.0810), or between the Cas9 Control clone ectopically expressing PKP1 and right this one transduced with the empty vector (p=0.3143).

In conclusion, this experiment demonstrated that PKP1 reconstitution is enough to significantly rescue the proliferation phenotype previously observed in this cellular model, and postulated PKP1 as one of the main effectors that may lead to NSCLC development.

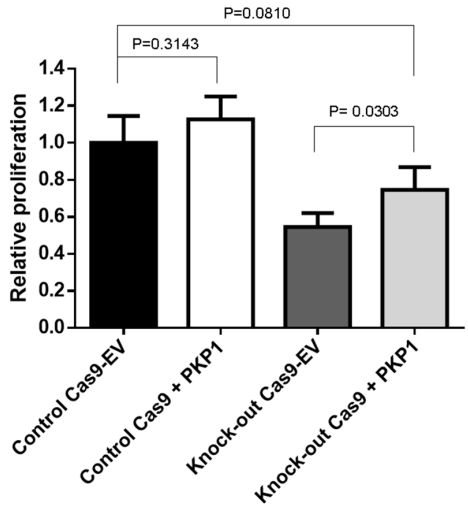

Figure 12. PKP1 reconstitution in Cas9 knock-out 1 cells significantly rescued the reduction in proliferation previously observed. Control Cas9-EV, Control Cas9 clone transduced with the empty vector; Control Cas9 + PKP1, Control Cas9 clone ectopically expressing PKP1; Knock-out Cas9 EV, PKP1 KO clone transduced with the empty vector; Knock-out Cas9 +PKP1, PKP1 KO clone with reconstructed PKP1 expression.

MIGRATION AND METASTASIS

The second main reason to achieve the PKP1 knock-out model was testing the effects of total PKP1 depletion in migration and metastasis. PKP1 knock-out clones suffer from poor desmosomes formation, and this lack of anchoring could induce a more migratory phenotype that may lead to metastasis and the invasion of other tissues. The *in vitro* scratch assay (Liang, Park, & Guan, 2007) was used to study cell migration in these 1(p=0.0038) and 2(p=0.0198) clones, finding a significant increase in cell migration versus controls (Figure 13).

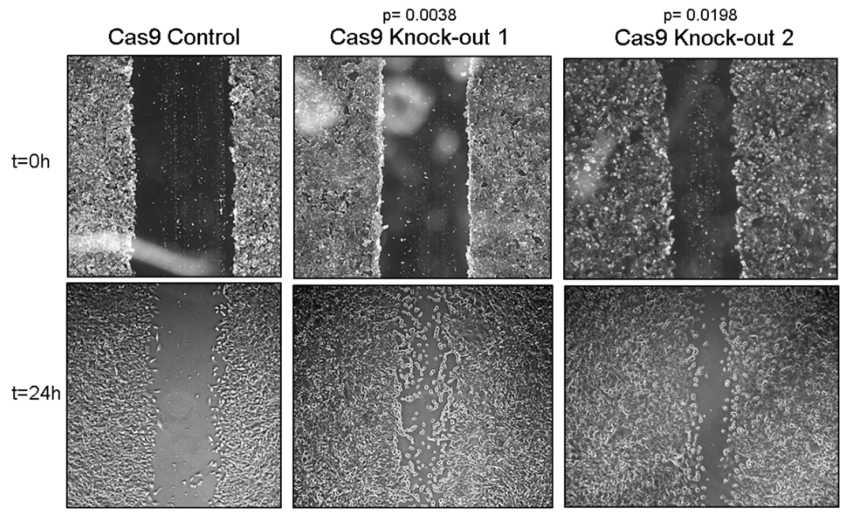

Figure 13. *In vitro* scratch assay of knock-out clones 1(p=0.0038) and 2(P=0.0198) in SK-MES-1 cells, showing enhanced cell migration in both knock-out clones versus control in three separate experiments. Cas9 Control, pspcas9(bb)-2a-puro empty vector-treated SK-MES-1 clonal cell line; Cas9 Knock-out 1, pspcas9(bb)-2a-puro sgRNA against PKP1 exon 3 treated SK-MES-1 clonal cell line 1; Cas9 Knock-out 2, pspcas9(bb)-2a-puro sgRNA against PKP1 exon 3 treated SK-MES-1 clonal cell line 2.

Intriguingly, these results indicate that PKP1 not only has a tumor-suppressor role but also oncogenic properties. Thus, PKP1 knock-outs showed both significantly lower proliferation and higher cell migration.

TESTING THE ONCOGENIC PHENOTYPE *IN VIVO*

DEVELOPMENT OF *IN VIVO* XENOGRAFTS

In order to evaluate and compare PKP1 tumor-suppressor and oncogenic effects *in vivo*, a xenograft model was developed with knock-out clones.

Immunodeficient NSG mice were used to perform tumor xenograft assays of PKP1 knock-out cells. Transfection of experimental (Cas9 knock-out 1 clone) and control (Cas9 Control clone) cells with luciferase (pUltra-chili-luc, Addgene) was conducted to facilitate tumor tracking with the *in vivo* imaging system (IVIS) and dTomato reporter signal was used to determine correct

transfection efficiency by flow cytometry. Finally, firefly luciferase expression was followed *in vivo* to characterize tumor behavior.

A total of 0.2 million cells were tail-vein injected to experimental and control groups (n=10 mice each). The arrival of tumor cells to the lung was checked by IVIS in both groups immediately after inoculation and the *in vivo* luminescence was studied at days 1, 4, 9, 15, and 24. IVIS results showed a sharp decline in the luminescence of xenografts from experimental cells (Cas9 knock-out 1 clone) over time and an increase of those from control cells (Cas9 Control clone) ($p = 0.0016$) (Figure 14A). In fact, the luminescence of xenografts from experimental cells disappeared so rapidly that it was difficult to properly evaluate their metastatic effect.

Organs from both groups of mice were extracted after sacrifice at day 24 and their *ex vivo* luminescence was measured. Luminescence remained mainly in lungs, and much higher in mice with PKP1-expressing cells than those with PKP1 knock-out cells, in which it was difficult to detect (Figure 14B).

Furthermore, as expected, some luminescence spots in a few of the analyzed livers were found in those mice injected with the PKP1-expressing clone, whereas luminescence was not detected in livers from mice injected with the PKP1 knock-out clone (Figure 15A).

Finally, a preliminary metastasis quantification was calculated in livers from both groups of study at 24 days after cell injection. Luminescence was significantly higher in livers from control mice than in those treated ($p= 0.0225$) (Figure 15B), indicating that PKP1 depletion may reduce metastasis *in vivo*, presumably through avoiding cancer cells establishment and growth.

A)

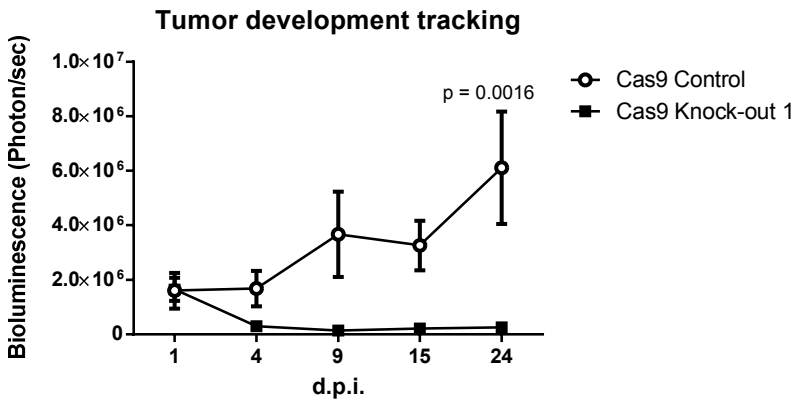

B)

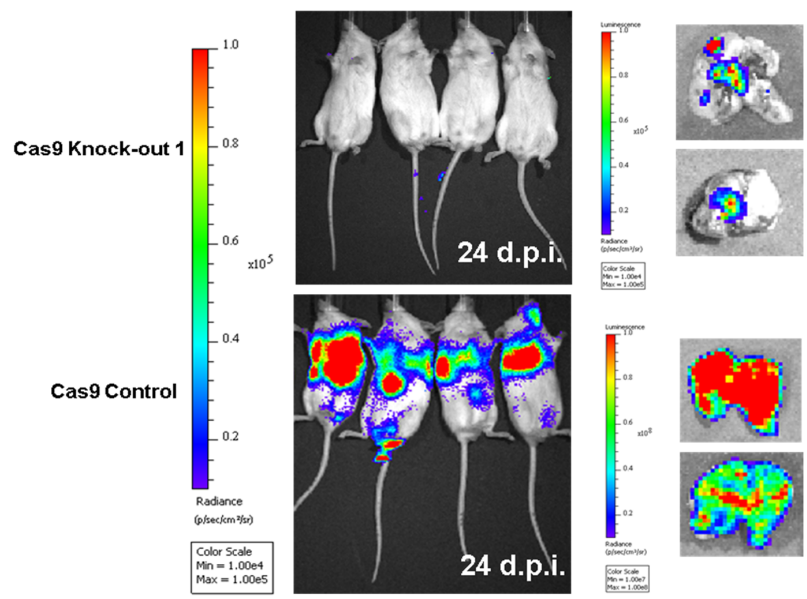

Figure 14. Tumor xenograft assay of PKP1 knock-out cells on immunodeficient NSG mice. A) Tumor development tracking at 24 days revealed a lower signal in mice injected with PKP1 knock-out versus PKP1-expressing clones over time (p = 0.0016). B) Luminescence analysis *in vivo* of mice and ex vivo of extracted organs at 24 days after cell injection, showing that luminescence was mainly observed in lungs and was considerably greater in mice injected with PKP1-expressing clones than in those injected with PKP1 knock-out cells, where it was difficult to detect. Cas9 Control, pspcas9(bb)-2a-puro empty vector treated SK-MES-1 clonal cell line; Cas9 Knock-out 1, pspcas9(bb)-2a-puro sgRNA against PKP1 exon 3 treated SK-MES-1 clonal cell line 1; d.p.i., days post-injection.

A)

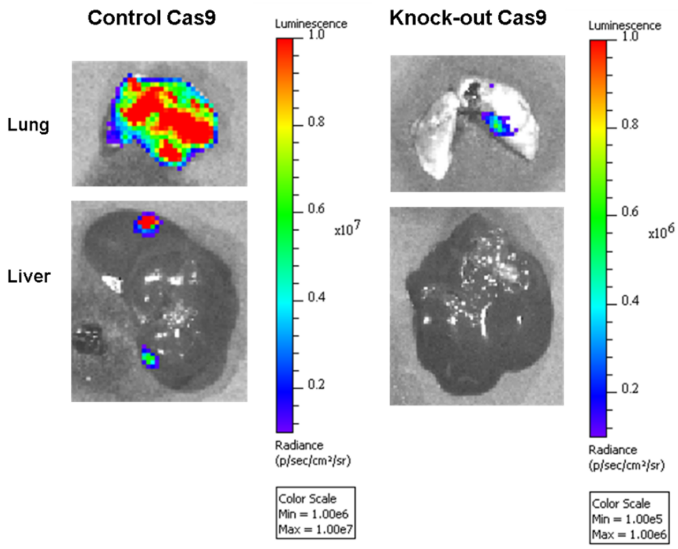

B)

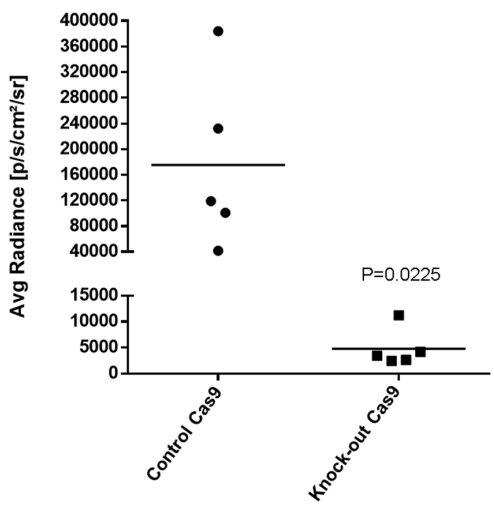

Figure 15. A) Representative pictures of extracted lungs and livers (mice of both groups) from the *ex vivo* luminescence analysis at 24 days after cell injection. B) Metastasis quantification in livers at 24 days after cell injection: knock-out Cas9 cells significantly metastasized less than control. Control Cas9, pspcas9(bb)-2a-puro empty vector treated SK-MES-1 clonal cell line; Knock-out Cas9, pspcas9(bb)-2a-puro sgRNA against PKP1 exon 3 treated SK-MES-1 clonal cell line.

A macroscopic analysis of the lung surface in control xenografts unveiled a granulated appearance in comparison to the smooth surface in experimental xenografts (similar to wild-type lungs) (Figure 16A). Lung tissue histological preparations were stained with hematoxylin-eosin and anti-human cytokeratin and anti-Ki-67 antibodies (Figure 16B). Tumor cells were difficult to detect in experimental preparations but easily observed in those derived from mice with control cells.

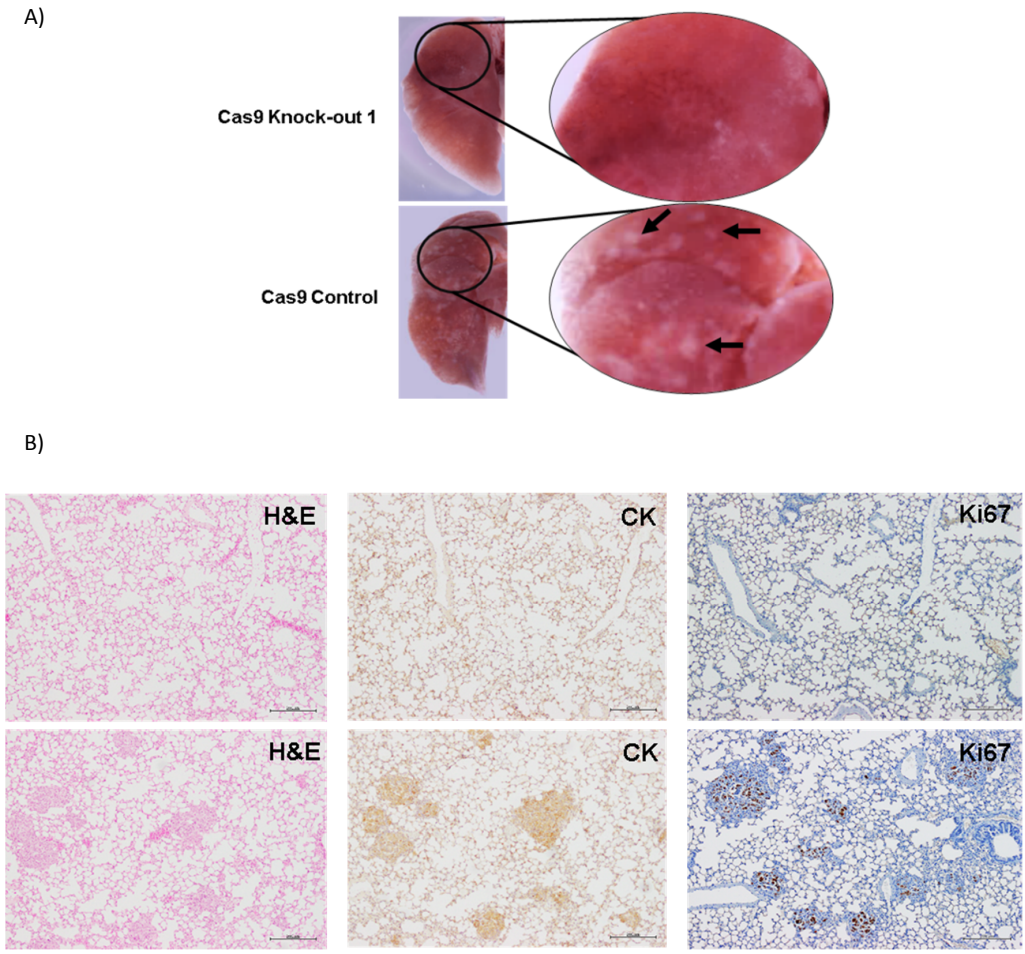

Figure 16. A) Macroscopic study of the lung surface, which appears granulated in PKP1-expressing xenografts but relatively smooth, similar to wild-type lung surface, in PKP1 knock-out xenografts. B) Hematoxylin-eosin and anti-human cytokeratin and anti-human Ki-67 antibodies staining results, revealing tumor structures in mice injected with PKP1-expressing clones (controls) but not in those injected with PKP1 knock-out clones; scale: 200um. Cas9 Control, pspcas9(bb)-2a-puro empty vector treated SK-MES-1 clonal cell line; Cas9 Knock-out 1, pspcas9(bb)-2a-puro sgRNA against PKP1 exon 3 treated SK-MES-1 clonal cell line 1; H&E, hematoxylin and eosin staining; CK; human cytokeratin immunostaining; Ki67, proliferation marker protein Ki-67 immunostaining.

In conclusion, the above results demonstrate that PKP1 knock-out impairs tumor xenograft engraftment and cell growth, placing the expression of PKP1 as a crucial effector for correct development and progression of *in vivo* xenografts, and for enhancing tumor growth *in vivo* in SqCLC.

ANALYSIS OF EXPRESSION PROFILES AFTER PKP1 DEPLETION

DETERMINATION OF DIFFERENTIALLY EXPRESSED GENES:

In order to shed light on the alternative PKP1 role in oncogenesis, which had been shown in the above experiments, a comparative transcriptome profile analysis between PKP1 knock-down and PKP1-expressing control cells was performed. Experiments were conducted in duplicate in SK-MES-1 cells, and a scrambled siRNA served as control. Criteria of fold change > 1.5 and $p < 0.05$ were adopted and 69 differentially expressed genes were found (42 up and 27 down), including PKP1, which was the most inhibited gene (fold change = -3.09, p = 0.01) (Figure 17).

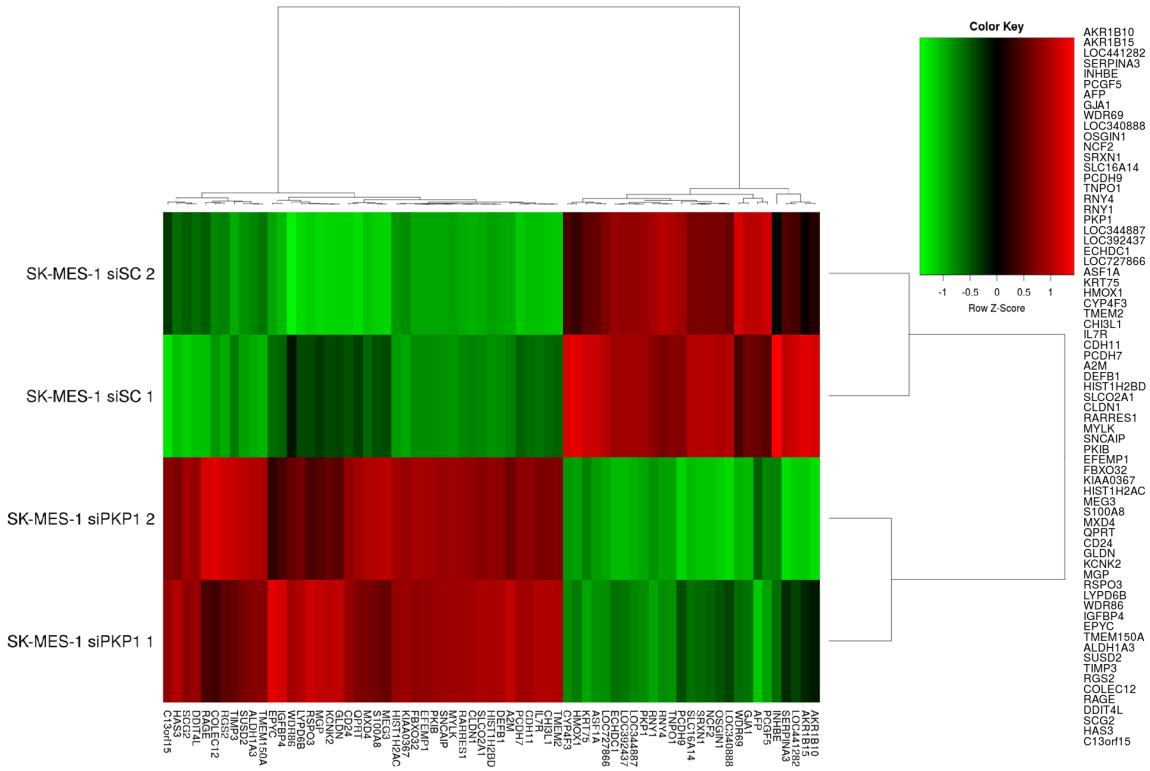

Figure 17. Heat map of differentially expressed genes obtained from a transcriptome profile analysis between SK-MES-1 PKP1 knock-down cells and their PKP1-expressing controls. Genes are listed from the right to the left. siPKP1, Knock-down siRNA-1 against PKP1 plus siRNA-2 against PKP1; siSC, scrambled-siRNA control.

FUNCTIONAL ANALYSIS OF EXPRESSION PROFILES AFTER PKP1 DEPLETION:

Geneset enrichment analysis (GSEA) was used to discover enriched biological functions and molecular signatures. A recommended false discovery rate cut-off of < 0.25 was applied and false positives were eliminated (i.e., gene sets with enrichment score peaks for both upregulation and downregulation). The top inhibited hallmark of cancer was "HALLMARK_MYC_TARGETS_V1", with a normalized enrichment score (NES) of -1.84. Furthermore, four other C-MYC-related gensets appeared also inhibited, and, interestingly, although C-MYC targets were downregulated, C-MYC mRNA levels itself remained unaltered (Figure 18A, B).

A)

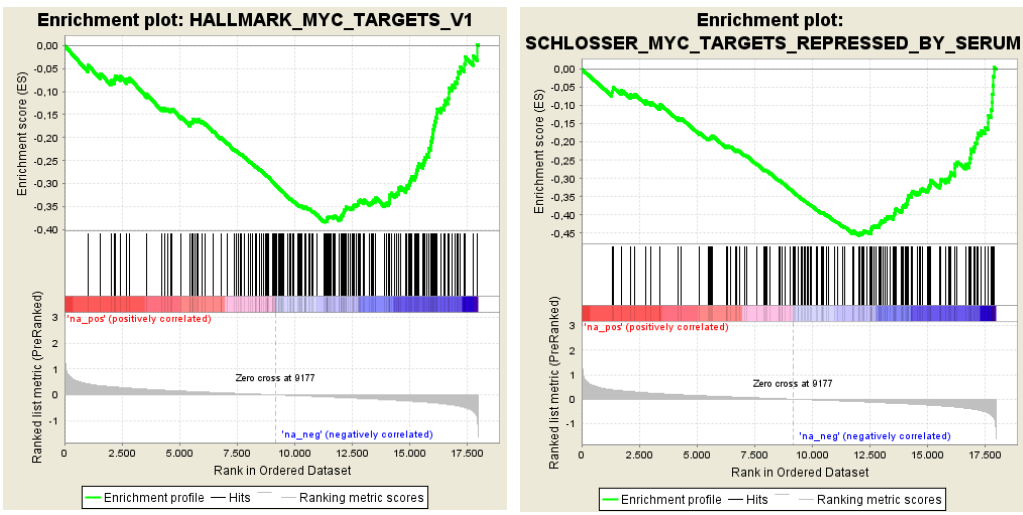

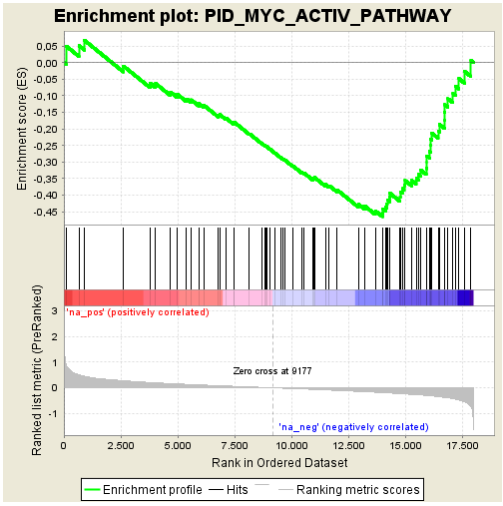

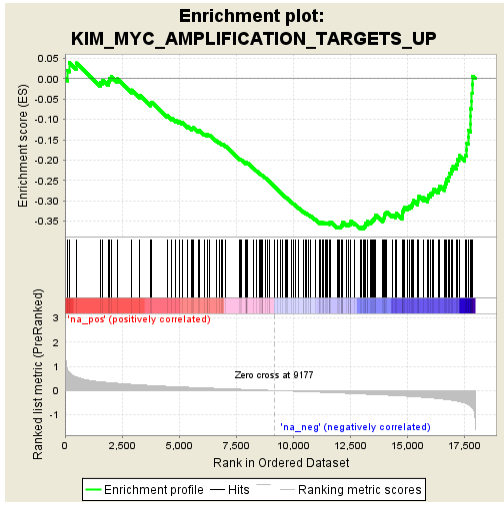

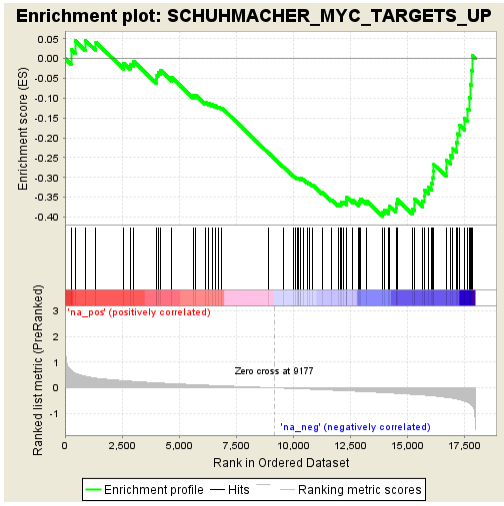

B)

Gene set	NES	FDR
HALLMARK_MYC_TARGETS_V1	-1.84	0.001
SCHLOSSER_MYC_TARGETS_REPRESSED_BY_SERUM	-2.18	0.002
PID_MYC_ACTIV_PATHWAY	-1.94	0.028
KIM_MYC_AMPLIFICATION_TARGETS_UP	-1.75	0.074
SCHUHMACHER_MYC_TARGETS_UP	-1.68	0.107

Figure 18. A) Top-scoring C-MYC-related gene sets in a gene set enrichment analysis (GSEA) of the transcriptome profiling results in PKP1 knock-down cells and their PKP1-expressing controls. These gensets were downregulated after PKP1 knock-down in the SK-MES-1 cell line. B) The table displays the top-scoring C-MYC-related gene sets alongside their normalized enrichment score (NES) and false discovery rate (FDR); the recommended FDR cutoff of < 0.25 was applied.

DISCOVERING A FUNCTIONAL RELATIONSHIP BETWEEN PKP1 AND C-MYC

PROTEIN AND mRNA VARIATIONS

Results obtained in the gene expression profiles after PKP1 depletion revealed a possible functional relationship between C-MYC and PKP1 that we decided to investigate:

Interestingly, C-MYC protein levels in SK-MES-1 cells were appreciably reduced after PKP1 knock-down (Figure 19A), but qPCR analysis showed no significant change in C-MYC mRNA (Figure 19B), suggesting that PKP1 regulates C-MYC expression at the post-transcriptional level. Furthermore, C-MYC knock-down in the SK-MES-1 cell line was followed by a remarkable PKP1 protein reduction and a significant ($p < 0.001$) depletion in PKP1 mRNA expression (Figure 19A, C). These results indicate that C-MYC, a well-known oncogenic transcription factor, regulates PKP1 at the transcriptional level.

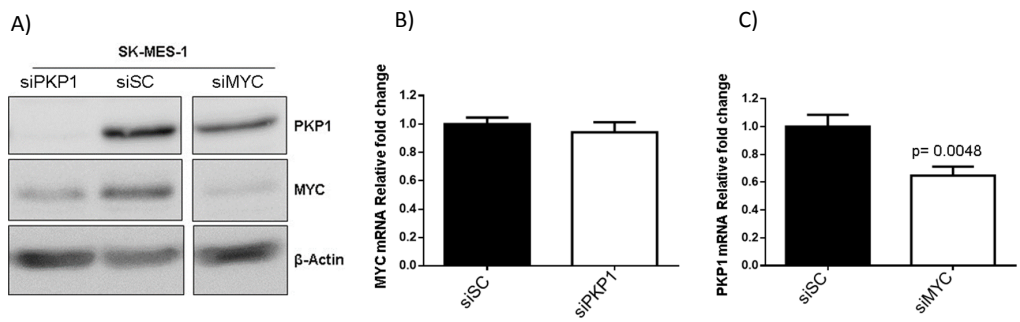

Figure 19. A) Western blot assay of PKP1 and C-MYC protein expression after the silencing of PKP1 or C-MYC. Reduction in PKP1 or C-MYC induces their reciprocal inhibition. B) qPCR analysis of C- MYC mRNA expression in SK-MES-1 cells after PKP1 silencing, showing that PKP1 inhibition does not affect C-MYC mRNA expression. C) qPCR analysis of PKP1 mRNA expression in SK-MES-1 cells after C-MYC silencing, showing that PKP1 mRNA expression is significantly reduced by C-MYC inhibition ($p = 0.0048$). PKP1, anti-plakophilin 1antibody; MYC, anti-C-MYC proto-oncogene antibody; B-Actin, anti-beta-actin antibody. siPKP1, Knock-down siRNA-1 against PKP1 plus siRNA-2 against PKP1; siMyc, knock-down siRNA against C- MYC; siSC, scrambled-siRNA control.

IMMUNOPRECIPITATION OF CYTOPLASMIC PKP1

Since translation mainly occurs in the cytoplasm, we decided to achieve a PKP1 cytoplasmic immunoprecipitation in order to identify new PKP1 partners and decode the mechanisms behind the PKP1-C-MYC regulation. Proteins pulled down with PKP1 were analyzed by means of liquid chromatography-tandem mass spectrometry (LC-MS/MS). Immunoprecipitation and LC-MS/MS of endogenous PKP1 were successful in the EPCL-272-H cell line, which has appreciably higher PKP1 levels compared to SK-MES-1 (in which we could not get proper performance). The pull-down with cytoplasmic PKP1 was analyzed with the Proteome Discoverer software using the SEQUEST engine. An output of 599 putative cytosolic PKP1-binding partners was obtained after quality filtering.

These cytosolic PKP1 partners were analyzed using DAVID 6.8 (https://david.ncifcrf.gov/) to identify enriched biological functions. As expected, clusters containing functions related to cell-cell adhesion obtained the highest enrichment score (57.09). Next positions were for clusters which included biological functions related to ATP binding (enrichment score = 22.56), RNA binding (enrichment score = 16.99), and ribosomes and translation (mainly translational initiation (enrichment score = 16.33)). These results pointed to a role for cytosolic PKP1 binding partners in translational initiation, binding rRNA and/or mRNA, as well as possible ATP-dependent roles (such as RNA helicase functions). A total of 38 proteins associated with the Gene Ontology term “translational initiation” were obtained in the list of putative PKP1 partners (Benjamini-adjusted enrichment p-value of $2.5 \cdot 10^{-20}$) and the top 20 are listed into Table 1.

ID	Gene Name	Coverage (%)	# Unique Peptides	Score Sequest HT
P11940	poly(A) binding protein cytoplasmic 1(PABPC1)	38.84	15	83.78
P61247	ribosomal protein S3A(RPS3A)	43.18	11	40.41
P23396	ribosomal protein S3(RPS3)	53.50	13	38.96
P46777	ribosomal protein L5(RPL5)	49.49	12	36.66
P39023	ribosomal protein L3(RPL3)	30.52	13	31.37
P62241	ribosomal protein S8(RPS8)	38.94	7	24.76
P61221	ATP binding cassette subfamily E member 1(ABCE1)	13.19	6	19.20
Q8NE71	ATP binding cassette subfamily F member 1(ABCF1)	11.01	6	18.84
P62424	ribosomal protein L7a(RPL7A)	26.69	6	18.26
P55884	eukaryotic translation initiation factor 3 subunit B(EIF3B)	11.06	7	17.16
P27635	ribosomal protein L10(RPL10)	26.17	5	16.94
P62917	ribosomal protein L8(RPL8)	16.34	4	15.83
P62829	ribosomal protein L23(RPL23)	41.43	4	14.37
P62280	ribosomal protein S11(RPS11)	34.18	4	13.38
P41091	eukaryotic translation initiation factor 2 subunit gamma(EIF2S3)	13.56	4	12.74
P23588	eukaryotic translation initiation factor 4B(EIF4B)	10.15	5	12.68
P18621	ribosomal protein L17(RPL17)	19.57	5	12.66
P62263	ribosomal protein S14(RPS14)	30.46	4	12.43
Q04637	eukaryotic translation initiation factor 4 gamma 1(EIF4G1)	4.75	4	11.73
P62753	ribosomal protein S6(RPS6)	20.08	3	11.19

Table 1. Top 20 translational initiation proteins from the PKP1 immunoprecipitation analysis followed by LC-MS/MS on PKP1 cytoplasmic native protein in EPLC-272H.

Finally, a western blot of the PKP1 immunoprecipitation protein extract was implemented in order to confirm the strong interaction of PKP1 with the PABP (poly(A) binding protein cytoplasmic 1) protein, which is part of the translation initiation factor complex, in the EPLC-272H cell line (Figure 20).

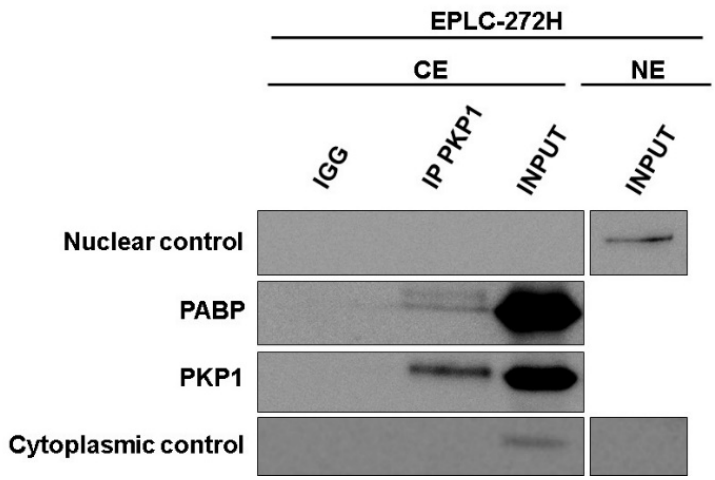

Figure 20. Western blot assay on the protein extract of PKP1 immunoprecipitation revealed strong interaction in the cytoplasm between PKP1 and poly(A) binding protein cytoplasmic 1 (PABP) proteins. Nuclear control (BRG1 antibody) and cytoplasmic control (GAPDH antibody) were used to check correct separation between the nucleus and cytoplasm. IgG, immunoprecipitation of negative control; IP PKP1, immunoprecipitation of PKP1 protein; INPUT; protein cellular extract; CE, cytoplasmic extract; NE, nucleus extract; Nuclear control, BRG1: SWI/SNF-related matrix-associated actin-dependent regulator of chromatin subfamily A member 4; Cytoplasmic control, GAPDH: glyceraldehyde-3-phosphate dehydrogenase; PKP1, plakophilin 1; PABP, poly(A) binding protein cytoplasmic 1.

CHECKING THE EFFECTS OF PKP1 IN "DE NOVO" PROTEIN SYNTHESIS

Interaction of PKP1 with different translation initiation factors pointed to a role of this plakophilin in either global or specific mRNA translation initiation.

In order to analyze the potential role of PKP1 in global translation, *de novo*-synthesized proteins were quantified by measuring the incorporation of puromycin on native peptide chains in our PKP1 inhibition model. Both PKP1 inhibited and scramble control SK-MES-1 cells showed no changes in the puromycylation pattern intensity by western blot, neither at the qualitative

(Figure 21A) or quantitative (Figure 21B) levels. The proper behavior of wild type (not treated cells), puromycin (which is incorporated in *de novo*-synthesized protein changes), emetine (an inhibitor of the protein synthesis), and puromycin+emitine treated cells, all of them used as controls, validated these results and confirmed that PKP1 does not affect global translation.

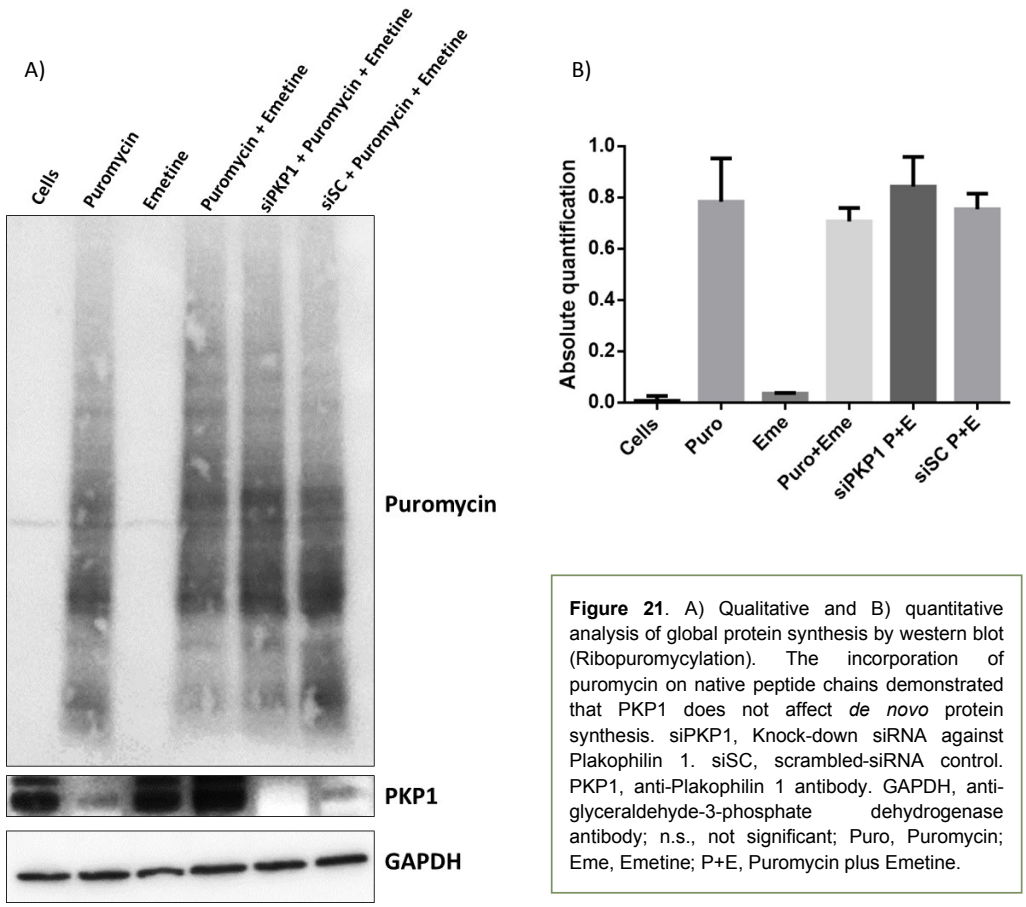

Figure 21. A) Qualitative and B) quantitative analysis of global protein synthesis by western blot (Ribopuromycylation). The incorporation of puromycin on native peptide chains demonstrated that PKP1 does not affect *de novo* protein synthesis. siPKP1, Knock-down siRNA against Plakophilin 1. siSC, scrambled-siRNA control. PKP1, anti-Plakophilin 1 antibody. GAPDH, anti-glyceraldehyde-3-phosphate dehydrogenase antibody; n.s., not significant; Puro, Puromycin; Eme, Emetine; P+E, Puromycin plus Emetine.

CHECKING THE EFFECTS OF PKP1 IN RIBOSOMES GLOBAL ACTIVITY:

Ribosomes global activity was quantified by analyzing changes in the polysome profiles in order to determine in a more precise way, or to discard, a possible role of PKP1 in global translation. Comparison of both, the PKP1 inhibited and control cells in the SK-MES-1 cell line, showed no significant changes in the resulted profiles or the calculated ratio area under the curve. Wild-type cells (not treated cells) and Na arsenite (an inhibitor of the translation initiation) treated cells were used as controls (Figure 22A, B, C). These results indicate no variation in the rate of active translation between PKP1 knock-down cells vs. control, and definitively discard a role of PKP1 in global translation.

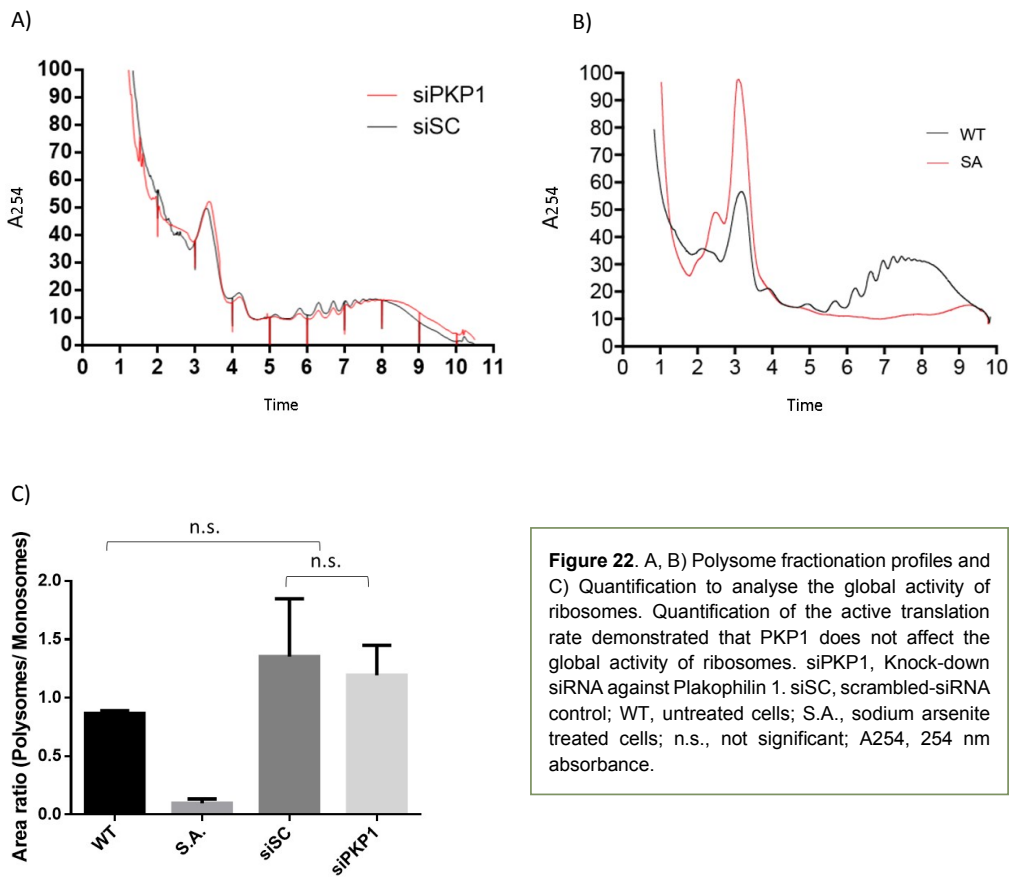

Figure 22. A, B) Polysome fractionation profiles and C) Quantification to analyse the global activity of ribosomes. Quantification of the active translation rate demonstrated that PKP1 does not affect the global activity of ribosomes. siPKP1, Knock-down siRNA against Plakophilin 1. siSC, scrambled-siRNA control; WT, untreated cells; S.A., sodium arsenite treated cells; n.s., not significant; A254, 254 nm absorbance.

PKP1 AND THE SPECIFIC TRANSLATIONAL INITIATION OF C-MYC

It is well known that C-MYC mRNA presents a highly structured 5´UTR, which requires to be uncoiled by the eIF4A1 subunit of the eIF4F complex, and, interestingly, a role of PKP1 in the increase of proliferation through its interaction with eIF4A1 in eIF4F-dependent translation has been described(Wolf & Hatzfeld, 2010)(Wolf et al., 2010).

In order to test whether or not PKP1 is directly involved in the translational initiation of C-MYC, luciferase assays were performed on the C-MYC 5'UTR through cloning it between the promoter and Renilla luciferase open reading frame in the psiCheck-2 plasmid. Firefly luciferase expression in the same bicistronic plasmid was used to normalize the transfection. Luciferase assay results showed a significant reduction (p = 0.0013) in luciferase expression after PKP1 knock-down (Figure 23), confirming the effect of PKP1 over C- MYC translation initiation.

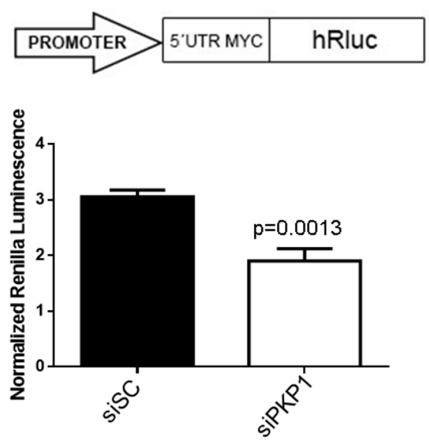

Figure 23. C-MYC 5'UTR cloning strategy in the psiCheck2 plasmid and Firefly luciferase assays on C-MYC 5'UTR, revealing a significant reduction in luciferase expression (p = 0.0013) after PKP1 silencing. Firefly luciferase expression in the same bicistronic psiCheck2 plasmid was used to normalize the signal. siPKP1, Knock-down siRNA-1 against PKP1 plus siRNA-2 against PKP1; siSC, scrambled-siRNA control; 5´UTR MYC, psiCheck2 plasmid expressing the 5´UTR of C-MYC. hRluc, Renilla luciferase.

CHECKING THE DIRECT INTERACTION BETWEEN PKP1 AND C-MYC mRNA:

RNA immunoprecipitation assay was developed in order to attest a direct interaction between PKP1 and C-MYC mRNA. The obtained 1.8-fold enrichment compared to the IgG control indicates a significant direct interaction (p = 0.0173) between them (Figure 24), unequivocally evidencing the role of PKP1 in the regulation of C-MYC translation.

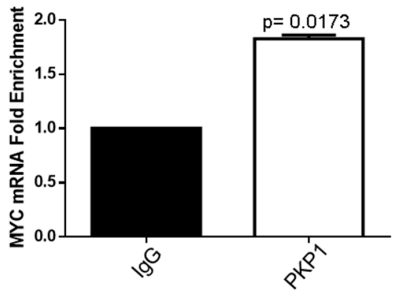

Figure 24. Fold enrichment of C-MYC mRNA level after PKP1 RNA immunoprecipitation (RIP). PKP1 antibody pulldown, normalized to IgG antibody pulldown control, has a significant fold enrichment of 1.8 (p = 0.0173). PKP1, immunoprecipitation of plakophilin 1; IgG, immunoprecipitation of the negative control.

CONFIRMING THE LINK BETWEEN THE OBSERVED PHENOTYPE AND PKP1-C-MYC FUNCTIONAL INTERACTION.

PKP1 effects on proliferation in SK-MES-1 cells after transducing C-MYC, with and without its 5'UTR, was measured in order to evaluate if the previously observed proliferation phenotypes were directed by the functional relationship between PKP1 and C-MYC. Interestingly, cells transduced with "5'UTR-CDS MYC" presented negative proliferation when PKP1 was inhibited, but this effect was not observed when C-MYC was transduced without its 5'UTR. These results indicate that the presence of the C-MYC 5'UTR in the transcript is key for the phenotype mediated by PKP1. Additionally, non-significant changes in proliferation, regardless if PKP1 was inhibited, were observed when C-MYC was transduced without its 5`UTR. However, proliferation trend drastically changed from positive to negative and became significant (p = 0.0231) when C-MYC was transduced with its 5'UTR (Figure 25).

These results pointed to an essential role of C-MYC in the oncogenic phenotype driven by PKP1 since it is dependent on the presence of its 5'UTR. Furthermore, PKP1 was revealed as a previously unknown C-MYC post-transcriptional activator, attributing novel oncogenic functions to the PKP1 cytoplasmic pool.

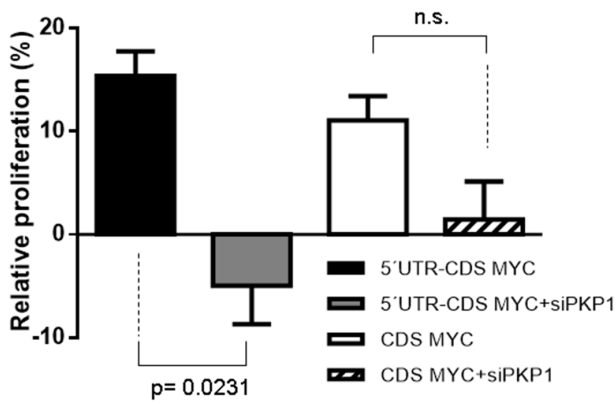

Figure 25. Phenotype rescue after 72 h of cell culture. Significative proliferation phenotype change trend (p = 0.0231) was observed after simultaneous 72h inhibition of PKP1 mRNA and ectopic expression of a C-MYC cDNA containing the 5´UTR and coding sequence, but not in the case that it only contained the coding sequence (p = 0.0904). 5´UTR-CDS MYC, C-MYC 5´UTR plus coding sequence plasmid transduction normalized to scramble transfection; 5´UTR-CDS MYC+siPKP1, C-MYC 5´UTR plus coding sequence plasmid transduction plus knock-down siRNA-1 against PKP1 plus siRNA-2 against PKP1 treatment and normalized to scramble transfection. CDS MYC, C-MYC coding sequence plasmid transduction normalized to scramble transfection; CDS MYC+siPKP1, C-MYC coding sequence plasmid transduction plus knock-down siRNA-1 against PKP1 plus siRNA-2 against PKP1 treatment and normalized to scramble transfection.

EVIDENCING POSITIVE CORRELATION BETWEEN PKP1 AND C-MYC mRNAs IN SQCLC TUMORS

After finding that PKP1 is a post-transcriptional activator of C-MYC, the effects of C-MYC on the regulation of PKP1 expression were explored.

A correlation between C-MYC and PKP1 expression levels was expected if C-MYC is an important transcriptional factor for PKP1 in SqCLC tumors. To test this hypothesis, we used the expression

levels determined in one of our previous studies (Sanchez-Palencia et al., 2011), finding a highly significant positive correlation (r = 0.68, p = 0.000019) between the mRNA levels of PKP1 and C-MYC in 32 SqCLC primary tumors (Figure 26).

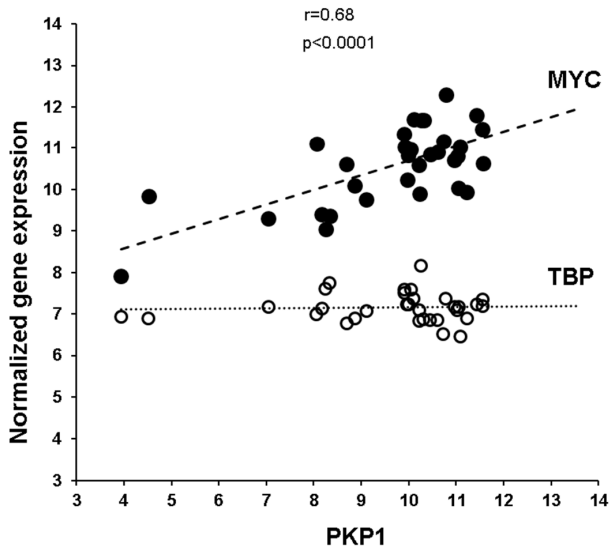

Figure 26. Correlation analysis of PKP1 and C-MYC mRNA expression in SqCLC tumors in our previous study, showing a significant correlation (r = 0.68, p = 0.000019) between C-MYC and PKP1 in 32 SqCLC primary tumors (Sanchez-Palencia et al., 2011). PKP1, plakophilin 1; MYC, C-MYC proto-oncogene; TBP, TATA-box binding protein.

CHECKING THE DIRECT EFFECT OF C-MYC IN PKP1 TRANSCRIPTION:

The direct interaction of C-MYC with the PKP1 promoter and its effects on PKP1 transcription were addressed through a classical luciferase experiment and a direct mutagenesis approach in which the Renilla luciferase gene was preceded by either the wild-type PKP1 promoter or one of its mutated versions in the psiCheck-2 plasmid, using the firefly luciferase expression in the same bicistronic plasmid to normalize the signal. "MYC-MAX complex" and "MYC-MAX heterodimer" binding sites present in the PKP1 promoter sequence (where the different site-directed mutagenesis were performed) were detected by the "MATinspertor" online tool.

The results showed a significant decrease (p = 0.0001) in luciferase expression under the PKP1 promoter when the protein levels of C-MYC were reduced using specific siRNA. On the contrary, although the mutation of two "MYC-MAX heterodimer" binding sites close to the 5'-end of the PKP1 promoter did not affect the regulation exerted by C-MYC (p = 0.0001), the mutation of the "MYC-MAX complex" binding sequence completely abolished the regulatory effect of C-MYC on the PKP1 promoter compared to the control (p = 0.6062). These findings indicate that C-MYC binds to the PKP1 promoter, significantly enhancing PKP1 expression (Figure 27).

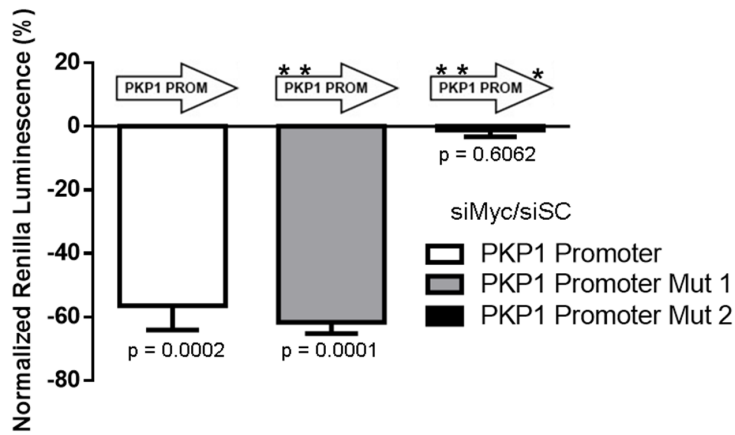

Figure 27. psiCheck2 cloning strategy for Firefly luciferase assays on the PKP1 promoter and PKP1 promoter mutated in different C-MYC binding sites and Firefly luciferase assay results showing a significant decrease in luciferase expression under the wild-type PKP1 promoter (p = 0.0002) and the version with two mutated "MYC-MAX heterodimer" binding sites close to the 5'-end of the PKP1 promoter (p = 0.0001). On the contrary, the mutation of the "MYC-MAX complex" binding sequence closest to the ATG start codon completely abolished the regulatory effect of C-MYC on the PKP1 promoter compared to the control(p=0.6062). Firefly luciferase expression in the same bicistronic psiCheck2 plasmid was used to normalize the signal. PKP1 promoter Mut 1, psiCheck2 plasmid expressing 5´-end mutated version of the PKP1 promoter; PKP1 promoter Mut 2, psiCheck2 plasmid expressing 3´-end mutated version of the PKP1 promoter; PKP1 promoter, psiCheck2 plasmid expressing wild-type PKP1 promoter.

All data obtained during the performance of this Ph.D. thesis point to a mechanistic relationship between PKP1 and C-MYC, in which PKP1 is regulated by C-MYC at the transcriptional level and C-MYC at the translational level by PKP1, placing C-MYC as key in the tumoral phenotype driven by PKP1. Interestingly, this kind of relationship has been previously described in the "EIF4F-MYC feedforward loop" in which was demonstrated that any player deregulation can lead to tumor development (C.-J. Lin et al., 2009)(C.-J. Lin, Cencic, Mills, Robert, & Pelletier, 2008)(Pelletier, Graff, Ruggero, & Sonenberg, 2015).

DISCUSSION

DATASETS OBTAINED FROM PATIENTS POINTED TO PKP1 AS A RELEVANT ACTOR IN DEVELOPMENT OF SqCLC TUMORS

Most of the advances in tumor mutations identification and abnormal gene expression variations in cancer context have been achieved through High-throughput genomics and transcriptomics technologies.

Our group has reported in two Independent studies that PKP1 is overexpressed in SqCLC (Angulo et al., 2008)(Sanchez-Palencia et al., 2011), and there are many other scientific publications supporting these data, such as those collected in the database of ONCOMINE expression profiles. It is worth noting two studies performed on lung cancer primary samples, compared to healthy lung tissue (Hou et al., 2010) (GEO access code, GSE19188)(Image 9); (Bhattacharjee et al., 2001) (GEO access code, GSE3526)(Image 10). In both, the result showed a significantly greater expression of the Pkp1 gene in samples corresponding to SqCLC compared to healthy samples or other lung cancer subtypes.

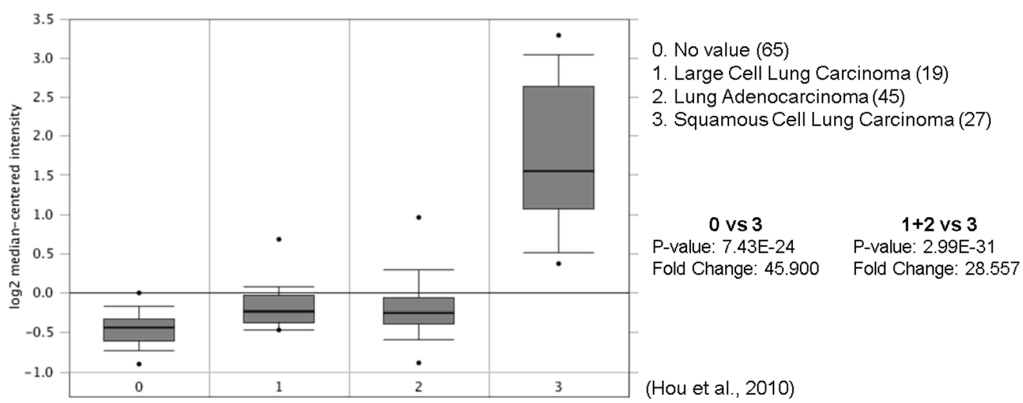

Image 9. Gene expression-based classification of non-small cell lung carcinomas. Ninety-one (91) non-small cell lung carcinoma and 65 adjacent normal lung samples were analyzed. Sample data includes age, sex, cancer sample site, and survival.

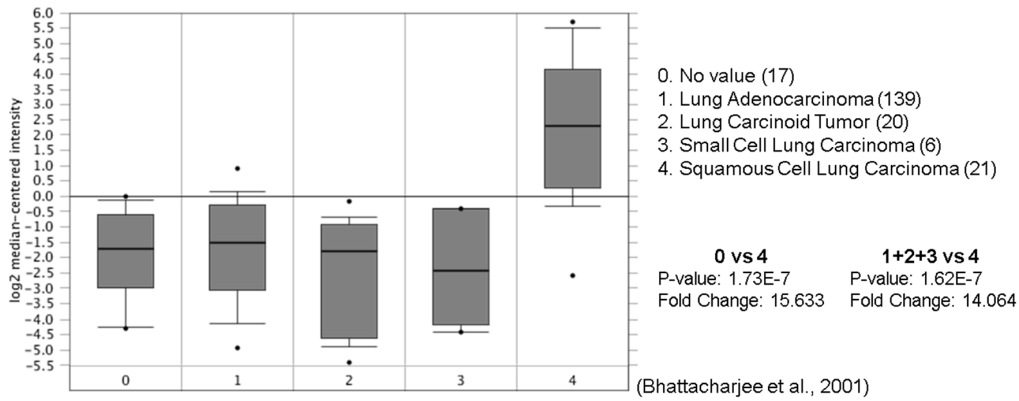

Image 10. Classification of human lung carcinomas by mRNA expression profiling. One hundred thirty-nine (139) lung adenocarcinoma, 21 squamous cell lung carcinoma, 20 lung carcinoid tumor, 6 small cell lung carcinoma, and 17 normal lung samples were analyzed on Affymetrix U95A microarrays. Sample data includes type, age, M stage, max tumor percentage, N stage, primary/metastatic, recurrence, sex, site of metastasis, smoking rate (packs per year), stage, survival, and T stage.

Furthermore, several bioinformatics methods to infer gene-subtype relationships based on AC and SqCLC specimens have been developed (Bowers, Cokus, Eisenberg, & Yeates, 2004). *Su, Yansen, and Linqiang Pan, 2014*, have reported that the expression of the genes DSG3, CLCA2, DSC3, and PKP1 was sufficient, and necessary, to the presence of SqCLC and the absence of AC. This finding suggests that these genes could distinguish between the two cancer subtypes(The analysis method applied took into consideration both, a single gene and a gene pair, which may influence lung cancer phenotypes)(Su & Pan, 2014)(Gomez-Morales et al., 2013). Furthermore, PKP1 showed a 20 times greater level of expression in SqCLC than in AC and normal lung, highlighting its histopathological diagnostic value, as it was previously noted by our group(Angulo et al., 2008)(Sanchez-Palencia et al., 2011)(Gomez-Morales et al., 2013).

Regarding high-throughput proteomic analysis, mass spectrometry studies have provided differences between protein profiles of normal and tumor lung tissue, which can be used to define useful protein biomarkers. Interestingly, these proteomic studies have identified PKP1 as an important and specific Squamous Cell Lung Cancer biomarker (Zamay et al., 2017).

More than never, it is necessary to perform useful functional experiments which allow us to understand the huge amount of descriptive data available and their relevance in the cancer development and progression context.

KNOWN FUNCTIONS OF PKP1 DEPEND ON ITS LOCALIZATION IN DESMOSOMES OR CYTOPLASM

PKP1 is a major component of desmosomes (M Hatzfeld et al., 2000) and its mutation results in a loss of epidermal integrity which is responsible for ectodermal dysplasia/skin fragility syndrome (EDSFS) (McGrath et al., 1997). Furthermore, desmosome activity is lost or disrupted in many tumors(Dusek & Attardi, 2011),and it is usually an important risk factor for promoting metastasis (Kundu et al., 2008). However, why PKP1 is overexpressed in cancer and how it contributes to tumorigenesis are still unresolved questions, although this overexpression has been frequently reported in many tumor types (Wolf et al., 2010)(Wolf & Hatzfeld, 2010).

The most plausible explanation could be related to the separated function that uncouples the adhesive and proliferative/survival roles of PKP1. Like other members of the armadillo protein family, PKP1 may play different cell functions with possibly opposite effects on cancer development. Also, PKP1 is present not only in desmosomes but also in the nucleus and cytoplasm (Gómez-Morales et al., 2013), and, therefore, it may have distinct functions in different cell compartments (Mechthild Hatzfeld, 2007). Accordingly, our results suggest that desmosomal PKP1 plays a tumor-suppressor role, enhancing cell cohesion, whereas cytoplasmic PKP1 plays a pro-oncogenic role and promotes cell proliferation, mainly by enhancing C-MYC expression at the post-transcriptional level.

Nowadays, it is known that phosphorylation-dependent subcellular localization of PKP1 is the main regulatory mechanism of its function, and it occurs via AKT2 as part of the Insulin signaling pathway:

On the one hand, in those cells with PKP1 expression, PKP1 is mainly associated with desmosomes, stabilizing desmosomal adhesion, and performing a tumor-suppressor function in the absence of growth factors signaling. Once the insulin pathway is activated, PKP1 becomes phosphorylated via AKT2 and, although it is still present in desmosomes (but in a less stable way), it mainly starts to accumulate in the cytoplasm, stimulating translation and proliferation and performing a tumor-promoter function. All this data is supported by several papers which describe unregulated activation of the growth factor/Akt pathway in several tumors (Lu-Hai Wang et al., 2008) (Memmott & Dennis, 2009) (Qiao, Sheng, & Pardee, 2008)(Steelman et al., 2008)(Tokunaga et al., 2008). Furthermore, elevated PKP1 protein levels in the cytoplasm have been reported in Oral squamous carcinoma (Narayana et al., 2010).

On the other hand, in those cells with low PKP1 expression, the lack of this protein could contribute to reduce intercellular adhesion and promote desmosome remodeling and carcinogenesis when, for example, the PI3K/Akt pathway is deregulated. It could explain why there are some tumors, such as colorectal, pancreatic, or prostate cancer, which express low levels of plakophilins (Breuninger et al., 2010) (Moll, Cowin, Kapprell, & Franke, 1986) (Schwarz et al., 2006) (C. Yang, Ströbel, Marx, & Hofmann, 2013).

The above described phosphorylation-dependent subcellular localization of PKP1 and its regulation by the growth factor signaling was previously described and summarized in 2013 by *Wolf et al.* (Image 11)(Wolf et al., 2013).

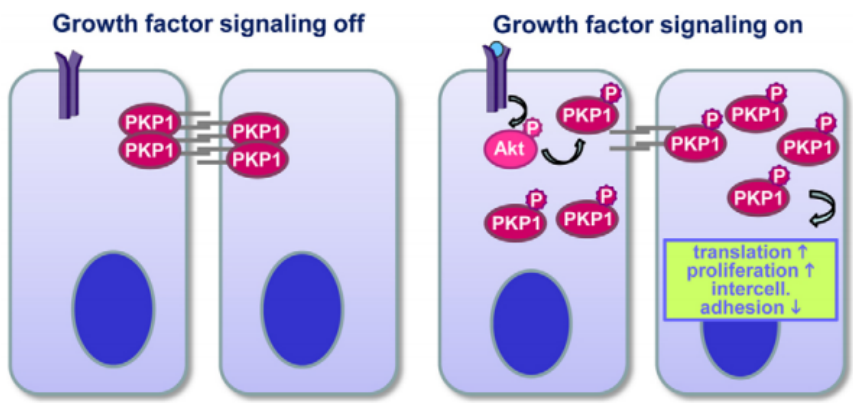

Adapted from (Wolf et al., 2013)

Image 11. Model for PKP1 regulation by growth factor signaling. In the absence of growth factors, PKP1 binds to desmoplakin and enhances desmosomal adhesion (left). Upon activation of the growth factor signaling cascade, PKP1 becomes phosphorylated by Akt2 and accumulates in the cytoplasm (right). The cytoplasmic pool of PKP1 stimulates translation and proliferation and reduces intercellular adhesion.

It is important to mention that desmosome disruption is an essential event to promote changes in cellular properties (as migratory and invasive characteristics) and morphology, which are necessary to transform epithelial into mesenchymal cells during the epithelial–mesenchymal transition (EMT). Although it plays a main role in morphogenesis during embryogenesis and is also implicated in wound healing, the EMT process is responsible for metastatic transformation in many tumoral contexts (Moustakas & Heldin, 2007).

Evidence suggests that the promotion of desmosome assembly may cause “mesenchymal-epithelial conversion”, which could prevent metastasis in a tumoral context. For example,

changes in morphology from fibroblastic to epithelial appearance have been obtained after the treatment of squamous carcinoma models with an epidermal growth factor receptor inhibitor (to promote desmosome assembly through avoiding the tyrosine phosphorylation of desmosomal proteins) (Lorch et al., 2004).

Our phenotypical assays have demonstrated that PKP1 knock-out induces a high decay in proliferation (Figure 11A, 11B), whereas the opposite effect occurs in ectopic expression models (Figure 3B and figure 4A). Moreover, the scratch-assay on PKP1 knock-out clones (Figure 13) revealed significant enhancement of cell dissemination after the loss of PKP1 expression, presumably because of disruption of desmosomes integrity and cell-cell junctions compromise (considered a PKP1 tumor-suppressor activity). However, according to our PKP1 knock-out xenograft experiments (Figures 14, 15, 16), the oncogenic activities of PKP1 seems to be stronger in SqCLC: PKP1 depletion not only does not increase metastasis *in vivo* but also it may reduce it, presumably through avoiding cancer cells establishment and growth. So, the higher level of PKP1 expression in Squamous Cell Lung Cancer may, in part, explain its lesser metastasization in comparison to lung adenocarcinoma, the other major NSCLC subtype (Budczies et al., 2015).

In this line, patients with ectodermal dysplasia/skin fragility syndrome (EDSFS), which is caused by homozygous or compound heterozygous PKP1 mutation, frequently present growth retardation and low birth weight as non-skin-related symptoms, and interestingly, there is no evidence of higher tumor susceptibility(McGrath et al., 1997). Furthermore, the same above phenotype was recently described in PKP1 knock-out mice, and keratinocytes isolated from these mice showed reduced proliferation rates (Rietscher et al., 2016). These phenotypical observations are in agreement with the results of our xenograft experiments (Figures 14, 15, 16) and support our hypothesis that PKP1 may play a more significant role in promoting cell growth than in enhancing cell cohesion, exerting an overall oncogenic effect in a tumoral context.

Cytoplasmic PKP1 was also described to act as a posttranscriptional regulator of gene expression through being a component of mRNA ribonucleoprotein particles (Fischer-Kešo et al., 2014). Furthermore, PKP1 was found in stress granules, where it influenced the translation and stability of attached mRNAs when cells were exposed to environmental stress (such as heat shock or oxidative stress) (Hofmann et al., 2006). Finally, a role of PKP1 in actin organization has been suggested since it has been observed in association with actin filaments(M Hatzfeld et al., 2000).

EVIDENCE ABOUT PKP1 FUNCTION IN THE NUCLEUS

The nuclear function of PKP1, unlike its desmosomal and cytoplasmic role, remains undefined.

In 2010, *Sobolik-Delmaire et al.* have demonstrated that the PKP1 nuclear pool interacted with Single-Stranded DNA *in vitro*, but not Double-Stranded DNA, in squamous carcinoma cell lines, postulating a role of PKP1 in DNA damage response (ssDNA occurs in the context of DNA repair). Furthermore, in the same study, PKP1 translocated to the nucleolus after DNA damage induction, which could indicate a possible function of this protein in suppressing ribosome biogenesis under these conditions(Sobolik-Delmaire et al., 2010). Although these results must be considered as preliminary data and more experiments have to be addressed to confirm them definitely, some preliminary results of PKP1 nuclear pool immunoprecipitation obtained in our group have confirmed direct interaction of PKP1 with different ribosomal subunits and rRNA in the nucleus, suggesting a role of PKP1 in ribosome assembly regulation (data not shown).

Finally, a hypothetical role of the PKP1 nuclear pool in transcription regulation has been postulated mainly due to its similarities to β-catenin. They are both plaque proteins working as structural components in cell-cell contacts (β-catenin is located in adherens junctions (AJs) whereas PKP1 is a desmosomal plaque protein). Thus, β-catenin also exhibits different subcellular localization and function depending on its phosphorylation status. When Wnt signaling is active, Akt-mediated phosphorylation of β-catenin causes its disassociation from AJs, where plays a tumor suppressor role. The subsequent accumulation in the cytoplasm and nucleus (where it binds to TCF- and LEF-family transcription factors) activates cell proliferation. Furthermore, it has been described that PKP2, a plakophilin that is close related with PKP1, can interact with β-catenin and can potentiate endogenous β-catenin–TCF transcriptional activity(X. Chen, Bonné, Hatzfeld, van Roy, & Green, 2002) (Schmidt et al., 1997)(Sobolik-Delmaire et al., 2010).

More research is required to unveil PKP1 functions in the nucleus and determine whether nuclear PKP1 is unequivocally involved in transcription regulation, ribosome biogenesis, and/ or DNA repair.

THE PKP1 AND C-MYC FEEDFORWARD LOOP

The functional interaction between PKP1 and C-MYC has been postulated as the best explanation for the observed phenotypes in this work, and several experiments have supported it. Presumably, this proposed model operates at two levels: PKP1 acts as a post-transcriptional activator of C-MYC, and C-MYC directly binds to the promoter of PKP1 and enhances its transcription.

Although it is true that inhibition of proliferation is indeed accompanied by downregulation of C-MYC expression in most cellular models, several experiments were achieved to demonstrate a direct relationship between inhibition of the C-MYC protein and inhibition of PKP1 expression:

On the one hand, results analysis from the expression array in the PKP1 inhibition model highlighted that C-MYC mRNA levels were not affected by the treatment (it was also lately proved by qPCR), while its targets were downregulated (Figure 18A, 18B). These results discarded a possible indirect C-MYC transcriptional regulation independent of PKP1 and caused by the treatment, and focus the attention on translation. Besides, various members of the translation initiation complex, including PABP (Table 1), were identified as direct PKP1 cytoplasmic partners in the PKP1 co-immunoprecipitation assay, suggesting that PKP1 may promote C-MYC translation by direct interaction with the translation initiation complex.

On the other hand, RNA immunoprecipitation assay pulling down the PKP1 protein indicated a significant direct interaction between C-MYC mRNA and PKP1 ($p = 0.0173$) (Figure 24), and a direct effect of PKP1 on C-MYC translation was confirmed by luciferase assay, which demonstrated the capacity of PKP1 to bind specifically to the C-MYC 5'UTR and enhance C-MYC protein expression (Figure 23). Furthermore, puromycilation and ribosome profiling experiments demonstrated that PKP1 is not implicated in global protein synthesis regulation, neither *the novo* protein synthesis (Figure 21A, 21B) or ribosomes global activity (Figure 22A,22B, 22C). So that, the effect over C-MYC translation cannot be attributed to changes in global translation, and it might be due to PKP1 regulation over a specific pool of mRNAs in which C-MYC mRNA would be included (as those containing complex 5´UTR sequences). This hypothesis is supported by previously published evidence of a role for PKP1 in translation in keratinocytes (Wolf & Hatzfeld, 2010)(Wolf et al., 2010).

Importantly, the essential role of PKP1 in the pro-tumoral phenotype due to the specific regulation of C-MYC translation through its 5'UTR, was also demonstrated in the experiment displayed on Figure 25: a significant change trend in proliferation phenotype ($p = 0.0231$) was observed after simultaneous 72h inhibition of PKP1 mRNA and ectopic expression of a C-MYC cDNA containing the 5´UTR and its coding sequence in SK-MES-1 cells, but not when it only contains the coding sequence ($p = 0.0904$).

The combination of direct mutagenesis in the PKP1 promoter and classical luciferase assays has allowed us to ensure that C-MYC binds to the PKP1 promoter and enhances its transcription. No variation was detected in the percentage of normalized luminescence between wild-type and twice-mutated promoter (corresponding to the "MYC/MAX heterodimer" mutated sites), indicating that these promoter sequences do not intervene in the C-MYC effect over PKP1 promoter activation. In other words, the C-MYC effect over PKP1 promoter would not be affected in a wild-type cell line with those two mutations randomly acquired. However, it is affected when the third mutation (corresponding to a "MYC-MAX binding site"), proximal to the ATG start codon, appeared (Figure 27). In support of these observations, a significant correlation between PKP1 and C-MYC expression levels in primary SqCLC tumor samples was observed (Figure 26).

In summary, all these data have allowed us to propose a functional interaction hypothesis in which PKP1 and C-MYC are components of a feedforward loop that links transcription and translation (PKP1 as post-transcriptional activator of C-MYC, and C-MYC as transcription factor that directly binds to the PKP1 promoter, enhancing its transcription), providing a possible molecular mechanism of cell transformation (Image 12).

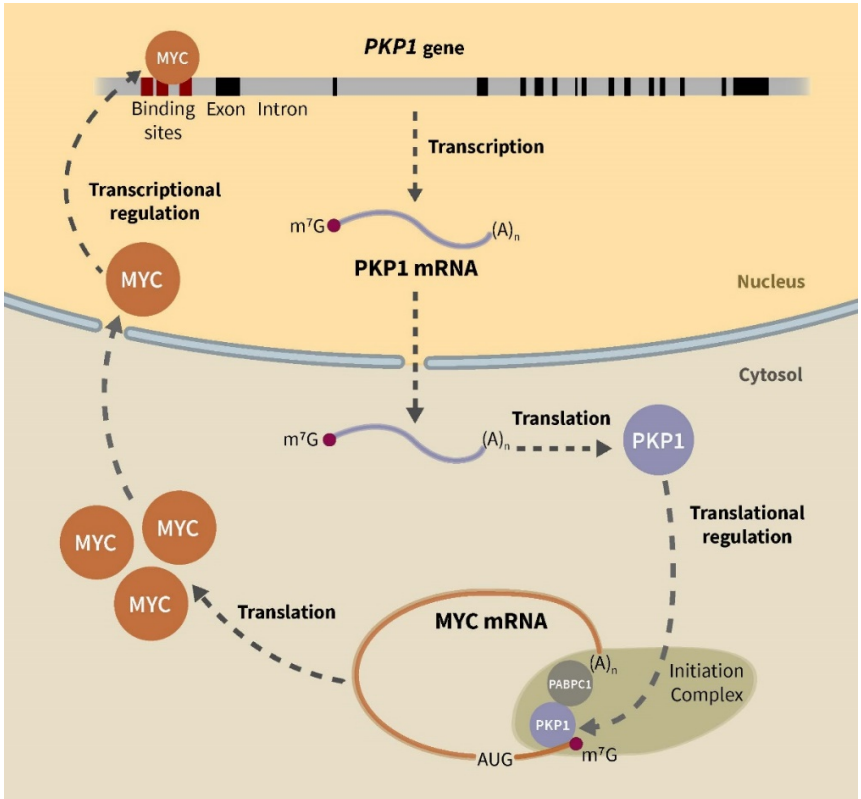

Image 12. Hypothesis of the functional interaction between PKP1 and C-MYC at two levels: PKP1 as a post-transcriptional activator of C-MYC, and C-MYC as a transcription factor that directly binds to the PKP1 promoter, enhancing its transcription. PKP1, plakophilin 1; MYC, C-MYC proto-oncogene; PABPC1, poly(A)-binding protein.

Several scientific data are supporting our observations. For example, a "Myc/eIF4F transcription/translation-coupled" mitogenic feedforward loop has been previously described, linking C-MYC with the translation machinery (C.-J. Lin et al., 2008) (C.-J. Lin et al., 2009). Interestingly, altered signaling of the PI3K/Akt/mTOR pathway in cancer is related to changes in eIF4F levels, which induce alterations in proteome due to the expression of malignancy-related mRNAs as C-MYC (C.-J. Lin et al., 2008)(Rajasekhar et al., 2003).

Moreover, polynuclear phenotype and mitosis aberrations were found in the knock-out model after some culture rounds, and a similar effect was described with the eif4F complex and the regulation of oncogenes such as C-MYC (Barna et al., 2008)(Annibali et al., 2014), suggesting that a rigorous control of PKP1 is necessary to regulate protein synthesis and oncogenesis. Although no variations in global translation and polysome profiling were found after PKP1 inhibition in the SK-MES-1 cell line (Figures 21 and 22), future experiments will be focused on obtaining

quantitative and qualitative results to understand the molecular mechanism by which PKP1 regulates the specific translation of C-MYC and, presumably, other mRNAs that could be implicated in oncogenesis. These experiments will include a polysomes profiling to isolate mRNAs bound to actively translating ribosomes and measuring the translational activity of selected mRNAs, as C-MYC mRNA, in response to PKP1 level alteration. It will help us to identify switch from light to heavy polysomes and global protein translation changes, not only of C-MYC mRNA but potentially others.

Finally, there are also some interesting similarities in the phenotype displayed by C-MYC and PKP1 knock-out mouse models, which underline their functional connection. For example, cells isolated from both knock-out mice showed reduced proliferation, and animal growth was impaired and presented high embryonic and/or neonatal mortality(Rietscher et al., 2016) (Pirity, Blanck, & Schreiber-Agus, 2006).

PKP1 AND CANCER THERAPY

Our results, most of them included in a recent publication(Martin-Padron et al., 2019), may be of clinical relevance. PKP1 appears to be an useful biomarker to differentiate between SqCLC and lung adenocarcinoma (the other main NSCLC cancer subtype), in which PKP1 expression levels are not significantly altered(Angulo et al., 2008)(Sanchez-Palencia et al., 2011)(Gomez-Morales et al., 2013). Also, PKP1 inhibition may be of potential therapeutic value against SqCLC, given our finding that it can impair the tumor phenotype *in vitro* (Figures 11 and 12) and *in vivo* (Figures 14, 15, and 16), presumably through altering the PKP1-C-MYC feedforward loop proposed in this Ph.D.

C-MYC plays an evolutionarily conserved role in the control of cell size and protein synthesis rates. It regulates the expression of multiple components of the machinery for protein synthesis (including ribosomal proteins, translation initiation factors, and rDNA), and it is widely described that C-MYC activity deregulation is causally implicated in most human tumors (Dang, 2012).

Given the importance of C-MYC in several cancers, further investigation regarding functional relationship between PKP1 and C-MYC must be achieved in order to discover new indirect targeting approaches against this “undruggable” oncogene, which is considered one of the “most-wanted” targets for cancer therapy(Whitfield et al., 2017).

CONCLUSIONS

1- PKP1 ectopic expression significantly enhances cell proliferation and reduces apoptosis in the NCI-H2170 cell line.

2- PKP1 ectopic expression shows high cell-transforming potential with a significant increment in focus formation in the NIH 3T3 murine fibroblast cell line.

3*- *PKP1* knock-out in the SK-MES-1 cell line significantly promotes cell dissemination but reduces cell proliferation *in vitro.

4- *PKP1* knock-out in the SK-MES-1 cell line significantly impairs tumor xenograft engraftment and cell growth *in vivo*.

5- Gene expression profile after PKP1 depletion revealed significant variation in C-MYC targets expression, but it did not affect C-MYC transcription.

6- Cytoplasmic immunoprecipitation of the PKP1 protein pool unveiled new PKP1 interactions with several components of the translation initiation complex as PABP.

7- PKP1 is revealed as a possible novel C-MYC post-transcriptional regulator, binding to the C-MYC mRNA 5'UTR, and enhancing its translation.

8- C-MYC seems to act as a PKP1 transcriptional regulator through directly interacting with the PKP1 promoter, and enhancing its transcription.

REFERENCES

Abdalla, E. M., & Has, C. (2014). A plakophilin-1 gene mutation in an egyptian family with ectodermal dysplasia-skin fragility syndrome. *Molecular Syndromology*, *5*(6), 304–306. https://doi.org/10.1159/000369267

Amini, A., Yeh, N., Gaspar, L. E., Kavanagh, B., & Karam, S. D. (2014). Stereotactic body radiation therapy (SBRT) for lung cancer patients previously treated with conventional radiotherapy: a review. *Radiation Oncology (London, England)*, *9*, 210. https://doi.org/10.1186/1748-717X-9-210

Anastasiadis, P. Z. (2007). p120-ctn: A nexus for contextual signaling via Rho GTPases. *Biochimica et Biophysica Acta (BBA) - Molecular Cell Research*, *1773*(1), 34–46. https://doi.org/https://doi.org/10.1016/j.bbamcr.2006.08.040

Anastasiadis, P. Z., & Reynolds, A. B. (2000). The p120 catenin family: complex roles in adhesion, signaling and cancer. *Journal of Cell Science*, *113*(8), 1319–1334. Retrieved from http://jcs.biologists.org/content/113/8/1319

Angulo, B., Suarez-Gauthier, A., Lopez-Rios, F., Medina, P. P., Conde, E., Tang, M., … Sanchez-Cespedes, M. (2008). Expression signatures in lung cancer reveal a profile for EGFR-mutant tumours and identify selective PIK3CA overexpression by gene amplification. *The Journal of Pathology*, *214*(3), 347–356. https://doi.org/10.1002/path.2267

Annibali, D., Whitfield, J. R., Favuzzi, E., Jauset, T., Serrano, E., Cuartas, I., … Soucek, L. (2014). Myc inhibition is effective against glioma and reveals a role for Myc in proficient mitosis. *Nature Communications*, *5*, 4632. https://doi.org/10.1038/ncomms5632

Bachmann, A. S., & Geerts, D. (2018). Polyamine synthesis as a target of MYC oncogenes. *Journal of Biological Chemistry* , *293*(48), 18757–18769. https://doi.org/10.1074/jbc.TM118.003336

Barna, M., Pusic, A., Zollo, O., Costa, M., Kondrashov, N., Rego, E., … Ruggero, D. (2008). Suppression of Myc oncogenic activity by ribosomal protein haploinsufficiency. *Nature*, *456*(7224), 971–975. https://doi.org/10.1038/nature07449

Bass-Zubek, A. E., Godsel, L. M., Delmar, M., & Green, K. J. (2009). Plakophilins: multifunctional scaffolds for adhesion and signaling. *Current Opinion in Cell Biology*, *21*(5), 708–716. https://doi.org/10.1016/j.ceb.2009.07.002

Bender, E. (2014). Epidemiology: The dominant malignancy. *Nature*, *513*, S2. Retrieved from https://doi.org/10.1038/513S2a

Bhattacharjee, A., Richards, W. G., Staunton, J., Li, C., Monti, S., Vasa, P., … Meyerson, M. (2001). Classification of human lung carcinomas by mRNA expression profiling reveals distinct adenocarcinoma subclasses. *Proceedings of the National Academy of Sciences*, *98*(24), 13790–13795. https://doi.org/10.1073/pnas.191502998

Bonne, S., van Hengel, J., Nollet, F., Kools, P., & van Roy, F. (1999). Plakophilin-3, a novel armadillo-like protein present in nuclei and desmosomes of epithelial cells. *Journal of Cell Science*, *112*(14), 2265–2276. Retrieved from http://jcs.biologists.org/content/112/14/2265

Bowers, P. M., Cokus, S. J., Eisenberg, D., & Yeates, T. O. (2004). Use of Logic Relationships to Decipher Protein Network Organization. *Science*, *306*(5705), 2246–2249. https://doi.org/10.1126/science.1103330

Boyce, A. E., McGrath, J. A., Techanukul, T., Murrell, D. F., Chow, C. W., McGregor, L., & Warren, L. J. (2012). Ectodermal dysplasia-skin fragility syndrome due to a new homozygous internal deletion mutation in the PKP1 gene. *Australasian Journal of Dermatology*, *53*(1), 61–65. https://doi.org/10.1111/j.1440-0960.2011.00846.x

Bray, F., Ferlay, J., Soerjomataram, I., Siegel, R. L., Torre, L. A., & Jemal, A. (2018). Global cancer statistics 2018: GLOBOCAN estimates of incidence and mortality worldwide for 36 cancers in 185 countries. *CA: A Cancer Journal for Clinicians*, *68*(6), 394–424. https://doi.org/10.3322/caac.21492

Breitling, R., Armengaud, P., Amtmann, A., & Herzyk, P. (2004). Rank products: a simple, yet powerful, new method to detect differentially regulated genes in replicated microarray experiments. *FEBS Letters*, *573*(1–3), 83–92. https://doi.org/10.1016/j.febslet.2004.07.055

Brennan, J., O\textquoterightConnor, T., Makuch, R. W., Simmons, A. M., Russell, E., Ilona Linnoila, R., … Johnson, B. E. (1991). myc Family DNA Amplification in 107 Tumors and Tumor Cell Lines from Patients with Small Cell Lung Cancer Treated with Different Combination Chemotherapy Regimens. *Cancer Research*, *51*(6), 1708–1712. Retrieved from http://cancerres.aacrjournals.org/content/51/6/1708

Brentjens, R. J., Davila, M. L., Riviere, I., Park, J., Wang, X., Cowell, L. G., … Sadelain, M. (2013). CD19-targeted T cells rapidly induce molecular remissions in adults with chemotherapy-refractory acute lymphoblastic leukemia. *Science Translational Medicine*, *5*(177), 177ra38-177ra38. https://doi.org/10.1126/scitranslmed.3005930

Breuninger, S., Reidenbach, S., Sauer, C. G., Ströbel, P., Pfitzenmaier, J., Trojan, L., & Hofmann, I. (2010). Desmosomal plakophilins in the prostate and prostatic adenocarcinomas: implications for diagnosis and tumor progression. *The American Journal of Pathology*, *176*(5), 2509–2519. https://doi.org/10.2353/ajpath.2010.090737

Brinkmeyer, J. K., & Moore, D. C. (2016). Necitumumab for the treatment of squamous cell non-small cell lung cancer. *Journal of Oncology Pharmacy Practice*, *24*(1), 37–41. https://doi.org/10.1177/1078155216682365

Buchbinder, E., & Hodi, F. S. (2015). Cytotoxic T lymphocyte antigen-4 and immune checkpoint blockade. *The Journal of Clinical Investigation*, *125*(9), 3377–3383. https://doi.org/10.1172/JCI80012

Budczies, J., von Winterfeld, M., Klauschen, F., Bockmayr, M., Lennerz, J. K., Denkert, C., … Stenzinger, A. (2015). The landscape of metastatic progression patterns across major human cancers. *Oncotarget*, *6*(1), 570–583. https://doi.org/10.18632/oncotarget.2677

Byers, L. A., & Rudin, C. M. (2015). Small cell lung cancer: where do we go from here? *Cancer*, *121*(5), 664–672. https://doi.org/10.1002/cncr.29098

Carrassa, L., & Damia, G. (2017). DNA damage response inhibitors: Mechanisms and potential applications in cancer therapy. *Cancer Treatment Reviews*, *60*, 139–151. https://doi.org/10.1016/j.ctrv.2017.08.013

Chen, L., & Han, X. (2015). Anti–PD-1/PD-L1 therapy of human cancer: past, present, and future. *The Journal of Clinical Investigation*, *125*(9), 3384–3391. https://doi.org/10.1172/JCI80011

Chen, X., Bonné, S., Hatzfeld, M., van Roy, F., & Green, K. J. (2002). Protein Binding and Functional Characterization of Plakophilin 2: EVIDENCE FOR ITS DIVERSE ROLES IN DESMOSOMES AND β-CATENIN SIGNALING . *Journal of Biological Chemistry* , *277*(12), 10512–10522. https://doi.org/10.1074/jbc.M108765200

Choi, H.-J., & Weis, W. I. (2005). Structure of the Armadillo Repeat Domain of Plakophilin 1. *Journal of Molecular Biology*, *346*(1), 367–376. https://doi.org/https://doi.org/10.1016/j.jmb.2004.11.048

Clark, G. J., Cox, A. D., Graham, S. M., & Der, C. J. B. T.-M. in E. (1995). Biological assays for Ras transformation. In *Small GTPases and Their Regulators, Part A: RAS Family* (Vol. 255, pp. 395–412). Academic Press. https://doi.org/https://doi.org/10.1016/S0076-6879(95)55042-9

collaborative group. (1995). Chemotherapy in non-small cell lung cancer: a meta-analysis using updated data on individual patients from 52 randomised clinical trials. Non-small Cell Lung Cancer Collaborative Group. *BMJ (Clinical Research Ed.)*, *311*(7010), 899–909. Retrieved from https://www.ncbi.nlm.nih.gov/pubmed/7580546

Collins, L. J., Kurland, C. G., Biggs, P., & Penny, D. (2009). The Modern RNP World of Eukaryotes. *Journal of Heredity*, *100*(5), 597–604. Retrieved from http://dx.doi.org/10.1093/jhered/esp064

Conacci-Sorrell, M., McFerrin, L., & Eisenman, R. N. (2014). An overview of MYC and its interactome. *Cold Spring Harbor Perspectives in Medicine*, *4*(1), a014357–a014357. https://doi.org/10.1101/cshperspect.a014357

Cory, S., & Adams, J. M. (2002). The Bcl2 family: regulators of the cellular life-or-death switch. *Nat Rev Cancer*, *2*(9), 647–656. https://doi.org/10.1038/nrc883

Cousin, S., Khalifa, E., Crombe, A., Laizet, Y., Lucchesi, C., Toulmonde, M., … Italiano, A. (2018). Targeting ERBB2 mutations in solid tumors: biological and clinical implications. *Journal of Hematology & Oncology*, *11*(1), 86. https://doi.org/10.1186/s13045-018-0630-4

Dalla-Favera, R., Bregni, M., Erikson, J., Patterson, D., Gallo, R. C., & Croce, C. M. (1982). Human c-myc onc gene is located on the region of chromosome 8 that is translocated in Burkitt lymphoma cells. *Proceedings of the National Academy of Sciences of the United States of America*, *79*(24), 7824–7827. Retrieved from https://www.ncbi.nlm.nih.gov/pubmed/6961453

Dang, C. V. (2012). MYC on the path to cancer. *Cell*, *149*(1), 22–35. https://doi.org/10.1016/j.cell.2012.03.003

Defranchi, S. A., Cassivi, S. D., Nichols, F. C., Allen, M. S., Shen, K. R., Deschamps, C., & Wigle, D. A. (2009). N2 disease in T1 non-small cell lung cancer. *The Annals of Thoracic Surgery*, *88*(3), 924–928. https://doi.org/10.1016/j.athoracsur.2009.05.039

Dohn, M. R., Brown, M. V, & Reynolds, A. B. (2009). An essential role for p120-catenin in Src- and Rac1-mediated anchorage-independent cell growth. *The Journal of Cell Biology*, *184*(3), 437–450. https://doi.org/10.1083/jcb.200807096

Drake, C. G., Jaffee, E., & Pardoll, D. M. B. T.-A. in I. (2006). Mechanisms of Immune Evasion by Tumors. In *Cancer Immunotherapy* (Vol. 90, pp. 51–81). Academic Press. https://doi.org/https://doi.org/10.1016/S0065-2776(06)90002-9

Drilon, A., Rekhtman, N., Ladanyi, M., & Paik, P. (2012). Squamous-cell carcinomas of the lung: emerging biology, controversies, and the promise of targeted therapy. *The Lancet Oncology*, *13*(10), e418–e426. https://doi.org/10.1016/S1470-2045(12)70291-7

Dusek, R. L., & Attardi, L. D. (2011). Desmosomes: new perpetrators in tumour suppression. *Nature Reviews Cancer*, *11*, 317. Retrieved from https://doi.org/10.1038/nrc3051

Ehrhardt, A., Bartels, T., Geick, A., Klocke, R., Paul, D., & Halter, R. (2001). Development of pulmonary bronchiolo-alveolar adenocarcinomas in transgenic mice overexpressing murine c-myc and epidermal growth factor in alveolar type II pneumocytes. *British Journal of Cancer*, *84*(6), 813–818. https://doi.org/10.1054/bjoc.2000.1676

Emens, L. A., Ascierto, P. A., Darcy, P. K., Demaria, S., Eggermont, A. M. M., Redmond, W. L., … Marincola, F. M. (2017). Cancer immunotherapy: Opportunities and challenges in the rapidly evolving clinical landscape. *European Journal of Cancer*, *81*, 116–129. https://doi.org/https://doi.org/10.1016/j.ejca.2017.01.035

Ersoy-Evans, S., Erkin, G., Fassihi, H., Chan, I., Paller, A. S., Sürücü, S., & McGrath, J. A. (2006). Ectodermal dysplasia-skin fragility syndrome resulting from a new homozygous mutation, 888delC, in the desmosomal protein plakophilin 1. *Journal of the American Academy of Dermatology*, *55*(1), 157–161. https://doi.org/10.1016/j.jaad.2005.10.002

Finn, O. J. (2012). Immuno-oncology: understanding the function and dysfunction of the immune system in cancer. *Annals of Oncology : Official Journal of the European Society for Medical Oncology*, *23 Suppl 8*(Suppl 8), viii6-viii9. https://doi.org/10.1093/annonc/mds256

Fischer-Kešo, R., Breuninger, S., Hofmann, S., Henn, M., Röhrig, T., Ströbel, P., … Hofmann, I. (2014). Plakophilins 1 and 3 bind to FXR1 and thereby influence the mRNA stability of desmosomal proteins. *Molecular and Cellular Biology*, *34*(23), 4244–4256. https://doi.org/10.1128/MCB.00766-14

Freeman-Keller, M., Goldman, J., & Gray, J. (2015). Vaccine immunotherapy in lung cancer: Clinical experience and future directions. *Pharmacology & Therapeutics*, *153*, 1–9. https://doi.org/https://doi.org/10.1016/j.pharmthera.2015.05.004

FUKAZAWA, T., MAEDA, Y., MATSUOKA, J., YAMATSUJI, T., SHIGEMITSU, K., MORITA, I., … NAOMOTO, Y. (2010). Inhibition of Myc Effectively Targets KRAS Mutation-positive Lung Cancer Expressing High Levels of Myc. *Anticancer Research* , *30*(10), 4193–4200. Retrieved from http://ar.iiarjournals.org/content/30/10/4193.abstract

Furukawa, C., Daigo, Y., Ishikawa, N., Kato, T., Ito, T., Tsuchiya, E., … Nakamura, Y. (2005). Plakophilin 3 Oncogene as Prognostic Marker and Therapeutic Target for Lung Cancer. *Cancer Research*, *65*(16), 7102–7110. https://doi.org/10.1158/0008-5472.CAN-04-1877

Gainor, J. F., Tan, D. S. W., De Pas, T., Solomon, B. J., Ahmad, A., Lazzari, C., … Shaw, A. T. (2015). Progression-Free and Overall Survival in ALK-Positive NSCLC Patients Treated with Sequential Crizotinib and Ceritinib. *Clinical Cancer Research : An Official Journal of the American Association for Cancer Research*, *21*(12), 2745–2752. https://doi.org/10.1158/1078-0432.CCR-14-3009

Garrod, D. R., Berika, M. Y., Bardsley, W. F., Holmes, D., & Tabernero, L. (2005). Hyper-adhesion in desmosomes: its regulation in wound healing and possible relationship to cadherin crystal structure. *Journal of Cell Science*, *118*(24), 5743–5754. https://doi.org/10.1242/jcs.02700

Gazzeri, S., Brambilla, E., Jacrot, M., Chauvin, C., Benabid, A. L., & Brambilla, C. (1991). Activation of myc Gene Family in Human Lung Carcinomas and during Heterotransplantation into Nude Mice. *Cancer Research*, *51*(10), 2566–2571. Retrieved from http://cancerres.aacrjournals.org/content/51/10/2566

George, J., Lim, J. S., Jang, S. J., Cun, Y., Ozretić, L., Kong, G., … Thomas, R. K. (2015). Comprehensive genomic profiles of small cell lung cancer. *Nature*, *524*(7563), 47–53. https://doi.org/10.1038/nature14664

Ghose, S., Min, Y., & Lin, P. C. (2015). δ-Catenin activates Rho GTPase, promotes lymphangiogenesis and growth of tumor metastases. *PloS One*, *10*(1), e0116338–e0116338. https://doi.org/10.1371/journal.pone.0116338

Glisovic, T., Bachorik, J. L., Yong, J., & Dreyfuss, G. (2008). RNA-binding proteins and post-transcriptional gene regulation. *FEBS Letters*, *582*(14), 1977–1986. https://doi.org/10.1016/j.febslet.2008.03.004

Goldstraw, P., Chansky, K., Crowley, J., Rami-Porta, R., Asamura, H., Eberhardt, W. E. E., … Yokoi, K. (2016). The IASLC Lung Cancer Staging Project: Proposals for Revision of the TNM Stage Groupings in the Forthcoming (Eighth) Edition of the TNM Classification for Lung Cancer. *Journal of Thoracic Oncology*, *11*(1), 39–51. https://doi.org/https://doi.org/10.1016/j.jtho.2015.09.009

Gomez-Morales, M., Camara-Pulido, M., Miranda-Leon, M. T., Sanchez-Palencia, A., Boyero, L., Gomez-Capilla, J. A., & Farez-Vidal, M. E. (2013). Differential immunohistochemical localization of desmosomal plaque-related proteins in non-small-cell lung cancer. *Histopathology*, *63*(1), 103–113. https://doi.org/10.1111/his.12126

Gómez-Morales, M., Cámara-Pulido, M., Miranda-León, M. T., Sánchez-Palencia, A., Boyero, L., Gómez-Capilla, J. A., & Fárez-Vidal, M. E. (2013). Differential immunohistochemical localization of desmosomal plaque-related proteins in non-small-cell lung cancer. *Histopathology*, *63*(1), 103–113. https://doi.org/10.1111/his.12126

González Baron, M. (2006). *Cáncer no microcítico de pulmón: Un reto para el siglo XXI.* Madrid: ARS MEDICA.

Govindan, R., Ding, L., Griffith, M., Subramanian, J., Dees, N. D., Kanchi, K. L., … Wilson, R. K. (2012). Genomic landscape of non-small cell lung cancer in smokers and never-smokers. *Cell*, *150*(6), 1121–1134. https://doi.org/10.1016/j.cell.2012.08.024

Greaves, M., & Maley, C. C. (2012). Clonal evolution in cancer. *Nature*, *481*(7381), 306–313. https://doi.org/10.1038/nature10762

Grupp, S. A., Kalos, M., Barrett, D., Aplenc, R., Porter, D. L., Rheingold, S. R., … June, C. H. (2013). Chimeric Antigen Receptor–Modified T Cells for Acute Lymphoid Leukemia. *New England Journal of Medicine*, *368*(16), 1509–1518. https://doi.org/10.1056/NEJMoa1215134

Hakimelahi, S., Parker, H. R., Gilchrist, A. J., Barry, M., Li, Z., Bleackley, R. C., & Pasdar, M. (2000). Plakoglobin Regulates the Expression of the Anti-apoptotic Protein BCL-2. *Journal of Biological Chemistry* , *275*(15), 10905–10911. https://doi.org/10.1074/jbc.275.15.10905

Hamada, T., South, A. P., Mitsuhashi, Y., Kinebuchi, T., Bleck, O., Ashton, G. H. S., … McGrath, J. A. (2002). Genotype–phenotype correlation in skin fragility-ectodermal dysplasia syndrome resulting from mutations in plakophilin 1. *Experimental Dermatology*, *11*(2), 107–114. https://doi.org/10.1034/j.1600-0625.2002.110202.x

Hanahan, D., & Weinberg, R. A. (2011). Hallmarks of Cancer: The Next Generation. *Cell*, *144*(5), 646–674. https://doi.org/10.1016/j.cell.2011.02.013

Hann, S. R. (2006). Role of post-translational modifications in regulating c-Myc proteolysis, transcriptional activity and biological function. *Seminars in Cancer Biology*, *16*(4), 288–302. https://doi.org/https://doi.org/10.1016/j.semcancer.2006.08.004

Hann, S. R., King, M. W., Bentley, D. L., Anderson, C. W., & Eisenman, R. N. (1988). A non-AUG translational initiation in c-myc exon 1 generates an N-terminally distinct protein whose synthesis is disrupted in Burkitt's lymphomas. *Cell*, *52*(2), 185–195. https://doi.org/10.1016/0092-8674(88)90507-7

Hatton, K. S., Mahon, K., Chin, L., Chiu, F. C., Lee, H. W., Peng, D., … DePinho, R. A. (1996). Expression and activity of L-Myc in normal mouse development. *Molecular and Cellular Biology*, *16*(4), 1794–1804. Retrieved from https://www.ncbi.nlm.nih.gov/pubmed/8657155

Hatzfeld, M. (2005). The p120 family of cell adhesion molecules. *European Journal of Cell Biology*, *84*(2), 205–214. https://doi.org/https://doi.org/10.1016/j.ejcb.2004.12.016

Hatzfeld, M. (2007). Plakophilins: Multifunctional proteins or just regulators of desmosomal adhesion? *Biochimica et Biophysica Acta (BBA) - Molecular Cell Research*, *1773*(1), 69–77. https://doi.org/https://doi.org/10.1016/j.bbamcr.2006.04.009

Hatzfeld, M. (2010). A Nuclear Function for Plakophilin-1 in the DNA Damage Response? *Journal of Investigative Dermatology*, *130*(11), 2538–2540. https://doi.org/10.1038/jid.2010.258

Hatzfeld, M., Haffner, C., Schulze, K., & Vinzens, U. (2000). The function of plakophilin 1 in desmosome assembly and actin filament organization. *The Journal of Cell Biology*, *149*(1), 209–222. Retrieved from https://www.ncbi.nlm.nih.gov/pubmed/10747098

Hatzfeld, M., Wolf, A., & Keil, R. (2014). Plakophilins in Desmosomal Adhesion and Signaling. *Cell Communication & Adhesion*, *21*(1), 25–42. https://doi.org/10.3109/15419061.2013.876017

Heid, H. W., Schmidt, A., Zimbelmann, R., Schäfer, S., Winter-Simanowski, S., Stumpp, S., … Franke, W. W. (1995). Cell type-specific desmosomal plaque proteins of the plakoglobin family: plakophilin 1 (band 6 protein). *Differentiation*, *58*(2), 113–131. https://doi.org/https://doi.org/10.1046/j.1432-0436.1995.5820113.x

Henriksson, M., & Lüscher, B. (1996). Proteins of the Myc Network: Essential Regulators of Cell Growth and Differentiation. In G. F. Vande Woude & G. B. T.-A. in C. R. Klein (Eds.) (Vol. 68, pp. 109–182). Academic Press. https://doi.org/https://doi.org/10.1016/S0065-230X(08)60353-X

Hirsh, V. (2015). Next-Generation Covalent Irreversible Kinase Inhibitors in NSCLC: Focus on Afatinib. *BioDrugs : Clinical Immunotherapeutics, Biopharmaceuticals and Gene Therapy*, *29*(3), 167–183. https://doi.org/10.1007/s40259-015-0130-9

Hofmann, I., Casella, M., Schnölzer, M., Schlechter, T., Spring, H., & Franke, W. W. (2006). Identification of the junctional plaque protein plakophilin 3 in cytoplasmic particles containing RNA-binding proteins and the recruitment of plakophilins 1 and 3 to stress granules. *Molecular Biology of the Cell*, *17*(3), 1388–1398. https://doi.org/10.1091/mbc.e05-08-0708

Hou, J., Aerts, J., den Hamer, B., van IJcken, W., den Bakker, M., Riegman, P., … Philipsen, S. (2010). Gene Expression-Based Classification of Non-Small Cell Lung Carcinomas and Survival Prediction. *PLOS ONE*, *5*(4), 1–12. https://doi.org/10.1371/journal.pone.0010312

Howington, J. A., Blum, M. G., Chang, A. C., Balekian, A. A., & Murthy, S. C. (2013). Treatment of Stage I and II Non-small Cell Lung Cancer: Diagnosis and Management of Lung Cancer, 3rd ed: American College of Chest Physicians Evidence-Based Clinical Practice Guidelines. *Chest*, *143*(5, Supplement), e278S–e313S. https://doi.org/https://doi.org/10.1378/chest.12-2359

Hurlin, P. J. (2013). Control of vertebrate development by MYC. *Cold Spring Harbor Perspectives in Medicine*, *3*(9), a014332–a014332. https://doi.org/10.1101/cshperspect.a014332

Imielinski, M., Berger, A. H., Hammerman, P. S., Hernandez, B., Pugh, T. J., Hodis, E., … Meyerson, M. (2012). Mapping the hallmarks of lung adenocarcinoma with massively parallel sequencing. *Cell*, *150*(6), 1107–1120. https://doi.org/10.1016/j.cell.2012.08.029

Iwakawa, R., Kohno, T., Kato, M., Shiraishi, K., Tsuta, K., Noguchi, M., … Yokota, J. (2011). MYC Amplification as a Prognostic Marker of Early-Stage Lung Adenocarcinoma Identified by Whole Genome Copy Number Analysis. *Clinical Cancer Research*, *17*(6), 1481–1489. https://doi.org/10.1158/1078-0432.CCR-10-2484

Jackstadt, R., & Hermeking, H. (2015). MicroRNAs as regulators and mediators of c-MYC function. *Biochimica et Biophysica Acta (BBA) - Gene Regulatory Mechanisms*, *1849*(5), 544–553. https://doi.org/https://doi.org/10.1016/j.bbagrm.2014.04.003

Johnson, B. E., Brennan, J. F., Ihde, D. C., & Gazdar, A. F. (1992). myc family DNA amplification in tumors and tumor cell lines from patients with small-cell lung cancer. *Journal of the National Cancer Institute. Monographs*, (13), 39—43. Retrieved from http://europepmc.org/abstract/MED/1327035

Johnson, B. E., Ihde, D. C., Makuch, R. W., Gazdar, A. F., Carney, D. N., Oie, H., … Minna, J. D. (1987). myc family oncogene amplification in tumor cell lines established from small cell lung cancer patients and its relationship to clinical status and course. *The Journal of Clinical Investigation*, *79*(6), 1629–1634. https://doi.org/10.1172/JCI112999

Jonkers, J. (2012). Tracking Evolution of BRCA1-Associated Breast Cancer. *Cancer Discovery*, *2*(6), 486 LP-488. https://doi.org/10.1158/2159-8290.CD-12-0186

Kalkat, M., De Melo, J., Hickman, K. A., Lourenco, C., Redel, C., Resetca, D., … Penn, L. Z. (2017). MYC Deregulation in Primary Human Cancers. *Genes*, *8*(6), 151. https://doi.org/10.3390/genes8060151

Kalos, M., Levine, B. L., Porter, D. L., Katz, S., Grupp, S. A., Bagg, A., & June, C. H. (2011). T cells with chimeric antigen receptors have potent antitumor effects and can establish memory in patients with advanced leukemia. *Science Translational Medicine*, *3*(95), 95ra73-95ra73. https://doi.org/10.1126/scitranslmed.3002842

Kashyap, S., Shanker, V., & Sharma, N. (2015). Ectodermal Dysplasia-Skin Fragility Syndrome: A Rare Case Report. *Indian Journal of Dermatology*, *60*(4), 421. https://doi.org/10.4103/0019-5154.160525

Keil, R., Wolf, A., Huettelmaier, S., & Hatzfeld, M. (2007). Beyond Regulation of Cell Adhesion: Local Control of RhoA at the Cleavage Furrow by the p0071 Catenin. *Cell Cycle*, *6*(2), 122–127. https://doi.org/10.4161/cc.6.2.3741

Kimura, T. E., Merritt, A. J., & Garrod, D. R. (2007). Calcium-Independent Desmosomes of Keratinocytes are Hyper-Adhesive. *Journal of Investigative Dermatology*, *127*(4), 775–781. https://doi.org/10.1038/sj.jid.5700643

Kimura, T. E., Merritt, A. J., Lock, F. R., Eckert, J. J., Fleming, T. P., & Garrod, D. R. (2012). Desmosomal adhesiveness is developmentally regulated in the mouse embryo and modulated during trophectoderm migration. *Developmental Biology*, *369*(2), 286–297. https://doi.org/https://doi.org/10.1016/j.ydbio.2012.06.025

Kolligs, F. T., Kolligs, B., Hajra, K. M., Hu, G., Tani, M., Cho, K. R., & Fearon, E. R. (2000). gamma-catenin is regulated by the APC tumor suppressor and its oncogenic activity is distinct from that of beta-catenin. *Genes & Development*, *14*(11), 1319–1331. Retrieved from https://www.ncbi.nlm.nih.gov/pubmed/10837025

Kowalczyk, A. P., Hatzfeld, M., Bornslaeger, E. A., Kopp, D. S., Borgwardt, J. E., Corcoran, C. M., … Green, K. J. (1999). The Head Domain of Plakophilin-1 Binds to Desmoplakin and Enhances Its Recruitment to Desmosomes: IMPLICATIONS FOR CUTANEOUS DISEASE . *Journal of Biological Chemistry* , *274*(26), 18145–18148. https://doi.org/10.1074/jbc.274.26.18145

Kumar, R., Collins, D., Dolly, S., McDonald, F., O'Brien, M. E. R., & Yap, T. A. (2017). Targeting the PD-1/PD-L1 axis in non–small cell lung cancer. *Current Problems in Cancer*, *41*(2), 111–124. https://doi.org/https://doi.org/10.1016/j.currproblcancer.2016.12.002

Kundu, S. T., Gosavi, P., Khapare, N., Patel, R., Hosing, A. S., Maru, G. B., … Dalal, S. N. (2008). Plakophilin3 downregulation leads to a decrease in cell adhesion and promotes metastasis. *International Journal of Cancer*, *123*(10), 2303–2314. https://doi.org/10.1002/ijc.23797

Lacasse, Y., Wong, E., Guyatt, G. H., & Cook, D. J. (1999). Transthoracic needle aspiration biopsy for the diagnosis of localised pulmonary lesions: a meta-analysis. *Thorax*, *54*(10), 884–893. Retrieved from https://www.ncbi.nlm.nih.gov/pubmed/10491450

Lee, E. Y. H. P., & Muller, W. J. (2010). Oncogenes and tumor suppressor genes. *Cold Spring Harbor Perspectives in Biology*, *2*(10), a003236–a003236. https://doi.org/10.1101/cshperspect.a003236

Liang, C.-C., Park, A. Y., & Guan, J.-L. (2007). In vitro scratch assay: a convenient and inexpensive method for analysis of cell migration in vitro. *Nature Protocols*, *2*, 329. Retrieved from https://doi.org/10.1038/nprot.2007.30

Lin, C.-J., Cencic, R., Mills, J. R., Robert, F., & Pelletier, J. (2008). c-Myc and eIF4F Are Components of a Feedforward Loop that Links Transcription and Translation. *Cancer Research*, *68*(13), 5326–5334. https://doi.org/10.1158/0008-5472.CAN-07-5876

Lin, C.-J., Malina, A., & Pelletier, J. (2009). c-Myc and eIF4F Constitute a Feedforward Loop That Regulates Cell Growth: Implications for Anticancer Therapy. *Cancer Research*, *69*(19), 7491–7494. https://doi.org/10.1158/0008-5472.CAN-09-0813

Lin, C. Y., Lovén, J., Rahl, P. B., Paranal, R. M., Burge, C. B., Bradner, J. E., … Young, R. A. (2012). Transcriptional amplification in tumor cells with elevated c-Myc. *Cell*, *151*(1), 56–67. https://doi.org/10.1016/j.cell.2012.08.026

Lin, J. J., & Shaw, A. T. (2017). Recent Advances in Targeting ROS1 in Lung Cancer. *Journal of Thoracic Oncology : Official Publication of the International Association for the Study of Lung Cancer*, *12*(11), 1611–1625. https://doi.org/10.1016/j.jtho.2017.08.002

Lodish, H., Berk, A., & Zipursky, S. (2000). *Molecular Cell Biology. Section 24.3: Oncogenic Mutations Affecting Cell Proliferation*. (W. . Freeman, Ed.) (4th editio). New York.

Lorch, J. H., Klessner, J., Park, J. K., Getsios, S., Wu, Y. L., Stack, M. S., & Green, K. J. (2004). Epidermal Growth Factor Receptor Inhibition Promotes Desmosome Assembly and Strengthens Intercellular Adhesion in Squamous Cell Carcinoma Cells. *Journal of Biological Chemistry* , *279*(35), 37191–37200. https://doi.org/10.1074/jbc.M405123200

Loubeyre, P., Copercini, M., & Dietrich, P.-Y. (2005). Percutaneous CT-Guided Multisampling Core Needle Biopsy of Thoracic Lesions. *American Journal of Roentgenology*, *185*(5), 1294–1298. https://doi.org/10.2214/AJR.04.1344

Lüscher, B., & Vervoorts, J. (2012). Regulation of gene transcription by the oncoprotein MYC. *Gene*, *494*(2), 145–160. https://doi.org/https://doi.org/10.1016/j.gene.2011.12.027

Martin-Padron, J., Boyero, L., Rodriguez, M. I., Andrades, A., Díaz-Cano, I., Peinado, P., … Medina, P. P. (2019). Plakophilin 1 enhances MYC translation, promoting squamous cell lung cancer. *Oncogene*. https://doi.org/10.1038/s41388-019-1129-3

Massagué, J., & Obenauf, A. C. (2016). Metastatic colonization by circulating tumour cells. *Nature*, *529*, 298. Retrieved from https://doi.org/10.1038/nature17038

Masters, G. A., Temin, S., Azzoli, C. G., Giaccone, G., Baker, S., Brahmer, J. R., … Johnson, D. H. (2015). Systemic Therapy for Stage IV Non–Small-Cell Lung Cancer: American Society of Clinical Oncology Clinical Practice Guideline Update. *Journal of Clinical Oncology*, *33*(30), 3488–3515. https://doi.org/10.1200/JCO.2015.62.1342

McGRATH, HOEGER, CHRISTIANO, McMILLAN, MELLERIO, ASHTON, … EADY. (1999). Skin fragility and hypohidrotic ectodermal dysplasia resulting from ablation of plakophilin 1. *British Journal of Dermatology*, *140*(2), 297–307. https://doi.org/10.1046/j.1365- https://doi.org/10.1016/j.cellsig.2009.01.004

Mertens, C., Kuhn, C., & Franke, W. W. (1996). Plakophilins 2a and 2b: constitutive proteins of dual location in the karyoplasm and the desmosomal plaque. *The Journal of Cell Biology*, *135*(4), 1009–1025. Retrieved from https://www.ncbi.nlm.nih.gov/pubmed/8922383

Meyer, N., & Penn, L. Z. (2008). Reflecting on 25 years with MYC. *Nature Reviews Cancer*, *8*, 976. Retrieved from https://doi.org/10.1038/nrc2231

Mirsadraee, S., Oswal, D., Alizadeh, Y., Caulo, A., & van Beek Jr, E. (2012). The 7th lung cancer TNM classification and staging system: Review of the changes and implications. *World Journal of Radiology*, *4*(4), 128–134. https://doi.org/10.4329/wjr.v4.i4.128

Moll, R., Cowin, P., Kapprell, H., & Franke, W. (1986). Desmosomal proteins: new markers for identification and classification of tumors. *Laboratory Investigation; a Journal of Technical Methods and Pathology*.

Mollaoglu, G., Guthrie, M. R., Böhm, S., Brägelmann, J., Can, I., Ballieu, P. M., … Oliver, T. G. (2017). MYC Drives Progression of Small Cell Lung Cancer to a Variant Neuroendocrine Subtype with Vulnerability to Aurora Kinase Inhibition. *Cancer Cell*, *31*(2), 270–285. https://doi.org/10.1016/j.ccell.2016.12.005

Morton, J. P., & Sansom, O. J. (2013). MYC-y mice: from tumour initiation to therapeutic targeting of endogenous MYC. *Molecular Oncology*, *7*(2), 248–258. https://doi.org/10.1016/j.molonc.2013.02.015

Moustakas, A., & Heldin, C.-H. (2007). Signaling networks guiding epithelial–mesenchymal transitions during embryogenesis and cancer progression. *Cancer Science*, *98*(10), 1512–1520. https://doi.org/10.1111/j.1349-7006.2007.00550.x

Munoz, W. A., Lee, M., Miller, R. K., Ahmed, Z., Ji, H., Link, T. M., … McCrea, P. D. (2014). Plakophilin-3 catenin associates with the ETV1/ER81 transcription factor to positively modulate gene activity. *PloS One*, *9*(1), e86784–e86784. https://doi.org/10.1371/journal.pone.0086784

Nair, S. K., & Burley, S. K. (2003). X-Ray Structures of Myc-Max and Mad-Max Recognizing DNA: Molecular Bases of Regulation by Proto-Oncogenic Transcription Factors. *Cell*, *112*(2), 193–205. https://doi.org/https://doi.org/10.1016/S0092-8674(02)01284-9

Narayana, N., Gist, J., Smith, T., Tylka, D., Trogdon, G., & Wahl, J. K. (2010). Desmosomal component expression in normal, dysplastic, and oral squamous cell carcinoma. *Dermatology Research and Practice*, *2010*, 649731. https://doi.org/10.1155/2010/649731

Nau, M. M., Brooks Jr, B. J., Carney, D. N., Gazdar, A. F., Battey, J. F., Sausville, E. A., & Minna, J. D. (1986). Human small-cell lung cancers show amplification and expression of the N-myc gene. *Proceedings of the National Academy of Sciences of the United States of America*, *83*(4), 1092–1096. Retrieved from https://www.ncbi.nlm.nih.gov/pubmed/2869482

Nau, M. M., Brooks, B. J., Battey, J., Sausville, E., Gazdar, A. F., Kirsch, I. R., … Minna, J. D. (1985). L-myc, a new myc-related gene amplified and expressed in human small cell lung cancer. *Nature*, *318*, 69. Retrieved from https://doi.org/10.1038/318069a0

Network, C. G. A. R. (2012). Comprehensive genomic characterization of squamous cell lung cancers. *Nature*, *489*(7417), 519–525. https://doi.org/10.1038/nature11404

Neuber, S., Mühmer, M., Wratten, D., Koch, P. J., Moll, R., & Schmidt, A. (2010). The desmosomal plaque proteins of the plakophilin family. *Dermatology Research and Practice*, *2010*, 101452. https://doi.org/10.1155/2010/101452

Pakkala, S., & Ramalingam, S. S. (2018). Personalized therapy for lung cancer: striking a moving target. *JCI Insight*, *3*(15), e120858. https://doi.org/10.1172/jci.insight.120858

Pao, W., & Hutchinson, K. E. (2012). Chipping away at the lung cancer genome. *Nature Medicine*, *18*, 349. Retrieved from https://doi.org/10.1038/nm.2697

Peifer, M., Fernández-Cuesta, L., Sos, M. L., George, J., Seidel, D., Kasper, L. H., … Thomas, R. K. (2012). Integrative genome analyses identify key somatic driver mutations of small-cell lung cancer. *Nature Genetics*, *44*(10), 1104–1110. https://doi.org/10.1038/ng.2396

Pelletier, J., Graff, J., Ruggero, D., & Sonenberg, N. (2015). Targeting the eIF4F translation initiation complex: a critical nexus for cancer development. *Cancer Research*, *75*(2), 250–263. https://doi.org/10.1158/0008-5472.CAN-14-2789

Pesch, B., Kendzia, B., Gustavsson, P., Jöckel, K.-H., Johnen, G., Pohlabeln, H., … Brüning, T. (2012). Cigarette smoking and lung cancer--relative risk estimates for the major histological types from a pooled analysis of case-control studies. *International Journal of Cancer*, *131*(5), 1210–1219. https://doi.org/10.1002/ijc.27339

Pesu, M., Laurence, A., Kishore, N., Zwillich, S. H., Chan, G., & O'Shea, J. J. (2008). Therapeutic targeting of Janus kinases. *Immunological Reviews*, *223*, 132–142. https://doi.org/10.1111/j.1600-065X.2008.00644.x

Pirity, M., Blanck, J. K., & Schreiber-Agus, N. (2006). Lessons Learned from Myc/Max/Mad Knockout Mice BT - The Myc/Max/Mad Transcription Factor Network. In R. N. Eisenman (Ed.) (pp. 205–234). Berlin, Heidelberg: Springer Berlin Heidelberg. https://doi.org/10.1007/3-540-32952-8_8

Qiao, M., Sheng, S., & Pardee, A. B. (2008). Metastasis and AKT activation. *Cell Cycle*, *7*(19), 2991–2996. https://doi.org/10.4161/cc.7.19.6784

Rajasekhar, V. K., Viale, A., Socci, N. D., Wiedmann, M., Hu, X., & Holland, E. C. (2003). Oncogenic Ras and Akt Signaling Contribute to Glioblastoma Formation by Differential Recruitment of Existing mRNAs to Polysomes. *Molecular Cell*, *12*(4), 889–901. https://doi.org/10.1016/S1097-2765(03)00395-2

Ramalingam, S., & Belani, C. (2008). Systemic Chemotherapy for Advanced Non-Small Cell Lung Cancer: Recent Advances and Future Directions. *The Oncologist* , *13*(suppl 1), 5–13. https://doi.org/10.1634/theoncologist.13-S1-5

Ran, F. A., Hsu, P. D., Wright, J., Agarwala, V., Scott, D. A., & Zhang, F. (2013). Genome engineering using the CRISPR-Cas9 system. *Nature Protocols*, *8*(11), 2281–2308. https://doi.org/10.1038/nprot.2013.143

Rapp, U. R., Korn, C., Ceteci, F., Karreman, C., Luetkenhaus, K., Serafin, V., … Potapenko, T. (2009). MYC is a metastasis gene for non-small-cell lung cancer. *PloS One*, *4*(6), e6029–e6029. https://doi.org/10.1371/journal.pone.0006029

Ready, N., Farago, A. F., de Braud, F., Atmaca, A., Hellmann, M. D., Schneider, J. G., … Antonia, S. J. (2019). Third-Line Nivolumab Monotherapy in Recurrent SCLC: CheckMate 032. *Journal of Thoracic Oncology*, *14*(2), 237–244. https://doi.org/https://doi.org/10.1016/j.jtho.2018.10.003

Richardson, G. ., & Johnson, B. E. (1993). The biology of lung cancer. *Seminars in Oncology*, *20*, 105–127.

Rietscher, K., Wolf, A., Hause, G., Rother, A., Keil, R., Magin, T. M., … Hatzfeld, M. (2016). Growth Retardation, Loss of Desmosomal Adhesion, and Impaired Tight Junction Function Identify a Unique Role of Plakophilin 1 In-Vivo. *Journal of Investigative Dermatology*, *136*(7), 1471–1478. https://doi.org/10.1016/j.jid.2016.03.021

Rivera, M. P., & Mehta, A. C. (2007). Initial Diagnosis of Lung Cancer: ACCP Evidence-Based Clinical Practice Guidelines (2nd Edition). *CHEST*, *132*(3), 131S–148S. https://doi.org/10.1378/chest.07-1357

Russo, A. E., Priolo, D., Antonelli, G., Libra, M., McCubrey, J. A., & Ferraù, F. (2017). Bevacizumab in the treatment of NSCLC: patient selection and perspectives. *Lung Cancer (Auckland, N.Z.)*, *8*, 259–269. https://doi.org/10.2147/LCTT.S110306

Sabò, A., Kress, T. R., Pelizzola, M., de Pretis, S., Gorski, M. M., Tesi, A., … Amati, B. (2014). Selective transcriptional regulation by Myc in cellular growth control and lymphomagenesis. *Nature*, *511*(7510), 488–492. https://doi.org/10.1038/nature13537

Sanchez-Palencia, A., Gomez-Morales, M., Gomez-Capilla, J. A., Pedraza, V., Boyero, L., Rosell, R., & Fárez-Vidal, M. E. (2011). Gene expression profiling reveals novel biomarkers in nonsmall cell lung cancer. *International Journal of Cancer*, *129*(2), 355–364. https://doi.org/10.1002/ijc.25704

Schackmann, R. C. J., Tenhagen, M., van de Ven, R. A. H., & Derksen, P. W. B. (2013). p120-catenin in cancer-mechanisms, models and opportunities for intervention. *Journal of Cell Science*, *126*(16), 3515–3525. https://doi.org/10.1242/jcs.134411

Schmidt, A., & Jäger, S. (2005). Plakophilins—hard work in the desmosome, recreation in the nucleus? *European Journal of Cell Biology*, *84*(2), 189–204. https://doi.org/https://doi.org/10.1016/j.ejcb.2004.12.020

Schmidt, A., Langbein, L., Rode, M., Prätzel, S., Zimbelmann, R., & Franke, W. (1997). Plakophilins 1a and 1b: Widespread nuclear proteins recruited in specific epithelial cells as desmosomal plaque components. *Cell and Tissue Research*, *290*, 481–499. https://doi.org/10.1007/s004410050956

Schreiber, R. D., Old, L. J., & Smyth, M. J. (2011). Cancer Immunoediting: Integrating Immunity´s Roles in Cancer Suppression and Promotion. *Science*, *331*(6024), 1565–1570. https://doi.org/10.1126/science.1203486

Schumacher, T. N., & Schreiber, R. D. (2015). Neoantigens in cancer immunotherapy. *Science*, *348*(6230), 69–74. https://doi.org/10.1126/science.aaa4971

Schwarz, J., Ayim, A., Schmidt, A., Jäger, S., Koch, S., Baumann, R., … Moll, R. (2006). Differential expression of desmosomal plakophilins in various types of carcinomas: correlation with cell type and differentiation. *Human Pathology*, *37*(5), 613–622. https://doi.org/https://doi.org/10.1016/j.humpath.2006.01.013

Seo, A. N., Yang, J. M., Kim, H., Jheon, S., Kim, K., Lee, C. T., … Paik, J. H. (2014). Clinicopathologic and prognostic significance of c-MYC copy number gain in lung adenocarcinomas. *British Journal of Cancer*, *110*(11), 2688–2699. https://doi.org/10.1038/bjc.2014.218

Shalapour, S., & Karin, M. (2015). Immunity, inflammation, and cancer: an eternal fight between good and evil. *The Journal of Clinical Investigation*, *125*(9), 3347–3355. https://doi.org/10.1172/JCI80007

Shi, W., de Graaf, C. A., Kinkel, S. A., Achtman, A. H., Baldwin, T., Schofield, L., … Smyth, G. K. (2010). Estimating the proportion of microarray probes expressed in an RNA sample. *Nucleic Acids Research*, *38*(7), 2168–2176. https://doi.org/10.1093/nar/gkp1204

Shi, W., Oshlack, A., & Smyth, G. K. (2010). Optimizing the noise versus bias trade-off for Illumina whole genome expression BeadChips. *Nucleic Acids Research*, *38*(22), e204–e204. https://doi.org/10.1093/nar/gkq871

Siddiqui, N., & Sonenberg, N. (2015). Signalling to eIF4E in cancer. *Biochemical Society Transactions*, *43*(5), 763–772. https://doi.org/10.1042/BST20150126

Sobolik-Delmaire, T., Reddy, R., Pashaj, A., Roberts, B. J., & Wahl III., J. K. (2010). Plakophilin-1 localizes to the nucleus and interacts with single-stranded DNA. *Journal of Investigative Dermatology*, *130*(11), 2638–2646. https://doi.org/10.1038/jid.2010.191

Sos, M. L., Dietlein, F., Peifer, M., Schöttle, J., Balke-Want, H., Müller, C., … Thomas, R. K. (2012). A framework for identification of actionable cancer genome dependencies in small cell lung cancer. *Proceedings of the National Academy of Sciences of the United States of America*, *109*(42), 17034–17039. https://doi.org/10.1073/pnas.1207310109

Soucek, L., Whitfield, J., Martins, C. P., Finch, A. J., Murphy, D. J., Sodir, N. M., … Evan, G. I. (2008). Modelling Myc inhibition as a cancer therapy. *Nature*, *455*(7213), 679–683. https://doi.org/10.1038/nature07260

South, A. P. (2004). Plakophilin 1: an important stabilizer of desmosomes. *Clinical and Experimental Dermatology*, *29*(2), 161–167. https://doi.org/10.1111/j.1365-2230.2004.01467.x

Spotts, G. D., Patel, S. V, Xiao, Q., & Hann, S. R. (1997). Identification of downstream-initiated c-Myc proteins which are dominant-negative inhibitors of transactivation by full-length c-Myc proteins. *Molecular and Cellular Biology*, *17*(3), 1459–1468. Retrieved from https://www.ncbi.nlm.nih.gov/pubmed/9032273

Sprecher, E., Molho-Pessach, V., Ingber, A., Sagi, E., Indelman, M., & Bergman, R. (2004). Homozygous Splice Site Mutations in PKP1 Result in Loss of Epidermal Plakophilin 1 Expression and Underlie Ectodermal Dysplasia/Skin Fragility Syndrome in Two Consanguineous Families. *Journal of Investigative Dermatology*, *122*(3), 647–651. https://doi.org/10.1111/j.0022-202X.2004.22335.x

Steelman, L. S., Stadelman, K. M., Chappell, W. H., Horn, S., Bäsecke, J., Cervello, M., … McCubrey, J. A. (2008). Akt as a therapeutic target in cancer. *Expert Opinion on Therapeutic Targets*, *12*(9), 1139–1165. https://doi.org/10.1517/14728222.12.9.1139

Steijlen, P. M., van Steensel, M. A. M., Jansen, B. J. H., Blokx, W., van de Kerkhof, P. C. M., Happle, R., & van Geel, M. (2004). Cryptic Splicing at a Non-Consensus Splice-Donor in a Patient with a Novel Mutation in the Plakophilin-1 Gene. *Journal of Investigative Dermatology*, *122*(5), 1321–1324. https://doi.org/10.1111/j.0022-202X.2003.22302.x

STEWART, B. W., & WILD, C. P. (2014). *World Cancer Report 2014*. (B. W. STEWART & C. P. WILD, Eds.). International Agency for Research on Cancer.

Su, Y., & Pan, L. (2014). Identification of logic relationships between genes and subtypes of non-small cell lung cancer. *PloS One*, *9*(4), e94644–e94644. https://doi.org/10.1371/journal.pone.0094644

Takahashi, H., Nakatsuji, H., Takahashi, M., Avirmed, S., Fukawa, T., Takemura, M., … Kanayama, H. (2012). Up-regulation of Plakophilin-2 and Down-regulation of Plakophilin-3 are Correlated With Invasiveness in Bladder Cancer. *Urology*, *79*(1), 240.e1-240.e8. https://doi.org/10.1016/j.urology.2011.08.049

STEWART, B. W., & WILD, C. P. (2014). *World Cancer Report 2014*. (B. W. STEWART & C. P. WILD, Eds.). International Agency for Research on Cancer.

Su, Y., & Pan, L. (2014). Identification of logic relationships between genes and subtypes of non-small cell lung cancer. *PloS One*, *9*(4), e94644–e94644. https://doi.org/10.1371/journal.pone.0094644

Takahashi, H., Nakatsuji, H., Takahashi, M., Avirmed, S., Fukawa, T., Takemura, M., … Kanayama, H. (2012). Up-regulation of Plakophilin-2 and Down-regulation of Plakophilin-3 are Correlated With Invasiveness in Bladder Cancer. *Urology*, *79*(1), 240.e1-240.e8. https://doi.org/10.1016/j.urology.2011.08.049

Tlsty, T. D., & Coussens, L. M. (2006). TUMOR STROMA AND REGULATION OF CANCER DEVELOPMENT. *Annual Review of Pathology: Mechanisms of Disease*, *1*(1), 119–150. https://doi.org/10.1146/annurev.pathol.1.110304.100224

Tokunaga, E., Oki, E., Egashira, A., Sadanaga, N., Morita, M., & Maehara, Y. K. and Y. (2008). Deregulation of the Akt Pathway in Human Cancer. *Current Cancer Drug Targets*. https://doi.org/http://dx.doi.org/10.2174/156800908783497140

Travis, W. D., Brambilla, E., Nicholson, A. G., Yatabe, Y., Austin, J. H. M., Beasley, M. B., … Wistuba, I. (2015). The 2015 World Health Organization Classification of Lung Tumors: Impact of Genetic, Clinical and Radiologic Advances Since the 2004 Classification. *Journal of Thoracic Oncology*, *10*(9), 1243–1260. https://doi.org/10.1097/JTO.0000000000000630

Weiss, J., Sos, M. L., Seidel, D., Peifer, M., Zander, T., Heuckmann, J. M., … Thomas, R. K. (2010). Frequent and focal FGFR1 amplification associates with therapeutically tractable FGFR1 dependency in squamous cell lung cancer. *Science Translational Medicine*, *2*(62), 62ra93-62ra93. https://doi.org/10.1126/scitranslmed.3001451

Whitfield, J. R., Beaulieu, M.-E., & Soucek, L. (2017). Strategies to Inhibit Myc and Their Clinical Applicability. *Frontiers in Cell and Developmental Biology*, *5*, 10. https://doi.org/10.3389/fcell.2017.00010

Whittock, N. V, Eady, R. A. J., McGrath, J. A., Haftek, M., Angoulvant, N., Wolf, F., & Perrot, H. (2000). Genomic Amplification of the Human Plakophilin 1 Gene and Detection of a New Mutation in Ectodermal Dysplasia/Skin Fragility Syndrome. *Journal of Investigative Dermatology*, *115*(3), 368–374. https://doi.org/10.1046/j.1523-1747.2000.00082.x

Wolf, A., & Hatzfeld, M. (2010). A role of plakophilins in the regulation of translation. *Cell Cycle*, *9*(15), 3045–3050. https://doi.org/10.4161/cc.9.15.12446

Wolf, A., Krause-Gruszczynska, M., Birkenmeier, O., Ostareck-Lederer, A., Hüttelmaier, S., & Hatzfeld, M. (2010). Plakophilin 1 stimulates translation by promoting eIF4A1 activity. *The Journal of Cell Biology*, *188*(4), 463–471. https://doi.org/10.1083/jcb.200908135

Wolf, A., Rietscher, K., Glaß, M., Hüttelmaier, S., Schutkowski, M., Ihling, C., … Hatzfeld, M. (2013). Insulin signaling via Akt2 switches plakophilin 1 function from stabilizing cell adhesion to promoting cell proliferation. *Journal of Cell Science*, *126*(8), 1832–1844. https://doi.org/10.1242/jcs.118992

Wolfer, A., & Ramaswamy, S. (2010). Prognostic signatures, cancer metastasis and MYC. *Cell Cycle*, *9*(18), 3639. https://doi.org/10.4161/cc.9.18.13220

Wong, A. J., Ruppert, J. M., Eggleston, J., Hamilton, Baylin, S. B., & Vogelstein, B. (1986). Gene amplification of c-myc and N-myc in small cell carcinoma of the lung. *Science*, *233*(4762), 461–464. https://doi.org/10.1126/science.3014659

Xia, A.-L., He, Q.-F., Wang, J.-C., Zhu, J., Sha, Y.-Q., Sun, B., & Lu, X.-J. (2019). Applications and advances of CRISPR-Cas9 in cancer immunotherapy. *Journal of Medical Genetics*, *56*(1), 4–9. https://doi.org/10.1136/jmedgenet-2018-105422

Yamaoka, T., Ohba, M., & Ohmori, T. (2017). Molecular-Targeted Therapies for Epidermal Growth Factor Receptor and Its Resistance Mechanisms. *International Journal of Molecular Sciences*, *18*(11), 2420. https://doi.org/10.3390/ijms18112420

Yang, C., Ströbel, P., Marx, A., & Hofmann, I. (2013). Plakophilin-associated RNA-binding proteins in prostate cancer and their implications in tumor progression and metastasis. *Virchows Archiv*, *463*(3), 379–390. https://doi.org/10.1007/s00428-013-1452-y

Yang, J. J., Zhou, Q., Yan, H. H., Zhang, X. C., Chen, H. J., Tu, H. Y., … Wu, Y. L. (2017). A phase III randomised controlled trial of erlotinib vs gefitinib in advanced non-small cell lung cancer with EGFR mutations. *British Journal of Cancer*, *116*(5), 568–574. https://doi.org/10.1038/bjc.2016.456

Zamay, T. N., Zamay, G. S., Kolovskaya, O. S., Zukov, R. A., Petrova, M. M., Gargaun, A., … Kichkailo, A. S. (2017). Current and Prospective Protein Biomarkers of Lung Cancer. *Cancers*, *9*(11), 155. https://doi.org/10.3390/cancers9110155

Zheng, X., Liu, D., Fallon, J. T., & Zhong, M. (2015). Distinct genetic alterations in small cell carcinoma from different anatomic sites. *Experimental Hematology & Oncology*, *4*, 2. https://doi.org/10.1186/2162-3619-4-2

Zimmerman, K., Legouy, E., Stewart, V., Depinho, R., & Alt, F. W. (1990). Differential regulation of the N-myc gene in transfected cells and transgenic mice. *Molecular and Cellular Biology*, *10*(5), 2096–2103. Retrieved from https://www.ncbi.nlm.nih.gov/pubmed/2183019

UNIVERSIDAD
DE GRANADA